

**Interlayer Organic Modification of  
1:1 Type Clay Mineral Kaolinite**

1:1 型粘土鉱物カオリナイトの層間有機修飾

Thesis Submitted to Waseda University

Tetsuro ITAGAKI

February, 2003



## *Preface*

Inorganic layered materials have been researched for the further application as adsorbent, catalysis, reaction media, and inorganic filler. Organic modification of inorganic layered materials is able to control these properties. Organic groups bonded to the interlayer surface improve the interlayer environment and sometimes add the new properties due to synergistic effects of inorganic and organic components. On the other hand, organic modification of inorganic layered materials is utilized to form two dimensional inorganic-organic nanohybrids. Highly ordered inorganic-organic nanocomposites are easily obtained because the ordering of organic components on inorganic interlayer surface are mainly depend on the positions of reactive groups on inorganic interlayer surface. This is the reason why this method is advantageous to materials design.

Kaolinite, a typical 1:1 type clay mineral, is used in this thesis. Kaolinite is composed of  $\text{SiO}_4$  tetrahedral and  $\text{AlO}_4(\text{OH})_2$  octahedral sheets and has an asymmetric interlayer environments between the layers. Organic modification proceeded on the  $\text{AlO}_4(\text{OH})_2$  octahedral sheet side. In this point, kaolinite is quite different from other inorganic layered materials having reactive groups on both interlayer surfaces. Due to the different interaction with both layers, intercalated guest molecules are sometimes ordered in  $c$  axis (the direction of layer stacking) as well as  $ab$  plane. However, kaolinite known as non-swelling clay has a low reactivity for intercalation. Organic modification of kaolinite has a potential to solve this problem because interlayer environments are improved and asymmetry in  $c$  direction are maintained after modification.

This thesis describes the synthesis of organically modified kaolinites and a kaolinite-nylon 6 intercalation compound for the purpose of extending the potential use of kaolinite. Furthermore, the structures and properties have been investigated.

Kaolinite was organically modified with alcohols by trans esterification to establish the

general synthesis method for organic modified kaolinites. Methoxy-modified kaolinite, a versatile intermediate for the further intercalation, was selected as an intermediate, and 1,2-(and 1,3-)propanediol were grafted by transesterification of methoxy groups on the interlayer surface and propanediol. Further esterification between AlOH groups and propanediol also proceeded during the reaction. Propanediols were grafted in two different manners, “one-side bonding” and “bridged”, and residual OH groups of propanediol were introduced between the layers of kaolinite in the case of “one-side bonding”. This method was extended to organic modification of kaolinite with glycerol. In the process of organic modification, some organically modified kaolinites were swollen into alcohols. When ethylene glycol, 1,2-(and 1,3-)propanediol, 1,2-(and 1,3-)butanediol, and aminoethanol reacted with methoxy-modified kaolinite, swelling behavior was observed.

A kaolinite–nylon 6 intercalation compound (Kao–nylon 6) was prepared and mechanical properties of the composites in which Kao–nylon 6 was blended with nylon 6 matrix. First a kaolinite–6-aminohexanoic acid intercalation compound was obtained by the reaction between methoxy-modified kaolinite and 6-aminohexanoic acid. Next, Kao–nylon 6 was obtained by in-situ polymerization of 6-aminohexanoic acid. Kao–nylon 6 and Nylon 6 was blended at 250 °C, and Kao–nylon 6 was not exfoliated in nylon 6. Reinforcement effects of Kao–nylon 6 was higher than kaolinite, suggesting the strong interaction between Kao–nylon 6 and nylon 6 matrix. Nylon 6 blended with Kao–nylon 6 showed almost similar impact strength to NCH, in which clay nanosheets derived from smectite were dispersed into nylon 6 matrix, though the tensile strength was much lower than that of NCH.

The method described in this thesis provide the efficient rout for prepare organically modified kaolinite and by organic modification swelling behavior was added to kaolinite. On the other hand, reinforcement effects of kaolinite were improved using the intercalation reaction. I believe that the results of this thesis expand the field of kaolinite in industry.

## *CONTENTS*

<b>Chapter 1 INTRODUCTION</b>	<b>1</b>
1.1 Organic modification of inorganic layered materials	3
1.2 Inorganic layered material for organic modification	4
1.2.1 Metal phosphates and phosphonates	4
1.2.2 Layered polysilicates	9
1.2.3 Kaolinite	10
1.2.4 Layered aluminum hydroxides	12
1.3 Applications	15
1.3.1 Adsorbents	15
1.3.2 Controlling the interlayer environments	16
1.3.3 Porous materials	19
1.4 References	22
<b>Chapter 2</b>	
<b>Organic Modification of the Interlayer Surface of Kaolinite with Propanediols by Transesterification</b>	<b>25</b>
2.1 Introduction	27
2.2 Experimental	29
2.3 Results and Discussion	30
2.4 Conclusions	35
2.5 References	36

## **Chapter 3**

### **Synthesis and Characterization of Organically-Modified kaolinite with**

#### **Glycerol 47**

3.1 Introduction	49
3.2 Experimental	50
3.3 Results and Discussion	51
3.4 Conclusion	54
3.5 References	55

## **Chapter 4**

### **Swelling Behavior of Kaolinite Induced by Organic Modification 63**

4.1 Introduction	65
4.2 Experimental	66
4.3 Results and Discussion	67
4.4 Conclusion	70
4.5 References	71

## **Chapter 5**

### **Synthesis and Mechanical Properties of Kaolinite/Polymer Nanocomposites**

**83**

#### **5.1 Preparation of a Kaolinite–Nylon 6 Intercalation Compound 85**

5.1.1 Introduction	85
5.1.2 Experimental	86
5.1.2 Characterization	87
5.1.3 Results and Discussion	88
5.1.4 Conclusions	94

5.1.5 References	95
<b>5.2 Preparation of Kaolinite–Nylon6 Composites by Blending Nylon6 and a Kaolinite–Nylon6 Intercalation Compound</b>	<b>104</b>
5.2.1 Introduction	104
5.2.2 Experimental	105
5.2.3 Results and Discussion	105
5.2.4 Conclusions	106
5.2.5 References	107
<b>Chapter 6 CONCLUSION</b>	<b>111</b>
<b>List of Publications</b>	<b>117</b>



# CHAPTER 1

## INTRODUCTION



## 1.1 Organic modification of inorganic layered materials

Organically-modified inorganic layered materials, one of inorganic-organic intercalation compounds, have been researched by many authors as a polytype of pillared inorganic layered materials for the further application of absorbent, reaction media etc. Organic groups between the layers were bonded to inorganic layer, and the covalent bonds improved the stability of grafted organics and sometimes that of inorganic layer. Organic modification of inorganic layered materials improved the interlayer environment and newly generated hydrophobic interlayer environments were able to intercalate solvent molecules. In the different viewpoint, the organically modified inorganic layers materials could be recognized as the well-ordered assemblies of inorganic-organic nanohybrid sheets, because their structures were composed of inorganic nanosheets that were covered by grafted organic units (Fig. 1-1). Due to crystalline inorganic parts, they has higher ordering than other nanohybrids obtained by other methods like sol-gel method. In many cases, ordered reactive groups on the inorganic surface arranged the organic groups. These characteristics had an advantage for the material design of nanometaterials. Usually, they are obtained by simple process, such as stirring or refluxing, or coprecipitation of the mixture containing inorganic layered materials and organic species.

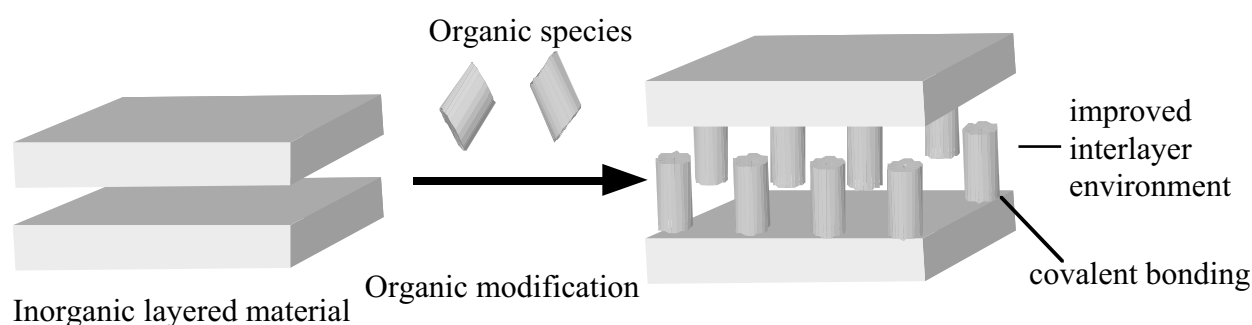


Fig. 1-1 organic modification of inorganic layered material

## 1.2 Inorganic layered material for organic modification

Various layered materials having the functional groups on their surface, such as metal phosphate, layered polysilicates, layered double hydroxides, kaolinite, boehmite were used for organic modification and various organically modified inorganic layered materials are obtained by changing the combination of inorganic layered materials and organic unit. Some combinations were known to give functions such as swelling behaviors<sup>1</sup>, selective-adsorption properties<sup>2</sup> to the materials. The basic structure of the materials depended on that of the starting inorganic layered materials, and the arrangement of organic units depended on the arrangement of reactive groups on the inorganic interlayer surface. Thus, the selection of inorganic layered materials are very important for materials design. In this section, crystal structures and features of typical inorganic layered materials for organic modification are described.

### 1.2.1 Metal phosphates and phosphonates

#### 1.2.1.1 Structure

Layered metal phosphates or phosphonates (metal = Ti, Zr, Hf, Ge, Sn, Pb, Ti etc.) are composed of octahedral and tetrahedral units. Among these layered materials, layered zirconium phosphates were most researched because of relatively high crystallinity. Main structures of layered zirconium phosphate were  $\alpha$ - and  $\gamma$ -layer structures (Fig. 1-2).  $\alpha$ -Zr(O<sub>3</sub>POH)<sub>2</sub>·H<sub>2</sub>O (also written as  $\alpha$ -Zr(HPO<sub>4</sub>)<sub>2</sub>) were composed of tetrahedral phosphate groups and each zirconium shares six oxygens with six O<sub>3</sub>POH groups (Fig. 1-2a). The basal spacing was 7.56 Å and the thickness of the layer is 0.63 Å. The distance between POH groups on one side of the interlayer surface was 5.3 Å. In  $\gamma$ -ZrPO<sub>4</sub>(H<sub>2</sub>PO<sub>4</sub>)·2H<sub>2</sub>O, zirconium atoms lie in the two different planes and were bonded by tetrahedral PO<sub>4</sub> and H<sub>2</sub>PO<sub>4</sub> groups (Fig. 1-2b). The basal spacing was 12.2

Å and the thickness of the layer is 7.41 Å. The free area of POH<sub>2</sub> group is 35.7 Å<sup>2</sup> larger than the free area of POH group in α-zirconium phosphate.

### 1.2.1.2 Organically modified metal phosphates and phosphonates

Organic modification of layered metal phosphates or phosphonates have been researched for the further application of sorbents, catalysts, and ion-exchangers by many authors<sup>3-6</sup>. VO(C<sub>6</sub>H<sub>13</sub>PO<sub>3</sub>)·H<sub>2</sub>O had a shape-selective intercalation property and adsorbed simple 1- and 2-butanol but bulky *s*- and *t*-butanol<sup>12</sup>. Zr(O<sub>3</sub>PCH<sub>2</sub>SO<sub>3</sub>H)<sub>2</sub> showed higher catalytic activity (21.8\*10<sup>-7</sup> mol g<sup>-1</sup> s<sup>-1</sup>) than hydrogen form of Nafion<sup>7</sup>. Properties of products were controlled by changing the centre metals of metal phosphates or phosphonates. For example, adsorption properties of M(O<sub>3</sub>PCH<sub>3</sub>) with amine and H<sub>2</sub>O were different by changing the centre metal atoms (M= Co, Zn, and Mg)<sup>8</sup>. Mg(O<sub>3</sub>PCH<sub>3</sub>) did not adsorb amine and absorbed H<sub>2</sub>O rapidly from air to form Mg(O<sub>3</sub>PCH<sub>3</sub>)·H<sub>2</sub>O. Whereas, Co or Zn(O<sub>3</sub>PCH<sub>3</sub>) adsorbed easily ammonia or amines and changed to Co or Zn(O<sub>3</sub>PCH<sub>3</sub>)(RNH<sub>2</sub>) (R = H to *n*-C<sub>8</sub>H<sub>17</sub>). Moreover, Zn(O<sub>3</sub>PCH<sub>3</sub>) adsorbed ethylamine and did not adsorb H<sub>2</sub>O from 70% ethylamine aqueous solution.

Because layered zirconium phosphate has a relative high crystallinity, crystal structures of zirconium phosphates fully covered by bulk organo-phosphate like phenylphosphonate<sup>9</sup>, butyl diphosphonate<sup>10</sup> were able to be refined (Fig. 1-3). The most specific feature of zirconium phosphate was that some kind of pillared layered materials, in which diphosphonate groups were bonded to each layer like a ladder, were obtained (Fig. 1-4). Some organically modified zirconium phosphates are listed in Table 1-3.

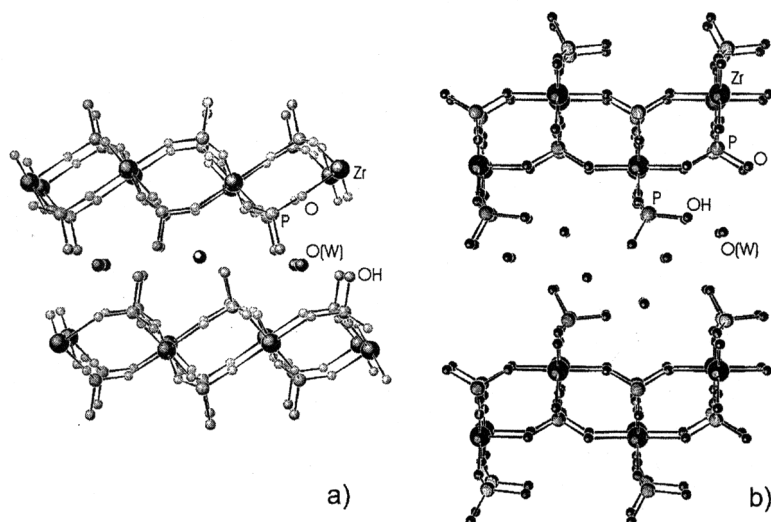


Fig.1-2 Structure of  $\alpha$ -zirconium phosphate and  $\gamma$ -zirconium phosphate<sup>3</sup>

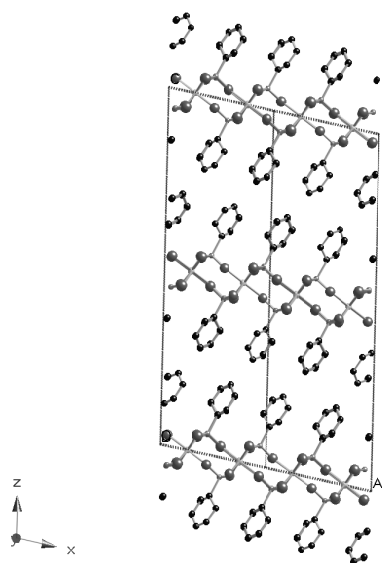


Fig. 1-3 Crystal structure of  $Zr(O_3PC_6H_5)_2$ <sup>9</sup>  
Space groups  $C_{2/c}$

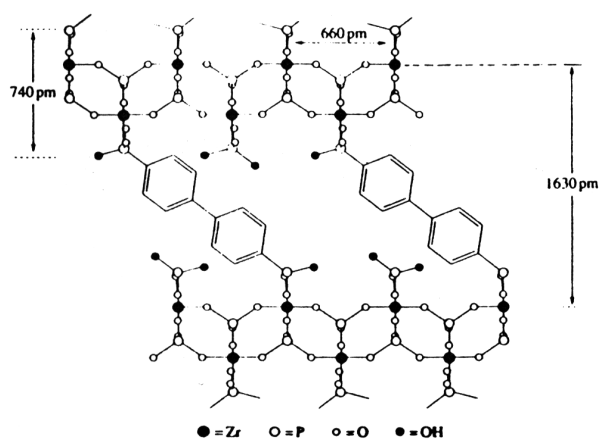


Fig. 1-4 The structure of  $Zr(PO_4)_{0.75}(HO_3PC_{12}H_8PO_3H)_{0.125}$   
(computer generated models)<sup>5</sup>

Table 1-1 Basal spacings of some zirconium bismonophosphates and organophosphates with  $\alpha$ -layered structure<sup>3</sup>

Compound	Basal spacing / Å	Compound	Basal spacing / Å
Zr(O <sub>3</sub> PH) <sub>2</sub> ·H <sub>2</sub> O	0.756	Zr(O <sub>3</sub> PCH=CH <sub>2</sub> ) <sub>2</sub>	10.6, 10.8
Zr(O <sub>3</sub> PCH <sub>3</sub> ) <sub>2</sub>	8.9	Zr(O <sub>3</sub> P(CH) <sub>2</sub> CH=CH <sub>2</sub> ) <sub>2</sub>	13.5
Zr(O <sub>3</sub> PCH <sub>2</sub> OH) <sub>2</sub> ·H <sub>2</sub> O	10.1	Zr(O <sub>3</sub> PC <sub>6</sub> H <sub>5</sub> ) <sub>2</sub>	14.7
Zr(O <sub>3</sub> P(CH <sub>2</sub> ) <sub>2</sub> Cl) <sub>2</sub>	12.3	Zr(O <sub>3</sub> PC <sub>6</sub> H <sub>11</sub> ) <sub>2</sub>	15.2
Zr(O <sub>3</sub> P(CH <sub>2</sub> ) <sub>2</sub> CN) <sub>2</sub>	11.8	Zr(O <sub>3</sub> PCH <sub>2</sub> C <sub>6</sub> H <sub>5</sub> ) <sub>2</sub>	19, 16.6
Zr(O <sub>3</sub> PC <sub>3</sub> H <sub>7</sub> ) <sub>2</sub>	14.0	Zr(O <sub>3</sub> PC <sub>2</sub> H <sub>4</sub> C <sub>5</sub> H <sub>4</sub> N)	18.6
Zr(O <sub>3</sub> PC <sub>6</sub> H <sub>13</sub> ) <sub>2</sub>	19.2	Zr(O <sub>3</sub> PCH <sub>2</sub> SO <sub>3</sub> H) <sub>2</sub>	15.4
Zr(O <sub>3</sub> PC <sub>12</sub> H <sub>25</sub> ) <sub>2</sub>	32.4	Zr(O <sub>3</sub> P(CH <sub>2</sub> ) <sub>3</sub> SO <sub>3</sub> H) <sub>2</sub>	17.3
Zr(O <sub>3</sub> PC <sub>22</sub> H <sub>45</sub> ) <sub>2</sub>	56.2	Zr[O <sub>3</sub> PO(CH <sub>2</sub> CH <sub>2</sub> O) <sub>2</sub> PO <sub>3</sub> ]	15.3
Zr(O <sub>3</sub> PC <sub>6</sub> H <sub>4</sub> NO <sub>2</sub> ) <sub>2</sub>	15.8	Zr(O <sub>3</sub> PCH <sub>2</sub> CH <sub>2</sub> NH <sub>2</sub> ) <sub>2</sub> ·HCl	14.3
Zr(O <sub>3</sub> P(CH <sub>2</sub> ) <sub>2</sub> COCl) <sub>2</sub>	13.5	Zr(O <sub>3</sub> P(C <sub>6</sub> H <sub>4</sub> ) <sub>2</sub> C <sub>6</sub> H <sub>5</sub> )	33
Zr(O <sub>3</sub> PCH <sub>2</sub> COOH) <sub>2</sub>	11.1	Zr(O <sub>3</sub> POC <sub>2</sub> H <sub>5</sub> ) <sub>2</sub>	11.7
Zr(O <sub>3</sub> P(CH <sub>2</sub> ) <sub>4</sub> COOH) <sub>2</sub>	16.7	Zr(O <sub>3</sub> POC <sub>4</sub> H <sub>9</sub> ) <sub>2</sub>	15.9
Zr(O <sub>3</sub> P(CH <sub>2</sub> ) <sub>5</sub> COOH) <sub>2</sub>	18.7	Zr(O <sub>3</sub> PO(CH <sub>2</sub> ) <sub>2</sub> CN) <sub>2</sub>	13.2

## Chapter 1

Table 1-2 Basal spacings of some derivatives of  $\alpha$ -zirconium phosphate with two different pendant groups.<sup>3</sup>

Compound	Basal spacing / Å
Zr(O <sub>3</sub> POH)(O <sub>3</sub> PC <sub>2</sub> H <sub>4</sub> COOH)·2H <sub>2</sub> O	12.9
Zr(O <sub>3</sub> POH) <sub>0.5</sub> (O <sub>3</sub> PC <sub>2</sub> H <sub>4</sub> COOH) <sub>1.5</sub> ·2H <sub>2</sub> O	13.8
Zr(O <sub>3</sub> PCH <sub>2</sub> OH) <sub>0.75</sub> (O <sub>3</sub> PC <sub>2</sub> H <sub>4</sub> COOH) <sub>1.25</sub>	13.6
Zr(O <sub>3</sub> PC <sub>2</sub> H <sub>5</sub> ) <sub>1.15</sub> (O <sub>3</sub> PC <sub>6</sub> H <sub>4</sub> SO <sub>3</sub> H) <sub>0.85</sub> ·3.7H <sub>2</sub> O	18.5
Zr(O <sub>3</sub> PC <sub>2</sub> H <sub>5</sub> ) <sub>1.03</sub> (O <sub>3</sub> PC <sub>6</sub> H <sub>4</sub> SO <sub>3</sub> H) <sub>0.97</sub> ·4.9H <sub>2</sub> O	19.6
Zr(O <sub>3</sub> PH) <sub>0.75</sub> (O <sub>3</sub> PC <sub>6</sub> H <sub>5</sub> ) <sub>1.25</sub>	15
Zr(O <sub>3</sub> POH) <sub>1.15</sub> (O <sub>3</sub> PC <sub>6</sub> H <sub>5</sub> ) <sub>0.85</sub> ·H <sub>2</sub> O*	24.8
Zr(O <sub>3</sub> POH)(O <sub>3</sub> PC <sub>6</sub> H <sub>5</sub> )*	22.5
Zr(O <sub>3</sub> PCH <sub>2</sub> OH)(O <sub>3</sub> PH)*	14
Zr(O <sub>3</sub> PC <sub>6</sub> H <sub>5</sub> ) <sub>0.7</sub> (O <sub>3</sub> PH) <sub>1.3</sub> *	21

\*:Asymmetrical layers;  $d_{001}$  is the sum of two interlayer distances.

Table 1-3 Basal spacings of some derivative compounds of  $\gamma$ -zirconium phosphate<sup>3</sup>

Compound	Basal spacing / Å
ZrPO <sub>4</sub> ·O <sub>2</sub> PHOH·2H <sub>2</sub> O	12.2
ZrPO <sub>4</sub> ·O <sub>2</sub> PH <sub>2</sub> ·H <sub>2</sub> O	8.8
ZrPO <sub>4</sub> ·O <sub>2</sub> POHCH <sub>3</sub> ·2H <sub>2</sub> O	12.8
ZrPO <sub>4</sub> ·O <sub>2</sub> POHC <sub>3</sub> H <sub>7</sub> ·1.2H <sub>2</sub> O	15.1
ZrPO <sub>4</sub> (H <sub>2</sub> PO <sub>4</sub> ) <sub>0.33</sub> (O <sub>2</sub> P(CH <sub>3</sub> ) <sub>2</sub> ) <sub>0.67</sub>	10.3
ZrPO <sub>4</sub> (H <sub>2</sub> PO <sub>4</sub> ) <sub>0.33</sub> (O <sub>2</sub> POHC <sub>6</sub> H <sub>5</sub> ) <sub>0.67</sub>	15.4
ZrPO <sub>4</sub> (H <sub>2</sub> PO <sub>4</sub> ) <sub>0.33</sub> (O <sub>2</sub> POHC <sub>6</sub> H <sub>11</sub> ) <sub>0.67</sub> ·H <sub>2</sub> O	16.9
ZrPO <sub>4</sub> ·O <sub>2</sub> PHC <sub>6</sub> H <sub>5</sub>	15.1

## 1.2.2 Layered polysilicates

### 1.2.2.1 Structure

Layered polysilicates were composed of  $\text{SiO}_4$  tetrahedral and OH and ONa groups were on the interlayer surfaces. Among very variety of layered polysilicates, magadiite ( $\text{Na}_2\text{H}_2\text{Si}_{14}\text{O}_{30}\cdot x\text{H}_2\text{O}$ ) were mainly used for organic modification (Table 1-4). Because of low crystal size, crystal structure of magadiite was not reported.

### 1.2.2.2 Organically modified layered polysilicates

Since organic modification of layered polysilicic acids and polysilicates was first reported by Ruiz-Hitzky *et al.*<sup>11</sup>, organically modified layered polysilicic acid and polysilicate have attracted many authors for the further application of absorbent<sup>1, 12-28</sup>. The various organically modified polysilicic acids and polysilicates were easily synthesized by changing the silylating agents, such as trimethylsilane<sup>11, 12, 14</sup>, diphenylmethylchlorosilane<sup>13</sup>. Several alcohols were also allowed to be grafted onto the interlayer surface of magadiite<sup>1</sup>. [2-(perfluorohexyl)ethyl]dimethoxychlorosilane-modified magadiite had a film-forming ability after swelling into (perfluorohexyl)ethanol<sup>23</sup>. Due to the variation of layered polysilicate, the thickness of an inorganic layer and the density of reactive silanol groups could be controlled. The inorganic layered material-polymer nanohybrid, containing the covalent bond between polymer chain and inorganic nanosheet, were also obtained by the intercalative polymerization of methylmethacrylate between the layers of  $\gamma$ -Methacryloxypropylsilane-modified magadiite<sup>25</sup>

## Chapter 1

Table 1-4 Basal spacing of organic derivatives of layered polysilicates, magadiite

Organic species	basal spacing / nm	Organic species	basal spacing / nm
$(\text{CH}_3)_3\text{SiCl}^{11, 14}$	1.94, 1.86	$(\text{C}_3\text{H}_7)_3\text{SiCl}^{24}$	2.08
$[(\text{CH}_3)_3\text{Si}]\text{NH}_2^{12}$	1.92	$(\text{C}_4\text{H}_9)(\text{CH}_3)_2\text{SiCl}^{24}$	1.95
$[(\text{CH}_3\text{CH}_2)_3\text{Si}]_2\text{NH}^{12}$	1.95	$(\text{C}_8\text{H}_{17})(\text{CH}_3)_2\text{SiCl}^{24}$	2.33
$\text{ClCH}_2(\text{CH}_3)_2\text{SiCl}^{12}$	1.99	$(\text{C}_{18}\text{H}_{37})(\text{CH}_3)_2\text{SiCl}^{24}$	3.25
$(\text{CH}_3)_2(\text{C}_6\text{H}_5)\text{SiCl}^{12}$	1.62	$\text{CH}_3(\text{CH}_2=)\text{CC}(=\text{O})\text{O}(\text{CH}_2)_3\text{Si}(\text{OCH}_3)_3^{25}$	2.15
$(\text{C}_6\text{H}_5)_3\text{SiCl}^{12}$	1.48	$\text{CH}_3\text{OH}^{29}$	1.35
$(\text{C}_6\text{H}_5)_2\text{CH}_3\text{SiCl}^{13}$	2.46	$\text{CH}_3\text{CH}_2\text{OH}^{29}$	1.39
$\text{CH}_2=\text{CHCH}_2(\text{CH}_3)_2\text{SiCl}^{16}$	1.79	$\text{CH}_3(\text{CH}_2)_3\text{OH}^{29}$	1.40
$\text{C}_6\text{H}_5\text{SiCl}_3^{15}$		$\text{CH}_3(\text{CH}_2)_4\text{OH}^{29}$	1.38
$\text{C}_6\text{H}_{11}\text{Si}_3\text{Cl}_3^{15}$		$\text{CH}_3(\text{CH}_2)_5\text{OH}^{29}$	1.37
Ethylene glycol <sup>20</sup>		$\text{CH}_3(\text{CH}_2)_7\text{OH}^{29}$	1.39
$\text{C}_8\text{H}_{17}\text{SiCl}_3^{22}$	2.18	$\text{CH}_3(\text{CH}_2)_8\text{OH}^{29}$	1.37
$\text{C}_8\text{H}_{17}\text{Si}(\text{CH}_3)_2\text{Cl}^{22}$	2.23	$\text{CH}_3(\text{CH}_2)_{13}\text{OH}^{29}$	1.38
$\text{C}_6\text{F}_{13}\text{C}_2\text{H}_4(\text{CH}_3)_2\text{SiCl}^{23}$	2.83	$\text{CH}_3(\text{CH}_2)_{15}\text{OH}^{29}$	1.38
$(\text{C}_2\text{H}_5)_3\text{SiCl}^{24}$	1.98	$(\text{CH}_3)_3\text{OH}^{29}$	1.55

### 1.2.3 Kaolinite

#### 1.2.3.1 Structure

Kaolinite ( $\text{Al}_2\text{Si}_2\text{O}_5(\text{OH})_4$ ) was composed of pairs of  $\text{AlO}_4(\text{OH})_2$  octahedral and  $\text{SiO}_4$  tetrahedral sheets and had an asymmetric interlayer environment sandwiched by two distinct sheets (Fig. 1-5 above). Because of this specific structure, some small polar intercalated guest molecules were arranged in three dimensions<sup>30</sup>, and organic-modification of kaolinite, quite

different from that of other inorganic layered materials, only took place at  $\text{AlO}_4(\text{OH})_2$  octahedral sheet side. That is to say, a synthesis of organically modified kaolinite was a generation of asymmetric interlayer environment.

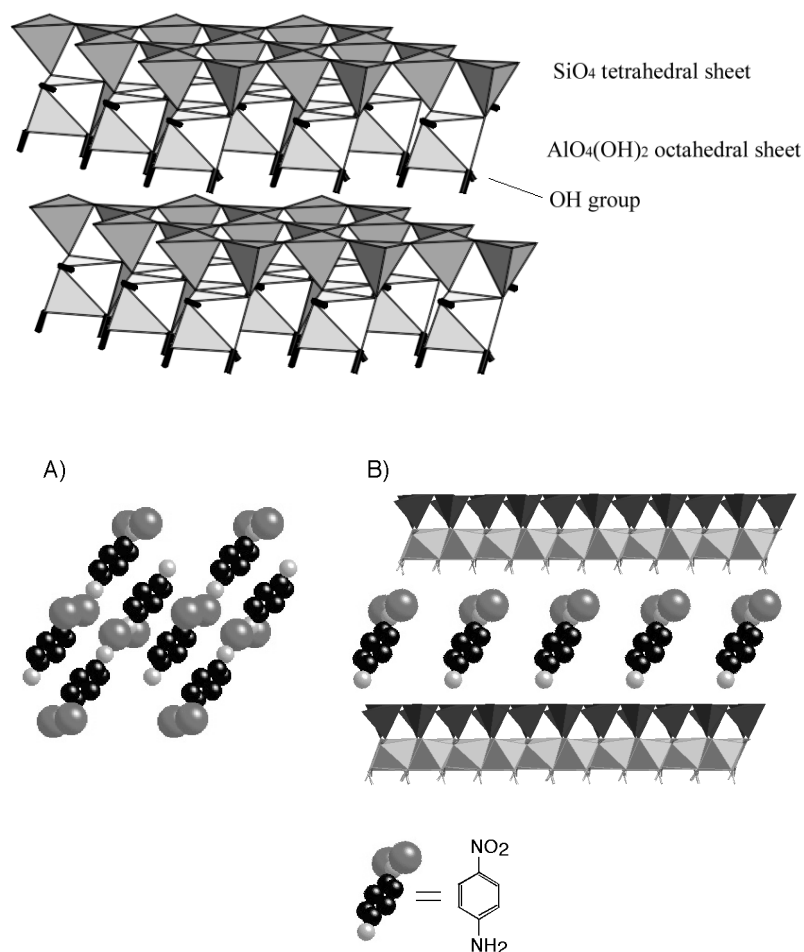


Fig.1-5 (above) structure of kaolinite and (below) illustration of *p*-nitroaniline in crysal (A) and between the layers of kaolinite

### 1.2.3.2 Organically modified kaolinite

There are several reports about the organic-modifications of kaolinite by refluxing with various alcohols; methanol<sup>31</sup>, ethylene glycol<sup>32,33</sup>, propanediol<sup>32</sup>, aminoethanol<sup>34</sup>, ethylene glycol

## Chapter 1

monomethyl ether<sup>32</sup>, diethyleneglycol monobutyl ether<sup>32</sup>. These reports mainly relied on the existence of exothermal peaks with mass loss in thermal analyses for evidence of organic modification. Komori *et al.* reported organic-modification of kaolinite with methanol proceed at room temperature and revealed the existence of Al-OCH<sub>3</sub> by NMR spectroscopy<sup>35</sup>. Methanol-modified kaolinite was a versatile intermediate with high reactivity for further intercalation and was able to incorporate guest like polymer that could not intercalate with conventional guest displacement methods<sup>29,36,37</sup>. A kaolinite-*p*-nitroaniline intercalation compound using methanol-modified kaolinite as an intermediate showed SHG properties<sup>38</sup>, in which *p*-nitroaniline was ordered without symmetric centre (Fig. 1-5 below). Methoxy group on the surface was exchangeable with other alcohol<sup>39,40</sup>. Thus, methanol-modified kaolinite was available as a versatile intermediate for further organic modification of kaolinite. However, organic modification of kaolinite did not proceed completely, at most one OH groups per Al<sub>2</sub>Si<sub>2</sub>O<sub>5</sub>(OH)<sub>4</sub> were reacted<sup>31</sup>.

### 1.2.4 Layered aluminum hydroxides

#### 1.2.4.1 Structure

Layered aluminum hydroxides such as gibbsite (Al(OH)<sub>3</sub>), boehmite (AlOOH) were composed of octahedral units. The basic structure of organically modified layered aluminum hydroxides is boehmite with lepidocrocite type structure, in which all octahedral groups are jointing by sharing the edge (Fig. 1-6). The bonding force between layers of boehmite is hydrogen bond and boehmite did not intercalate.

#### 1.2.4.1 Organically modified boemite

Inoue *et al.* reported the synthesis of alcohol-modified boemite (AlOOH) by the two routes. One route was autoclaving the gibbsite into alcohol (HO(CH<sub>2</sub>CH<sub>2</sub>)<sub>n</sub>OH, H(OCH<sub>2</sub>CH<sub>2</sub>)<sub>n</sub>OH (n =

1-3), glycerol etc.) at high pressure and the other route was hydrolysis of the aluminum alcoxides in alcohol.

In the first route, the structure of aluminum hydroxides was converted from gibbsite ( $\text{Al}(\text{OH})_3$ ; starting material) to boehmite ( $\text{AlOOH}$ )<sup>41-44</sup> during the organic modification. In this reaction, controlling of starting particle size was very important, and pure organically modified boehmite phase was obtained when the particle size of gibbsite was under 0.2  $\mu\text{m}$ <sup>44</sup>. This reaction was elucidated as the dissolution-crystallization mechanism because morphology of aluminum hydroxides was changed during the reaction. In case of adding 15-25 vol%  $\text{H}_2\text{O}$  to alcohol, organically modified boehmite having the second stage structure was obtained<sup>41</sup> (Fig. 1-7). The role of  $\text{H}_2\text{O}$  was explained as follows. The formation of Al-OR bond was described as the equilibrium;  $\text{AlOH} + \text{ROH} \leftrightarrow \text{AlOR} + \text{H}_2\text{O}$ . The coexistence of  $\text{H}_2\text{O}$  shifted the equilibrium to left hand and increased alkoxy/hydroxy ratio of the product.

The other route was the reaction between aluminum isopropoxide and various alcohols ( $\text{CH}_3\text{C}_n\text{H}_{2n}\text{OH}$  ( $n=0-11$ ), glycols, 3-methyl-1-butanol) at 300  $^\circ\text{C}$ <sup>45,46</sup>. XRD result revealed the inorganic framework of product was a boehmite structure. The experimental formula was  $\text{AlO}(\text{OH})_{(1-x)}(\text{OR})_x$  ( $X = 0.61-0.21$ ;  $x$  depended on the alcohol). The hydrolysis of aluminum isopropoxide proceeded with the help of  $\text{H}_2\text{O}$  that was supplied by the thermal decomposition of

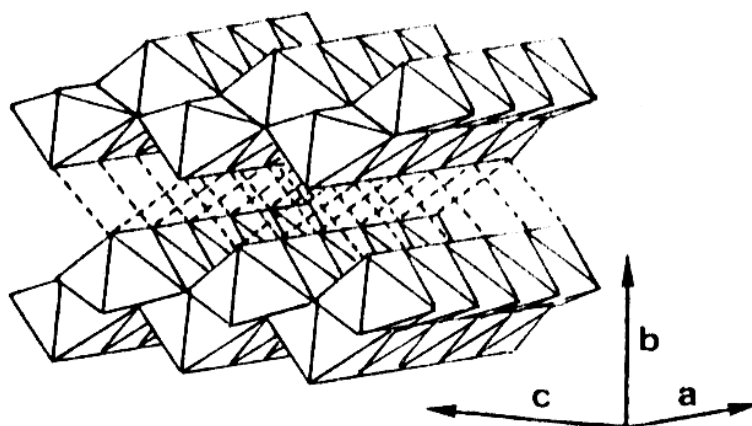


Fig. 1-6 Structure of boehmite<sup>43</sup>

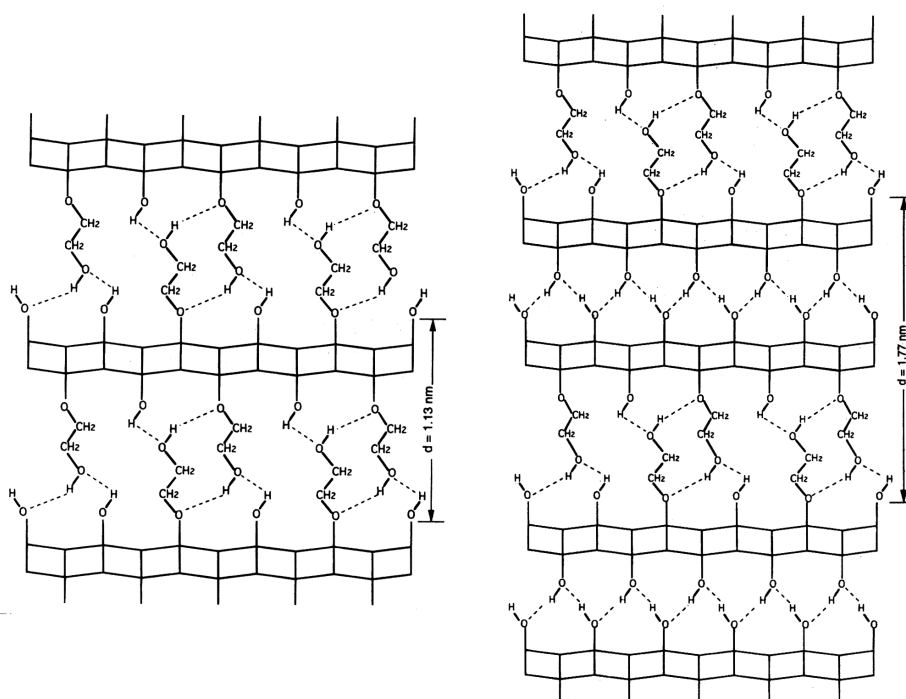


Fig. 1-7 Illustration of organically modified boehmite with first stage (left) and with second stage (right)<sup>41</sup>

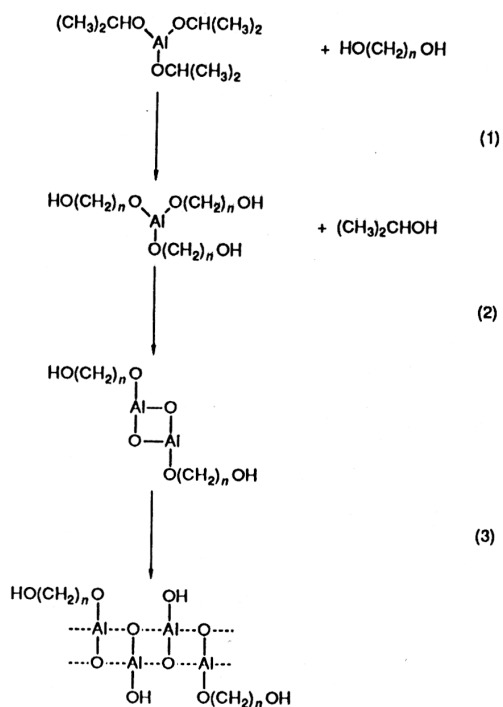


Fig. 1-8 Formation of organically modified boehmite from aluminum isopropoxide<sup>46</sup>

alcohol and/or that may be in alcohols (Fig. 1-8). This was the very important method to obtain the organically modified inorganic layered material with the crystalline inorganic framework using the metal alkoxides.

## 1.3 Applications

### 1.3.1 Adsorbents

There were some reports about organically modified zirconium phosphates, which had various basal spacings and pore sizes by adsorption and desorption of polar molecules. Such “accordion-like movement” was sometimes able to be controlled by chemical process (i.e. pH control). Alberti *et al.* synthesized alkyldisulfuric acid-modified  $\gamma$ -zirconium phosphate with various percentage of pillaring ( $\text{ZrPO}_4[\text{O}_2\text{P}(\text{OH})_2]_{1-x}(\text{O}_2\text{POH}-(\text{CH}_2)_n-\text{HOPO}_2)_{x/2} \cdot m\text{H}_2\text{O}$  ( $n=4, 6, 8, 10, 12, 16$ ))<sup>47</sup>. Alkyldisulfuric acid between the layers was grafted on each layer. At the high percentage of pillaring ( $\geq 60$ ), the basal spacing increased with the alkyl chain length, and alkyl chain between the layers inclined with  $52.7^\circ$  and packed. At the low percentage of pillaring, the basal spacing depended on the amount of  $\text{H}_2\text{O}$ . In the hydrated sample, the basal spacing was independent from the percentage of pillaring and was fixed on the same basal spacing of fully modified sample because the gallery between the pillars was filled with  $\text{H}_2\text{O}$ . In the dried sample, the basal spacing decreased with the alkyl chain length because alkyl chain was not able to maintain the extended conformation. Then, the basal spacing was independent from the percentage of pillaring and was fixed. Alberti *et al.* also reported the synthesis of polyethylene oxide-modified  $\gamma$ -zirconium phosphate ( $\text{ZrPO}_4[\text{O}_2\text{P}(\text{OH})_2]_{0.76}(\text{O}_2\text{POH-R-HOPO}_2)_{0.12} \cdot n\text{H}_2\text{O}$  ( $\text{R}=\text{diethylene glycol or pentaethylene glycol}$ ) and investigated the pH dependency about the adsorption properties<sup>48</sup>. In spite that the interlayer environment was more hydrophilic than that of alkyldisulfuric acid-modified  $\gamma$ -zirconium phosphate, the sample did not hydrate fully until

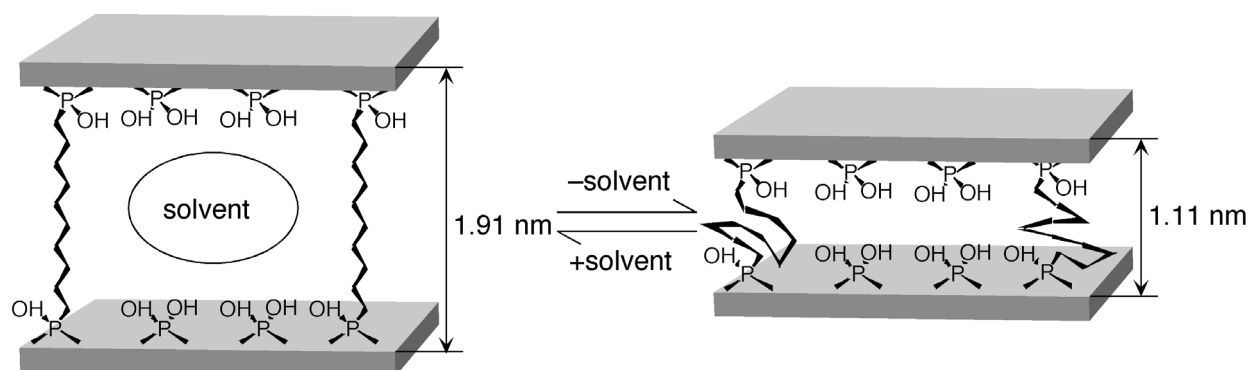


Fig. 1-9 illustration of “accordion-like movement” for 1,10-decanediphosphonate-modified  $\gamma$ -ZrP

polyethylene oxide chain took the extended conformation (from 13.2 Å to 15.7 Å; in case of R = diethylene glycol). This was explained by high affinity of polyethylene oxide to the layer. On the contrary, methylamine was easily adsorbed and the basal spacing of the sample increased to 21.6 Å (R = diethylene glycol). When swelled sample was dispersed into HCl aq. sol. (pH = 2.5), methylamine between the layers was deintercalated and the basal spacing was back to 15.7 Å.

### 1.3.2 Controlling the interlayer environments

Recently, Okutomo *et al.* reported the alcohol absorption of organically modified magadiite<sup>22,24</sup>. This organically modified magadiite was synthesized by reacting octylchlorosilane and dodecyltrimethylammonium-magadiite and washing the product with an acetone/water mixture. In the <sup>29</sup>Si NMR spectrum of the sample, the broad signal at -55.0 ppm, showing T<sup>2</sup> and/or T<sup>1</sup> environments of silicone, was observed, and the signal assigned to T<sup>3</sup> environment was not observed. This means that an intercalated organotricholasilane was bonded to silicate sheets with one or two Si-O-Si bonds, and unreacted Si-Cl groups changed to Si-OH groups. Newly generated Si-OH groups were nearby the interlayer surface of magadiite, and the product had unique interlayer environment that was mainly hydrophobic but over interlayer surface was

hydrophilic. This characteristic interlayer environment produced an alcohol adsorption (Fig. 1-10). In case of magadiite modified by organomonochlorosilane, such behavior was not observed. The absorption model of octyltrichlorosilane-modified magadiite by 1-hexanol and 1-butanol, and the amount of absorbed alcohol was discussed by Fujita *et al.*<sup>7</sup>. Moreover, the amount of organic affected the alcohol adsorption. This method for designing the interlayer environment was useful of the design of absorbent and has a potential for that of selective absorbent.

The crystal structure of magadiite, which is one of the most researched polysilicates in an organic modification, was not reported because of its small particle size. In the concern of material design, this was a weak point. Shimojima *et al.* reported the synthesis of organically modified kanemite with mono-, di-, trichloroalkylsilanes and showed the possibility of the controlling the polysilicate structure by revealing the bonding manner between organosilicon and kanemite (Fig. 1-11)<sup>26</sup>. Kanemite was one of the simplest types of layered polysilicates and the silicate frameworks were composed of only six-membered rings. By the organic-modification of di- or trichloroalkylsilanes, new silicate frameworks with five- and six- members rings were formed. Reactive Si-OH groups of kanemite were uniform. Thus, bonding manners between organosilicon and kanemite was restricted to several types. These attempts of designing of interlayer environments and inorganic framework were different form the conventional pillared layered materials and further development was expected. Mochizuki *et al.* focused on the structural feature of octosilicate and reported organic modified octosilicate with unique bonding manners (Fig. 1-12). The layer structure of octosilicate ( $\text{Na}_8[\text{Si}_{32}\text{O}_{64}(\text{OH})_8 \cdot 32\text{H}_2\text{O}]$ ) is composed of five-membered ring and the distance between reactive Si-OH and/or Si-O<sup>-</sup> groups on the *a* direction were different form that on the *b* direction. Thus,  $(\text{C}_n\text{H}_{n+1}\text{O})_2\text{SiCl}_2$  were grafted onto octosilicate with unique <sup>29</sup>Si environment of T<sup>2</sup>. Grafted dialkoxy group has a potential for generating new Si-OH groups by hydrolysis, and this method showed the opportunity for the design the silicate frameworks.

Chapter 1

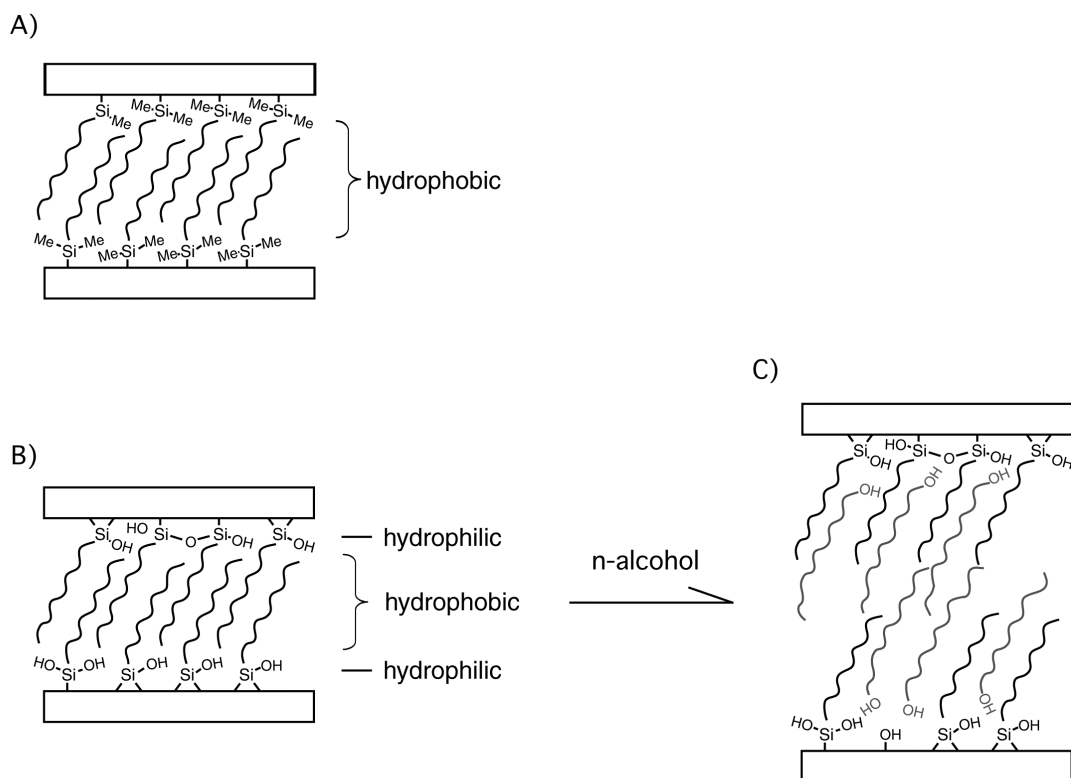


Fig. 1-10 Organically modified magadiites (a) with octyldimethylchlorosilane and (b) with octyltrichlorosilane, and alcohol adsorption of b.

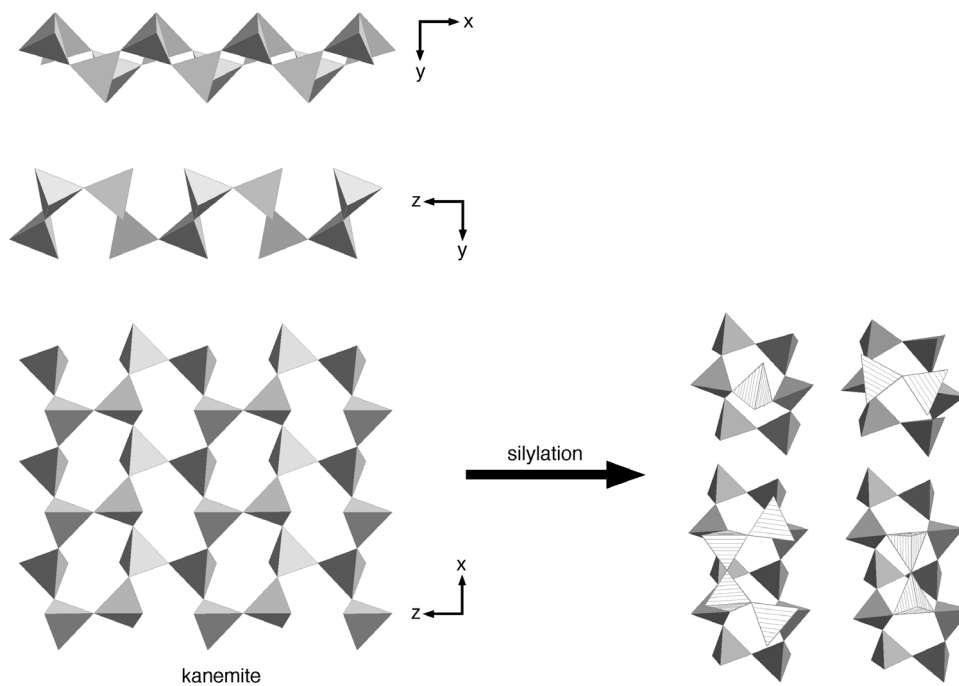


Fig. 1-11 Generation of new silicate framework

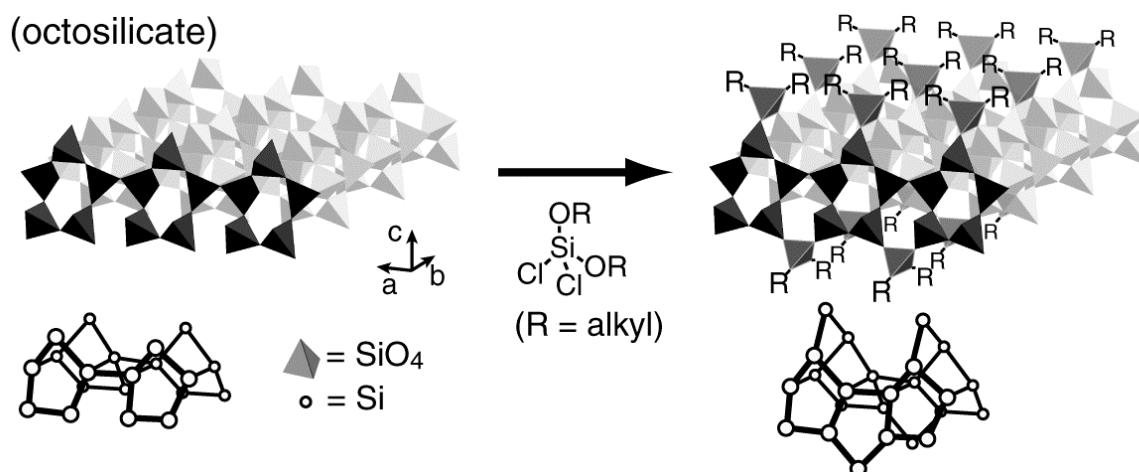


Fig. 1-12 Silylation of octosilicate

### 1.3.3 Porous materials

$\alpha$ -Zirconium phosphate possessed exchangeable  $\text{O}_3\text{PH}$  groups per  $24 \text{ \AA}^2$  on the surface. In a word,  $\text{O}_3\text{PH}$  groups were at regular intervals of  $5.3 \text{ \AA}$ . That is the reason why that cross section of organo-phosphate need be less than  $5.3 \text{ \AA}$  for complete organic modification. Alberti *et al.* focused on this structural feature and synthesized organically modified  $\alpha$ -zirconium phosphate with uniform pore size by using dumbbell-shaped diphosphate. In this material, surface was closely covered by organics and uniform pore was generated between the layers (Fig. 1-13 and 1-14A). When 4,4'-(3,3', 5,5'-tetramethyl)biphenyl diphosphonic acid was used, uniform pore with  $5 \text{ \AA}$  was created<sup>49,50</sup>. As mentioned above,  $\alpha$ -zirconium phosphate was suitable for the ordered and uniform organic modification. However, it was unsuitable for partial organic modification because organically modified  $\alpha$ -zirconium phosphates were directly synthesized from organic phosphoric acid and zirconium fluoro complexes.

On the contrary, organic modification of  $\gamma$ -zirconium phosphate proceeded by the topochemical reaction between  $\gamma$ -zirconium phosphate and organic phosphoric acid, and it was possible to control the organic amount of organically modified  $\gamma$ -zirconium phosphate by reacting

## Chapter 1

under the adequate synthesis condition. The product in the reaction between  $\text{ZrPO}_4(\text{H}_2\text{PO}_4)$  and  $\text{C}_{12}\text{H}_8(\text{PO}_2\text{OH})_2$  was single phase with the pillaring percentage over 1/4, and segregated phase with lower pillaring percentage. The sample with the pillaring percentage of 1/4 had uniform micropores with average diameter of  $5.8 \text{ \AA}$ <sup>51</sup> (Fig. 1-14b). These organically modified zirconium phosphates utilized the gallery between the ordered pillars as micropores, and sometimes possessed the mesopores. Alberti *et al.* reported that  $\text{Zr}(\text{O}_3\text{PH})_x(\text{O}_3\text{P-C}_6\text{H}_4\text{PO}_3)_y$  has mesopores with surface area of  $230\text{-}400 \text{ m}^2\text{g}^{-1}$  of the pore size  $4\text{-}14 \text{ nm}$ . Zhang *et al.* also reported  $\text{Zn}_2(\text{O}_3\text{PC}_{12}\text{H}_8\text{PO}_3)_{0.75}(\text{HPO}_4)_{0.5}\cdot 2.5\text{H}_2\text{O}$  with mesopores<sup>52</sup>. These phenomenon explained due to the card house structure<sup>52, 53</sup>(Fig. 1-15).

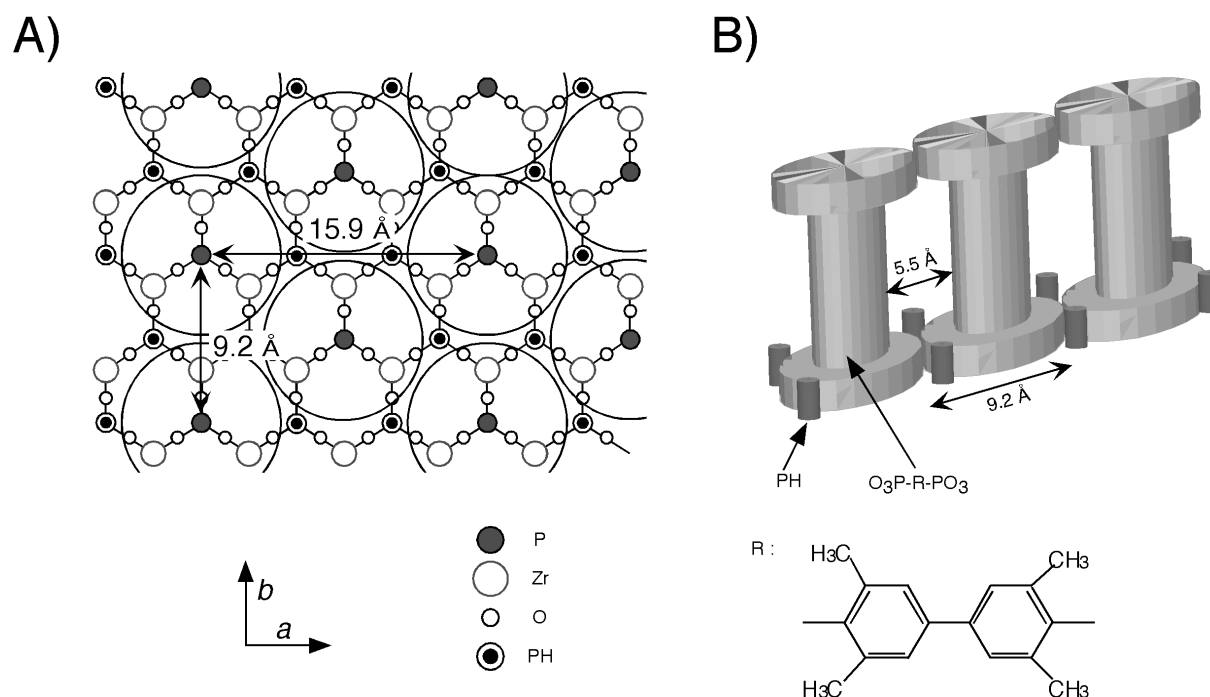


Fig. 1-13 ideal arrangement of large phosphite groups on the surface of  $\alpha\text{-ZrP}$  (A) and in case of large phosphite groups were dumbbell-like structure (B)<sup>4</sup>

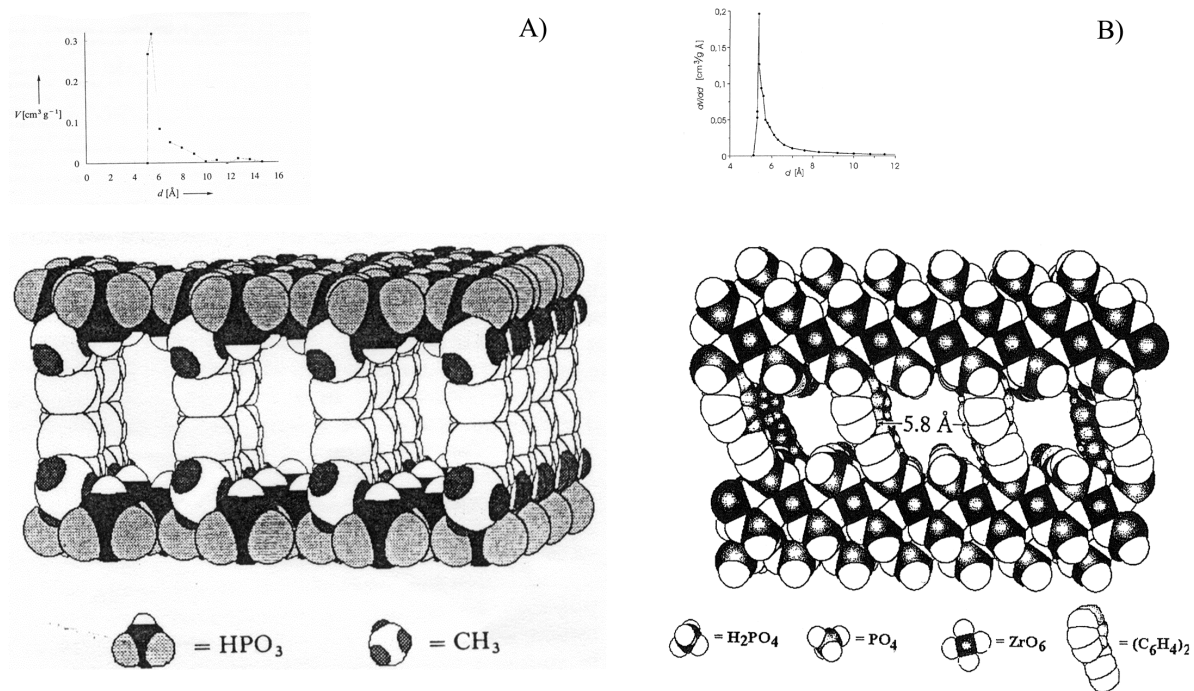


Fig. 1-14 illustration and pore size distribution of organically modified zirconium phosphate with unique pore size of a)  $\alpha$ -layer structure and b)  $\gamma$ -layer structure

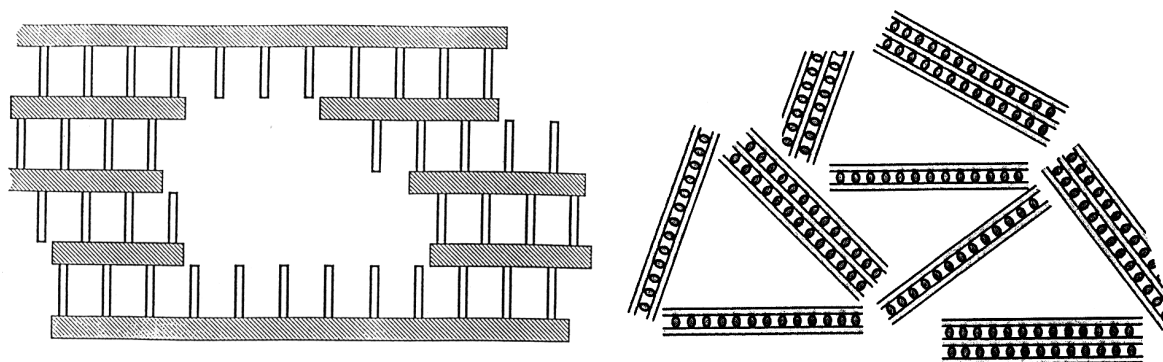


Fig. 1-15 conceptual model of mesopore formation (left: Clearfield<sup>5</sup> and right: Alberti<sup>54</sup>)

## 1.4 References

- 1 Y. Mitamura, Y. Komori, S. Hayashi, Y. Sugahara and K. Kuroda, *Chem. Mater.*, 2001, **13**, 3747.
- 2 J. W. Johnson, A. J. Jacobson, W. M. Butler, S. E. Rosenthal, J. F. Brody and J. T. Lewandowski, *J. Am. Chem. Soc.*, 1989, **111**, 381.
- 3 G. Alberti, M. Casciola, U. Constantino and R. Vivani, *Adv. Mater.*, 1996, **8**, 291.
- 4 G. Alberti, R. Vivani, F. Marmottini and P. Zappelli, *J. Porous. Mater.*, 1998, **5**, 205.
- 5 A. Clearfield, *Chem. Mater.*, 1998, **10**, 2801.
- 6 A. Clearfield, C. V. K. Sharma and B. P. Zhang, *Chem. Mater.*, 2001, **13**, 3099.
- 7 K. Segawa, N. Kihara and H. Yamamoto, *J. Mol. Catal.*, 1992, **74**, 213.
- 8 G. Cao and T. E. Mallouk, *Inorg. Chem.*, 1991, **30**, 1434.
- 9 M. D. Poojary, H.-L. Hu, F. L. Campbell III and A. Clearfield, *Acta Cryst.*, 1993, **B49**, 996.
- 10 G. Alberti, G. M. Lombardo, G. C. Pappalardo and R. Vivani, *Chem. Mater.*, 2002, **14**, 295.
- 11 E. Ruiz-Hitzky and J. M. Rojo, *Nature*, 1980, **287**, 28.
- 12 E. Ruiz-Hitzky, J. M. Rojo and G. Lagaly, *Colloid Polym. Sci.*, 1985, **263**, 1025.
- 13 T. Yanagisawa, K. Kuroda and C. Kato, *Bull. Chem. Soc. Jpn.*, 1988, **61**, 3743.
- 14 T. Yanagisawa, K. Kuroda and C. Kato, *React. Solid*, 1988, **5**, 167.
- 15 R. Sprung, M. E. Davis, J. S. Kauffman and C. Dybowski, *Ind. Eng. Chem. Res.*, 1990, **29**, 213.
- 16 T. Yanagisawa, M. Harayama, K. Kuroda and C. Kato, *Solid State Ionics*, 1990, **42**, 15.
- 17 T. Yanagisawa, K. Kuroda, A. Doi and C. Kato, *Clay Sci.*, 1991, **8**, 107.
- 18 J. S. Dailey and T. J. Pinnavaia, *Chem. Mater.*, 1992, **4**, 855.
- 19 K. Endo, Y. Sugahara and K. Kuroda, *Bull. Chem. Soc. Jpn.*, 1994, **67**, 3352.
- 20 L. Mercier, G. A. Facey and C. Detellier, *J. Chem. Soc., Chem. Commun.*, 1994, 2111.
- 21 S.-Y. Jeong, O.-Y. Kwon, J.-K. Suh, H. Jin and J. M. Lee, *J. Colloid Interface. Sci.*, 1995,

- 175, 253.
- 22 M. Ogawa, S. Okutomo and K. Kuroda, *J. Am. Chem. Soc.*, 1998, **120**, 7361.
- 23 M. Ogawa, M. Miyoshi and K. Kuroda, *Chem. Mater.*, 1998, **10**, 3787.
- 24 S. Okutomo, K. Kuroda and M. Ogawa, *Appl. Clay Sci.*, 1999, **15**, 253.
- 25 K. Isoda and K. kuroda, *Chem. Mater.*, 2000, **12**, 1702.
- 26 A. Shimojima, D. Mochizuki and K. Kuroda, *Chem. Mater.*, 2001, **13**, 3603.
- 28 I. Fujita and K. Kuroda, *Chem. Mater.*, in press.
- 29 A. Matsumura, Y. Komori, T. Itagaki, Y. Sugahara and K. Kuroda, *Bul. Chem. Soc. Jpn.*, 2001, **74**, 1153.
- 30 J. G. Thompson, N. Gabbitas and P. J. R. Uwins, *Clays Clay Miner*, 1993, **41**, 73.
- 31 J. J. Tunney and C. Detellier, *J. Mater. Chem.*, 1996, **6**, 1679.
- 32 J. J. Tunney and C. Detellier, *Chem. Mater.*, 1993, **5**, 747.
- 33 J. J. Tunney and C. Detellier, *Clays Clay Miner*, 1994, **42**, 552.
- 34 J. J. Tunney and C. Detellier, *Can. J. Chem.*, 1997, **75**, 1766.
- 35 Y. Komori, H. Enoto, R. Takenawa, S. Hayashi, Y. Sugahara and K. Kuroda, *Langmuir*, 2000, **16**, 5506.
- 36 Y. Komori, Y. Sugahara and K. Kuroda, *J. Mater. Res.*, 1998, **13**, 930.
- 37 Y. Komori, Y. Sugahara and K. Kuroda, *Chem. Mater.*, 1999, **11**, 3.
- 38 R. Takenawa, Y. Komori, S. Hayashi, J. Kawamata and K. Kuroda, *Chem. Mater.*, 2001, **13**, 3741.
- 39 T. Itagaki and K. Kuroda, *J. Mater. Chem.* in press. (See Chapter 2)
- 40 See Chapter 3
- 41 M. Inoue, H. Kominami, Y. Kondo and T. Inui, *Chem. Mater.*, 1997, **9**, 1614.
- 42 M. Inoue, H. Tanino, Y. Kondo and T. Inui, *Clays Clay Miner*, 1991, **39**, 151.
- 43 M. Inoue, Y. Kondo and T. Inui, *Inorg. Chem.*, 1988, **27**, 215.
- 44 M. Inoue, Y. Kondo and T. Inui, *Chem. Lett.*, 1986, 1421.

## Chapter 1

- 45 M. Inoue, M. Kimura and T. Inui, *Chem. Mater.*, 2000, **12**, 55.
- 46 M. Inoue, H. Kominami and T. Inui, *J. Chem.Sco. Dalton Trans.*, 1991, 3331.
- 47 G. Alberti, S. Murcia-Mascarós and R. Vivani, *J. Am. Chem. Soc.*, 1998, **120**, 9291.
- 48 G. Alberti, E. Brunet, C. Dionigi, O. Juanes, M. J. de la Mata, J. C. Rodríguez-Ubis and R. Vivani, *Angew. Chem. Int. Ed. Engl.*, 1999, **38**, 3351.
- 49 G. Alberti, U. Constantino, F. Marmottini, R. Vivani and P. Zappelli, *Angew. Chem. Int. Ed. Engl.*, 1993, **32**, 1357.
- 50 G. Alberti, U. Constantino, F. Marmottini, R. Vivani and P. Zappelli, *Miropo. Mesopo.*, 1998, **21**, 297.
- 51 G. Alberti, F. Marmottini, S. Murcia-Mascarós and R. Vivani, *Angew. Chem. Int. Ed. Engl.*, 1994, **33**, 1594.
- 52 B. Zhang, D. M. Poojary and A. Clearfield, *Inorg. Chem.*, 1998, **37**, 1844.
- 53 G. Alberti, F. Marmottini and R. Vivani, *J. Porous. Mater.*, 1998, **5**, 221.
- 54 G. Alberti, M. Casciola, F. Marmottini and R. Vivani, *J. Porous. Mater.*, 1999, **6**, 299.

## CHAPTER 2

Organic Modification of the Interlayer Surface of Kaolinite with  
Propanediols by Transesterification



## 2.1 Introduction

Organically-modified inorganic layered materials, composed of inorganic layers linked directly with organic groups, are typical of inorganic-organic nanohybrids and have attracted many researchers for a couple of decades. This type of organic-inorganic nanohybrids inherently contain two-dimensional crystalline inorganic layers and their properties mainly depend on the nature of organic groups and/or synergistic effects of inorganic and organic components, which is advantageous to materials design.

There have been many reports on organic grafting of inorganic layered materials. Layered zirconium phosphates,<sup>1-3</sup> zirconium phosphonates,<sup>4-7</sup> layered polysilicates,<sup>8-12</sup> boehmites,<sup>13-16</sup> etc.<sup>17-19</sup> have been modified in various ways.  $\text{VO}(\text{O}_3\text{PC}_6\text{H}_{13})\cdot\text{H}_2\text{O}$  has a shape-selective intercalation property for alcohols.<sup>20</sup>  $\text{Zr}(\text{O}_3\text{PCH}_2\text{SO}_3\text{H})_2$  has a high catalytic activity.<sup>21</sup> Silylation of a layered polysilicate magadiite with different degree of silylation and variable organic groups generates unusual interlayer environments for alcohol adsorption.<sup>11,22</sup> Alberti *et al.* reported the synthesis of organically-modified zirconium phosphate with uniform pore size by controlling the ordering of organic units.<sup>23,24</sup> We reported that different kinds of layered polysilicates provide distinctive interlayer environments after silylation.<sup>8,9</sup>

Kaolinite, a typical 1:1 type clay mineral, was used in this work as an inorganic layered material because of its structural uniqueness. Kaolinite is composed of aluminosilicate layers which have two kinds of interlayer surfaces, i.e., oxygen surfaces of  $\text{SiO}_4$  tetrahedral sheets and hydroxy surfaces of  $\text{AlO}_4(\text{OH})_2$  octahedral sheets. Owing to this characteristic structure, kaolinite is a unique layered material with an asymmetric interlayer space which induces specific orientations of guest species.<sup>25-27</sup>

Because the interlayer surface grafting of kaolinite with organic substances can occur only on the side of  $\text{AlO}_4(\text{OH})_2$  sheets, organically-modified kaolinites afford very unique asymmetric environments where only one side is covered by organic groups, which is in clear

## Chapter 2

contrast to all other inorganic layered systems. Therefore, it is quite attractive to design the asymmetric environments toward future potential applications such as selective adsorption, regioselective reactions, and molecular recognition. Komori *et al.* have already reported the synthesis of methoxy-modified kaolinite in which some OH groups in the interlayer surface were displaced by methoxy groups and its versatility as an intermediate for further intercalation of poly(vinylpyrrolidone) and alkylamines.<sup>28-30</sup>

Alkanediols are excellent grafting reagents for creating new interlayer environments because organohydroxy groups are arrayed in one side only. Among a wide variety of diols, propanediols were used in this study because they have simple 1,2-dihydroxy and 1,3-dihydroxy isomers. In addition, propanediols can bond to kaolinite possibly by two different manners; that is, only one OH group out of two in the molecule can bond to the layers and/or both of the OH groups can be linked to the surfaces. The difference is very interesting for the control of the interlayer environment. Though the preparation of kaolinites modified with propanediols was mentioned by using a kaolinite-dimethylsulfoxide (DMSO) intercalation compound as the intermediate,<sup>31</sup> the products have not been fully characterized.

Here I report the synthesis of kaolinites modified with propanediols by using methoxy-modified kaolinite as an intermediate because the interlayer surfaces can be modified more efficiently through transesterification reaction rather than by simple guest displacement. The usual intermediates used for guest displacement reactions of kaolinite are kaolinite-*N*-methylformamide (NMF) and -DMSO intercalation compounds. Detellier *et al.* reported intercalation and grafting of some alcohols including methanol,<sup>32</sup> ethylene glycol monomethyl ether,<sup>31</sup> diethylene glycol monobutyl ether,<sup>31</sup> aminoethanol,<sup>33</sup> and ethylene glycol<sup>31, 34</sup> by using these intermediates. However, kaolinite–NMF and DMSO intercalation compounds are less reactive than a kaolinite–ammonium acetate intercalation compound<sup>35</sup> and methoxy-modified kaolinite.<sup>28,29</sup> To date there have been no reports on diol modification by using methoxy-modified kaolinite and I believe this method is feasible for intercalation and grafting with various alcohols.

## 2.2 Experimental

### *Materials.*

Well-crystallized kaolinite from Georgia (KGa-1), obtained from the Source Clays Repository of Clay Minerals Society (U.S.A.), was used after grinding for a few minutes to pass a 100-mesh sieve. According to our previous report,<sup>28</sup> wet methoxy-modified kaolinite ( $d_{001} = 1.11$  nm) was synthesized by stirring a suspension of a kaolinite-*N*-methylformamide intercalation compound ( $d_{001} = 1.08$  nm) with methanol repeatedly at room temperature, and was used without any drying processes.

### *Synthetic procedures.*

Grafting of 1,2- or 1,3-propanediol on kaolinite was achieved by refluxing a suspension of wet methoxy-modified kaolinite (ca. 0.5 g) in 50 ml of 1,2- or 1,3-propanediol for 1 d. For comparison, kaolinite-propanediol molecularly intercalated compounds without grafting were obtained by stirring the mixtures for 3 d at room temperature. All samples were washed several times with 1,4-dioxane and dried *in vacuo* to obtain 1,2- and 1,3-propanediol-grafted kaolinites (abbreviated as Kao-1,2PD<sub>graft</sub> and Kao-1,3PD<sub>graft</sub>, respectively) and kaolinite-1,2- and 1,3-propanediol molecular intercalation compounds (Kao-1,2PD<sub>int</sub> and Kao-1,3PD<sub>int</sub>, respectively). In order to examine the formation of “bridge” type grafted kaolinite, where both OH groups of 1,3-propanediol were bound to the AlOH groups, the refluxing time was extended to 5 d for the case of 1,3-propanediol (Kao-1,3PD<sub>bridge</sub>).

### *Characterisation.*

Powder XRD patterns were obtained by a Rigaku RINT-2500X diffractometer with graphite monochromated CuK $\alpha$  radiation. DTA and TG curves were recorded with a MAC Science TG-DTA 2010S instrument under a dry air flow (200 ml min<sup>-1</sup>) with a heating rate of 10 °C min<sup>-1</sup>. IR

## Chapter 2

spectra were recorded on a Perkin Elmer Spectrum One spectrometer using KBr-disk technique. The amounts of organic fractions were determined by a Perkin-Elmer 2400II CHN analyzer. All Solid-state NMR spectra were measured on a JEOL JNM-CMX-400 spectrometer. The  $^{13}\text{C}$  and  $^{29}\text{Si}$  CP/MAS NMR spectra were recorded at 100.52 MHz and 79.42 MHz with the contact times of 2 and 5 ms using the spinning rates of 10 kHz and 5 kHz, respectively. All the chemical shifts were referred with respect to external TMS.

### 2.3 Results and Discussion

#### *Formation of kaolinite-propanediol molecular intercalation compounds.*

The basal spacings of Kao-1,2PD<sub>int</sub> and Kao-1,3PD<sub>int</sub> were 1.14 nm and 1.11 nm, respectively, as determined by powder XRD (Fig. 2-1B and 2-1D). The peak due to dry methoxy-modified kaolinite ( $d_{001} = 0.86$  nm) disappeared. In the  $^{13}\text{C}$  CP/MAS NMR spectrum of Kao-1,2PD<sub>int</sub> (Fig. 2-2B), the signals due 1,2-propanediol were observed at 20.3 ppm ( $-\underline{\text{C}}\text{H}_3$ ), 69.5 ppm ( $-\underline{\text{C}}\text{H}_2\text{OH}$ ), and 70.7 ppm ( $-\underline{\text{C}}\text{H}(\text{OH})-$ ) as well as that due to methoxy groups (50.3 ppm). The spectrum of Kao-1,3PD<sub>int</sub> (Fig. 2-2D) shows the signals at 34.9 ppm ( $-\underline{\text{C}}\text{H}_2(\text{OH})$ ) and 60.8 ppm ( $-\underline{\text{C}}\text{H}_2-$ ) with that of methoxy groups (50.4 ppm).

After stirring the suspension of Kao-1,3PD<sub>int</sub> with ethanol several times, the XRD pattern of the product showed the decrease of the basal spacing to 0.86 nm, suggesting the reappearance of the phase due to methoxy-modified kaolinite (Fig. 2-3B and 2-3C). The  $^{13}\text{C}$  CP/MAS NMR spectrum of the product (not shown) showed the complete disappearance of the signals due to 1,3-propanediol, whereas the signal at 51 ppm ( $\text{O}\underline{\text{C}}\text{H}_3$ ) was still observed. The IR band at 2891  $\text{cm}^{-1}$  ( $\nu_{\text{s}}\text{CH}_2$ ) due to intercalated 1,3-propanediol disappeared and the bands at ca. 2960 ( $\nu_{\text{as}}\text{CH}_3$ ) and 2842  $\text{cm}^{-1}$  ( $\nu_{\text{s}}\text{CH}_3$ ) were observed. All these data indicate deintercalation of 1,3-propanediol. Kao-1,2PD<sub>int</sub> also showed similar results. Consequently, we conclude that 1,2- and 1,3-

propanediols were molecularly intercalated into methoxy-modified kaolinite at room temperature.

### ***Formation of propanediol-grafted kaolinites.***

By refluxing methoxy-modified kaolinite in 1,2- and 1,3-propanediols, the diols were grafted onto kaolinite, which was proved by the XRD (Fig. 2-1) and DTA-TG results (Fig. 2-4). After refluxing the mixtures, the basal spacings of the products were expanded from 0.86 nm to 1.08 nm for Kao-1,2PD<sub>graft</sub>, 1.11 nm for Kao-1,3PD<sub>graft</sub>, and 1.10 nm for Kao-1,3PD<sub>bridge</sub>, respectively (Fig. 2-1C, 2-1E, and 2-1F). The major exothermic peaks accompanied with evident mass losses were observed at ca. 400 °C in the DTA-TG curves of Kao-1,2PD<sub>graft</sub>, Kao-1,3PD<sub>graft</sub>, and Kao-1,3PD<sub>bridge</sub> (Fig. 3), whereas methoxy-modified kaolinite itself did not exhibit any noticeable changes in the DTA-TG curve. These data show that 1,2- and 1,3-propanediols were not desorbed until ca. 300 °C but decomposed thermally at higher temperatures, strongly suggesting the bonding to the aluminosilicate layers.

After washing Kao-1,3PD<sub>graft</sub> with ethanol several times, the XRD pattern of the product hardly changed, in contrast to the case of Kao-1,3PD<sub>int</sub> (Fig. 2-3D and 2-3E). Kao-1,2PD<sub>graft</sub> also showed similar results. Consequently, we conclude that 1,2- and 1,3-propanediols are grafted into kaolinite by refluxing.

The influences of the intercalation and grafting of propanediols on the framework of kaolinite were examined by <sup>29</sup>Si CP/MAS NMR. Kaolinite exhibits two signals at -90.9 and -91.4 ppm in the <sup>29</sup>Si NMR spectrum (Fig. 2-5A).<sup>36</sup> Generally the split disappears and the signals are normally observed at lower frequencies by intercalation of organic guest molecules. This shift is explained by weaker interactions between the silicate layers and intercalated guests than the pristine interlayer interactions.<sup>37</sup> In fact, the spectrum of methoxy-modified kaolinite (Fig. 2-5B) shows the signal at -91.6 ppm. Considering these results, we initially thought that the signals of Kao-PD<sub>graft</sub> and Kao-PD<sub>int</sub> should exhibit the signals in higher frequencies than methoxy-modified kaolinite because newly introduced OH groups should induce stronger interactions.

## Chapter 2

However, in the  $^{29}\text{Si}$  CP/MAS NMR spectra of Kao-1,2PD<sub>graft</sub> and Kao-1,3PD<sub>graft</sub>, three signals were observed ( $-92.7$ ,  $-91.2$ , and  $-90.6$  ppm for Kao-1,2PD<sub>graft</sub> (Fig. 2-5D) and  $-92.1$ ,  $-91.4$ , and  $-90.7$  ppm for Kao-1,3PD<sub>graft</sub> (Fig. 2-5F)). In the spectrum of Kao-1,3PD<sub>bridge</sub> a broad signal was observed at  $-92.0$  ppm (Fig. 2-5G). In all the cases, the main signals were at the lower frequencies than that of methoxy-modified kaolinite, though the weak signals at higher frequencies (around  $-90 \sim -91$  ppm) were observed. In the  $^{29}\text{Si}$  CP/MAS NMR spectra of Kao-1,2PD<sub>int</sub> and Kao-1,3PD<sub>int</sub>, the broad signals at around  $-91.5 \sim -92$  ppm were detected (Fig. 2-5C and 2-5E), being at somewhat lower frequencies than that of methoxy-modified kaolinite. These findings can be explained by the following reasons. The interactions between the layers of methoxy-modified kaolinite must have been reduced by the interlayer expansion, which should induce the shift to lower frequencies. The other factor of the introduction of OH groups of propanediols to cause the shift to higher frequencies does not contribute so much possibly because the expansion is too large for the interactions to influence.

The finding that the signals due to Kao-1,2PD<sub>graft</sub> and Kao-1,3PD<sub>graft</sub> were found at lower frequencies than those found for Kao-1,2PD<sub>int</sub> and Kao-1,3PD<sub>int</sub> may be ascribed to the lower interactions between the silicate layers and the guest species because the number of OH groups of propanediols interacting with the silicate sheets should be decreased. The small signal at  $-92.7$  ppm in the  $^{29}\text{Si}$  CP/MAS NMR spectrum of Kao-1,2PD<sub>int</sub> suggests that a small amount of 1,2-propanediol may have been grafted onto kaolinite even at room temperature.

The information on the interactions between kaolinite and propanediols was also obtained by the IR results. Kaolinite has four characteristic n(OH) bands (Fig. 2-6A), and three bands at  $3653$ ,  $3669$ , and  $3695\text{ cm}^{-1}$  are perturbed by intercalation of guest molecules,<sup>38</sup> whereas the band at  $3620\text{ cm}^{-1}$  assigned to inner hydroxy groups is not perturbed. By the modification with methoxy group, the three n(OH) bands were reasonably reduced and the bands at  $3500 \sim 3550$ , ca.  $3631$  and ca.  $3646$  appeared (Fig. 2-6B). The band at  $3500 \sim 3550\text{ cm}^{-1}$  is ascribed to the OH stretching arising from the interactions between cointercalated H<sub>2</sub>O and AlOH groups of kaolinite.<sup>28</sup> Thus,

the new bands at ca. 3631 and ca. 3646  $\text{cm}^{-1}$  are characteristic of OH groups of residual AlOH groups in methoxy-modified kaolinite. By the intercalation of propanediol into methoxy-modified kaolinite (Fig. 2-6C and 2-6E), the intensities of the bands at ca. 3630 and 3649  $\text{cm}^{-1}$  were decreased remarkably, and a new band at 3600  $\text{cm}^{-1}$  appeared. This band at 3600  $\text{cm}^{-1}$  is due to  $\nu(\text{OH})$  hydrogen-bonded with molecularly intercalated 1,2- and 1,3-propanediols.

By the grafting of propanediol, the intensity of the bands at ca. 3630 and ca. 3550  $\text{cm}^{-1}$  were decreased largely but the broad band at 3640 ~ 3650  $\text{cm}^{-1}$  did not change (Fig. 2-6D and 2-6F). The intensity of the band at ca. 3550  $\text{cm}^{-1}$  in the spectrum of Kao-PD<sub>graft</sub> was weaker than that of Kao-PD<sub>int</sub>, which means that the amounts of cointercalated H<sub>2</sub>O in the grafted samples were smaller than those in the intercalated samples. It was in agreement with the TG results (not shown). The amounts of cointercalated H<sub>2</sub>O may be affected by the number of OH groups of propanediol. The bands at 3640 ~ 3650  $\text{cm}^{-1}$  observed in the spectra of methoxy-modified kaolinite, Kao-1,2PD<sub>graft</sub>, and Kao-1,3PD<sub>graft</sub> were hardly shifted, independent of the kind of grafting species. The characteristic bands at 3600  $\text{cm}^{-1}$  of Kao-1,2PD<sub>int</sub> and Kao-1,3PD<sub>int</sub> were hardly observed in the IR spectra of Kao-1,2PD<sub>graft</sub> and Kao-1,3PD<sub>graft</sub>. All these differences in the profiles found for intercalated and grafted samples mean the different interactions of the organic groups with the AlOH groups and probably imply the different interlayer environments.

The organic modification with 1,2- and 1,3-propanediols proceeded under transesterification with methoxy groups and further grafting onto the AlOH groups of AlO<sub>4</sub>(OH)<sub>2</sub> sheets, which is shown by the <sup>13</sup>C CP/MAS NMR (Fig. 2-2), IR (Fig. 2-6), and CHN results (Table 2-1). The signal at 50.8 ppm derived from methoxy groups in methoxy-modified kaolinite was not observed in the <sup>13</sup>C CP/MAS NMR spectra of Kao-1,2PD<sub>graft</sub>, Kao-1,3PD<sub>graft</sub>, and Kao-1,3PD<sub>bridge</sub> (Fig. 2-2C, 2-2E, and 2-2F). Methoxy groups on the kaolinite are stable under 350 °C<sup>28</sup> and the temperature was higher than the boiling points of 1,2- and 1,3-propanediols (187.85 and 213.5 °C, respectively). These data show that the transesterification reaction between 1,2- or 1,3-propanediol and methoxy groups in methoxy-modified kaolinite proceeded during the refluxing.

## Chapter 2

The  $\nu(\text{OH})$  bands of 1,2- and 1,3-propanediol were still observed at ca.  $3400\text{ cm}^{-1}$  in the IR spectra of Kao-1,2PD<sub>graft</sub> and Kao-1,3PD<sub>graft</sub> (Fig. 2-6D and 2-6F). This suggests that one OH group out of two in 1,2- or 1,3-propanediol was grafted onto the aluminosilicate layers.

In the  $^{13}\text{C}$  CP/MAS NMR spectrum of Kao-1,3PD<sub>bridge</sub> (Fig. 2-2F), a new signal at 30.5 ppm and a broadened signal at 62.3 ppm were observed in addition to the signal at 35.0 ppm which was also found for Kao-1,3PD<sub>graft</sub>. The ratio of the peak area at 30.5 ppm to that of 35.0 ppm was 45:55 from the  $^{13}\text{C}$  MAS NMR data without cross polarization. Consequently, the broad signal at 62.3 ppm should be composed of two peaks due to two types of the grafted diols. In the IR spectrum of Kao-1,3PD<sub>bridge</sub>, the band due to OH stretching of propanediol at ca.  $3400\text{ cm}^{-1}$  was halved and the intensity of the band at  $3646\text{ cm}^{-1}$  was reduced (Fig. 2-6G). On the basis of these results, the signals at 30.5 and 62.3 ppm in the  $^{13}\text{C}$  CP/MAS NMR spectrum of Kao-1,3PD<sub>bridge</sub> are ascribable to 1,3-propanediol where both of the OH groups are reacted to form a bridge. By extending the refluxing time to 5 d, a part (about half) of the OH groups on the other side of grafted 1,3-propanediol are linked to the AlOH groups on the surfaces.

The amounts of the organic fractions in the grafted samples were calculated from the CHN data (Table 2-1). The amounts of the alkoxy groups per the  $\text{Al}_2\text{Si}_2\text{O}_5(\text{OH})_4$  unit were 0.63 (Kao-1,2PD<sub>graft</sub>), 0.68 (Kao-1,3PD<sub>graft</sub>), and 0.61 (Kao-1,3PD<sub>bridge</sub>), and these values are higher than that of methoxy-modified kaolinite (0.40). Because transesterification reaction does not lead such larger amounts of the alkoxy groups, the increment of the amounts should be brought about by further esterification reaction between propanediols and AlOH groups. The reaction pathways are illustrated in scheme 2-1. The complete disappearance of methoxy groups suggests that the transesterification occurred first.

## **2.4 Conclusions**

Propanediols (1,2- and 1,3-propanediols) were grafted onto the interlayer surface of kaolinite via transesterification of methoxy-modified kaolinite. Further esterification also occurred. Two kinds of organic derivatives of kaolinites modified with 1,3-propanediol were prepared. One OH group out of two in the diol was linked to the interlayer surface by refluxing for 1 d. By extending the refluxing time to 5 d, a new phase appeared in which two OH groups can be bound to the surface (bridged type). Residual OH groups of propanediols have a potential for further modification by reactive organic substances. Kaolinite–1,2- and 1,3-propanediol intercalation compounds, in which the diols were molecularly intercalated, were synthesized by stirring the suspension of methoxy-modified kaolinite in 1,2- and 1,3-propanediols at room temperature, respectively. All the spectroscopic data clarify the differences between propanediol-modified kaolinites and molecularly intercalated compounds. Grafting with 1,2- and 1,3-propanediols affects the aluminosilicate layers as well as the interlayer environments. The method using transesterification reaction is suited for other large alcohols because methoxy-modified kaolinite is a versatile intermediate.

## 2.5 References

- 1 G. Alberti, G. M. Lombardo, G. C. Pappalardo and R. Vivani, *Chem. Mater.*, 2002, **14**, 295.
- 2 G. Alberti, M. Casciola, U. Constantino and R. Vivani, *Adv. Mater.*, 1996, **8**, 291.
- 3 G. Alberti, R. Vivani, F. Marmottini and P. Zappelli, *J. Porous Mater.*, 1998, **5**, 205.
- 4 G. Alberti, E. Brunet, C. Dionigi, O. Juanes, M. J. de la Mata, J. C. Rodríguez-Ubis and R. Vivani, *Angew. Chem. Int. Ed. Engl.*, 1999, **38**, 3351.
- 5 A. Clearfield, *Chem. Mater.*, 1998, **10**, 2801.
- 6 A. Clearfield and Z. Wang, *J. Chem. Soc., Dalton Trans.*, 2002, 2937.
- 7 A. Clearfield, C. V. K. Sharma and B. P. Zhang, *Chem. Mater.*, 2001, **13**, 3099.
- 8 D. Mochizuki, A. Shimojima and K. Kuroda, *J. Am. Chem. Soc.*, 2002, **124**, 12082.
- 9 A. Shimojima, D. Mochizuki and K. Kuroda, *Chem. Mater.*, 2001, **13**, 3603.
- 10 E. Ruiz-Hitzky and J. M. Rojo, *Nature*, 1980, **287**, 28.
- 11 M. Ogawa, S. Okutomo and K. Kuroda, *J. Am. Chem. Soc.*, 1998, **120**, 7361.
- 12 Y. Mitamura, Y. Komori, S. Hayashi, Y. Sugahara and K. Kuroda, *Chem. Mater.*, 2001, **13**, 3747.
- 13 M. Inoue, M. Kimura and T. Inui, *Chem. Mater.*, 2000, **12**, 55.
- 14 M. Inoue, Y. Kondo and T. Inui, *Inorg. Chem.*, 1988, **27**, 215.
- 15 M. Inoue, H. Tanino, Y. Kondo and T. Inui, *Clays Clay Miner.*, 1991, **39**, 151.
- 16 M. Inoue, H. Kominami, Y. Kondo and T. Inui, *Chem. Mater.*, 1997, **9**, 1614.
- 17 V. Prévot, C. Forano and J. P. Besse, *Appl. Clay Sci.*, 2001, **18**, 3.
- 18 S. Ogata, H. Tagaya, M. Karasu and J. Kadokawa, *J. Mater. Chem.*, 2000, **10**, 321.
- 19 H. Suzuki, K. Notsu, Y. Takeda, W. Sugimoto and Y. Sugahara, *Chem. Mater.*, in press.
- 20 J. W. Johnson, A. J. Jacobson, W. M. Butler, S. E. Rosenthal, J. F. Brody and J. T. Lewandowski, *J. Am. Chem. Soc.*, 1989, **111**, 381.
- 21 K. Segawa, N. Kihara and H. Yamamoto, *J. Mol. Catal.*, 1992, **74**, 213.

- 22 I. Fujita, K. Kuroda and M. Ogawa, *Chem. Mater.*, in press.
- 23 G. Alberti, U. Constantino, F. Marmottini, R. Vivani and P. Zappelli, *Angew. Chem., Int. Ed. Engl.*, 1993, **32**, 1357.
- 24 G. Alberti, U. Constantino, F. Marmottini, R. Vivani and P. Zappelli, *Microporous Mesoporous Mater.*, 1998, **21**, 297.
- 25 R. Takenawa, Y. Komori, S. Hayashi, J. Kawamata, Y. Sugahara and K. Kuroda, *Chem. Mater.*, 2001, **13**, 3741.
- 26 J. G. Thompson and C. Cuff, *Clays Clay Miner.*, 1985, **33**, 490.
- 27 A. Weiss, W. Thielepape, G. G`ring, W. Ritter and W. Schäfer, *Proc. Int. Clay. Conf.*, 1963, **1**, 287.
- 28 Y. Komori, H. Enoto, R. Takenawa, S. Hayashi, Y. Sugahara and K. Kuroda, *Langmuir*, 2000, **16**, 5506.
- 29 Y. Komori, Y. Sugahara and K. Kuroda, *J. Mater. Res.*, 1998, **13**, 930.
- 30 Y. Komori, Y. Sugahara and K. Kuroda, *Chem. Mater.*, 1999, **11**, 3.
- 31 J. J. Tunney and C. Detellier, *Chem. Mater.*, 1993, **5**, 747.
- 32 J. J. Tunney and C. Detellier, *J. Mater. Chem.*, 1996, **6**, 1679.
- 33 J. J. Tunney and C. Detellier, *Can. J. Chem.*, 1997, **75**, 1766.
- 34 J. J. Tunney and C. Detellier, *Clays Clay Miner.*, 1994, **42**, 552.
- 35 T. Itagaki, Y. Komori, Y. Sugahara and K. Kuroda, *J. Mater. Chem.*, 2001, **11**, 3291.
- 36 P. Barron, R. L. Frost, J. O. Skjemstad and A. J. Koppi, *Nature*, 1983, **302**, 49.
- 37 J. G. Thompson, *Clays Clay Miner.*, 1985, **33**, 173.
- 38 R. L. Ledoux and J. L. White, *Science*, 1964, **143**, 244.

Table 2-1 The amounts of alkoxy groups in modified kaolinites.

Sample Name	C / mass%	N / mass%	alkoxy groups / Al <sub>2</sub> Si <sub>2</sub> O <sub>5</sub> (OH) <sub>4</sub>
methoxy-modified kaolinite	2.24	0.16 <sup>a</sup>	0.40
Kao-1,2PD <sub>graft</sub>	7.60	0.0	0.63
Kao-1,3PD <sub>graft</sub>	8.33	0.0	0.68
Kao-1,3PD <sub>bridge</sub>	7.78	0.0	0.61

<sup>a</sup> This means that a small amount of *N*-methylformamide remained. The amount of methoxy group was calculated from the carbon content after subtracting the amount due to *N*-methylformamide.

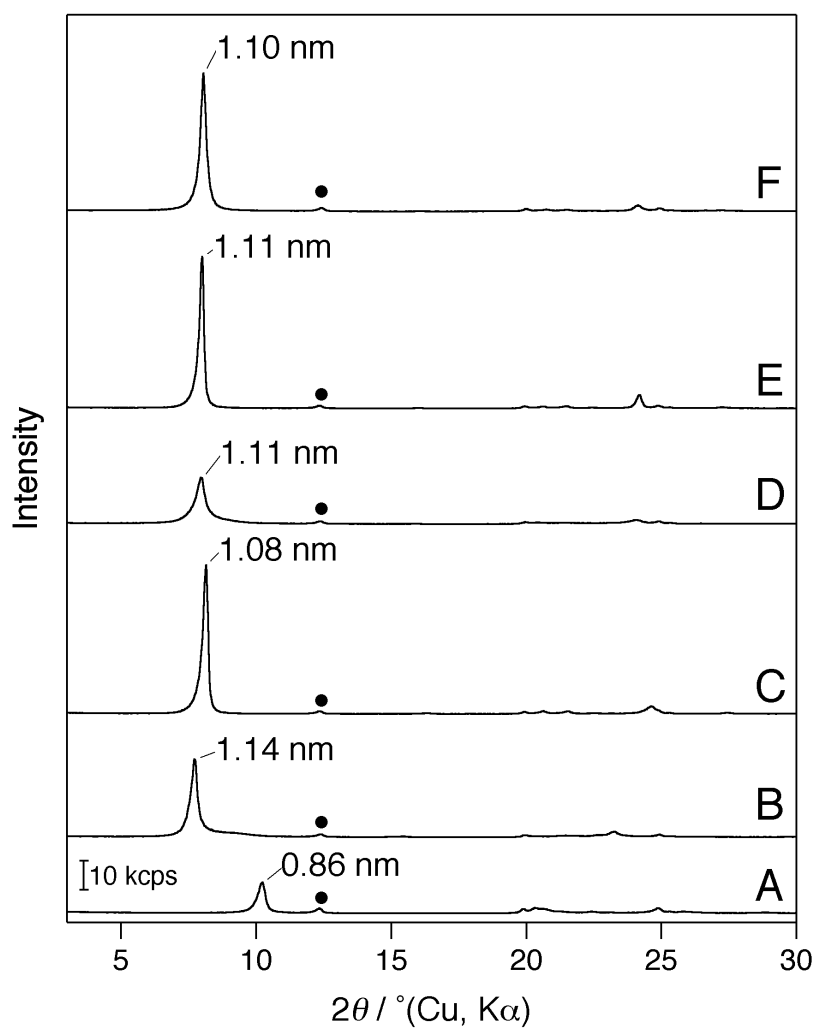


Fig. 2-1 XRD patterns of (A) methoxy-modified kaolinite, (B) Kao-1,2PD<sub>int</sub>, (C) Kao-1,2PD<sub>graft</sub>, (D) Kao-1,3PD<sub>int</sub>, (E) Kao-1,3PD<sub>graft</sub>, and (F) Kao-1,3PD<sub>bridge</sub>. The peaks of unreacted kaolinite are marked by filled circles.

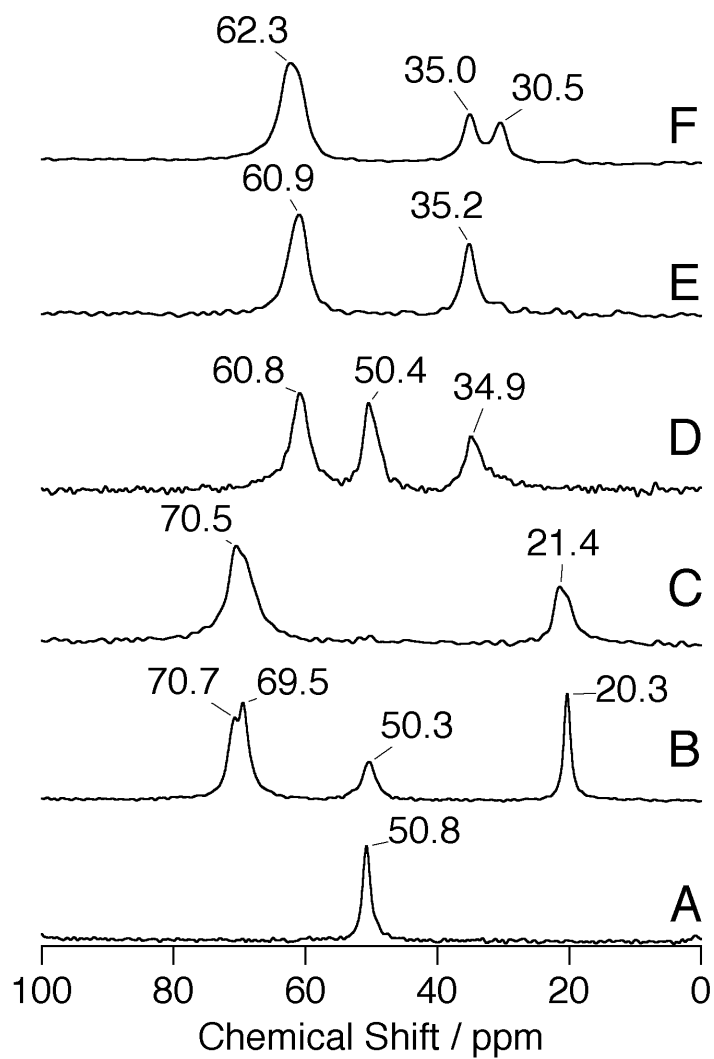


Fig. 2-2  $^{13}\text{C}$  CP/MAS NMR spectra of (A) methoxy-modified kaolinite, (B) Kao-1,2PD<sub>int</sub>, (C) Kao-1,2PD<sub>graft</sub>, (D) Kao-1,3PD<sub>int</sub>, (E) Kao-1,3PD<sub>graft</sub>, and (F) Kao-1,3PD<sub>bridge</sub>.

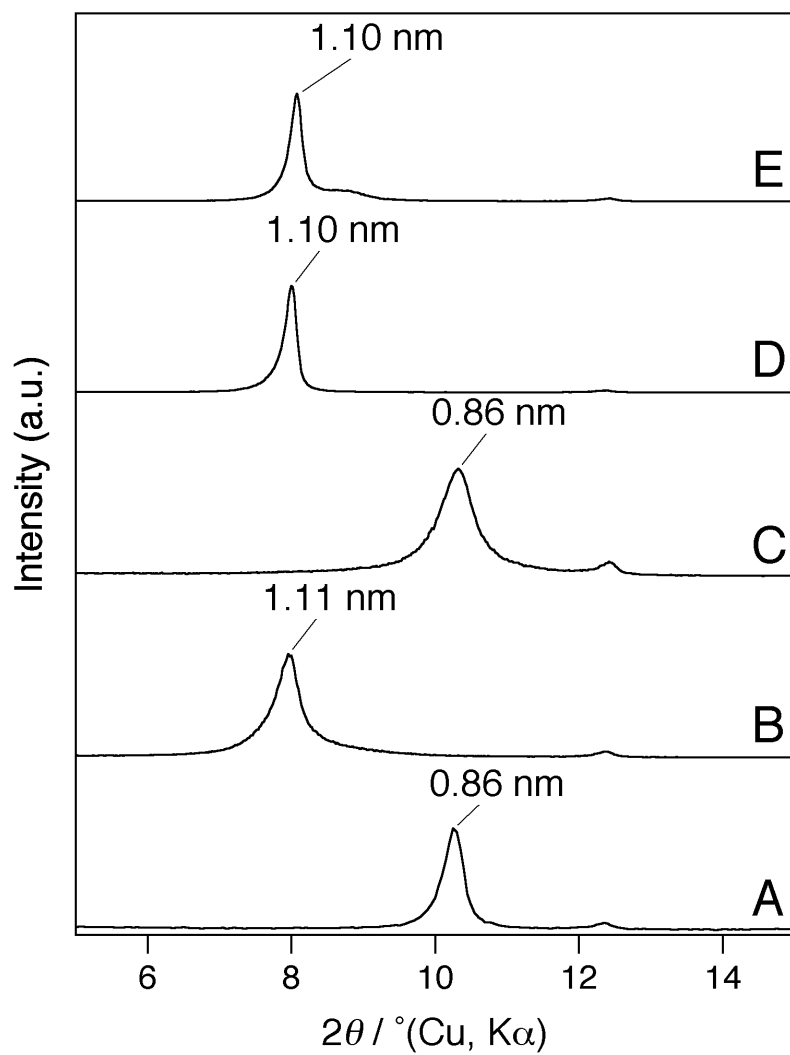


Fig. 2-3Figure S1 XRD patterns of (A) methoxy-modified kaolinite, (B) Kao-1,3PDint, (C) Kao-1,3PDint washed by ethanol, (D) Kao-1,3PDgraft, and (E) Kao-1,3PDgraft washed by ethanol

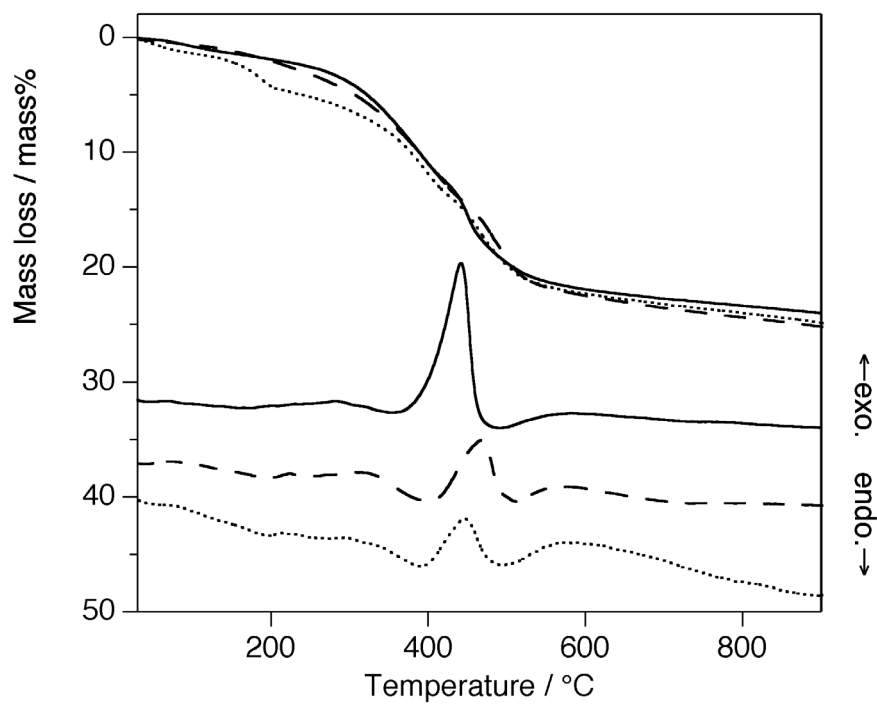


Fig. 2-4 DTA-TG curves of (solid line) Kao-1,2PD<sub>graft</sub>, (dash line) Kao-1,3PD<sub>graft</sub>, and (dotted line) Kao-1,3PD<sub>bridge</sub>.

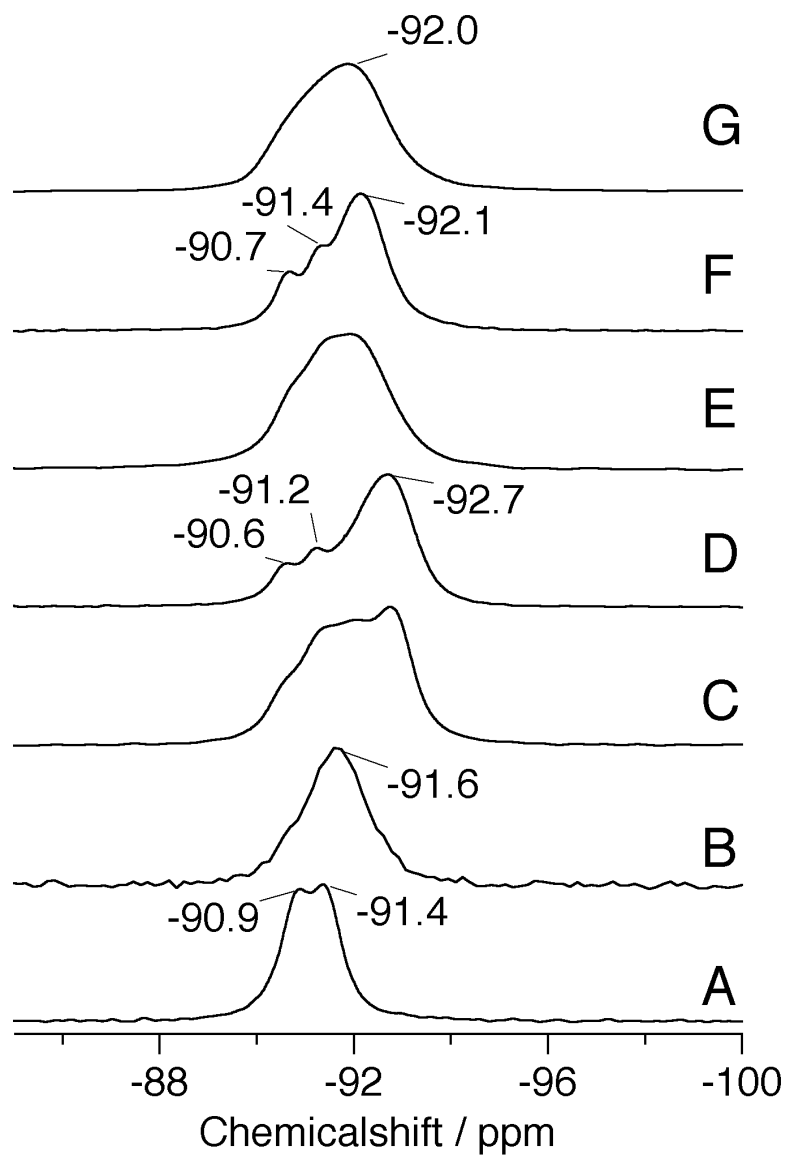


Fig. 2-5  $^{29}\text{Si}$  CP/MAS NMR spectra of (A) kaolinite, (B) methoxy-modified kaolinite, (C) Kao-1,2PD<sub>int</sub>, (D) Kao-1,2PD<sub>graft</sub>, (E) Kao-1,3PD<sub>int</sub>, (F) Kao-1,3PD<sub>graft</sub>, and (G) Kao-1,3PD<sub>bridge</sub>.

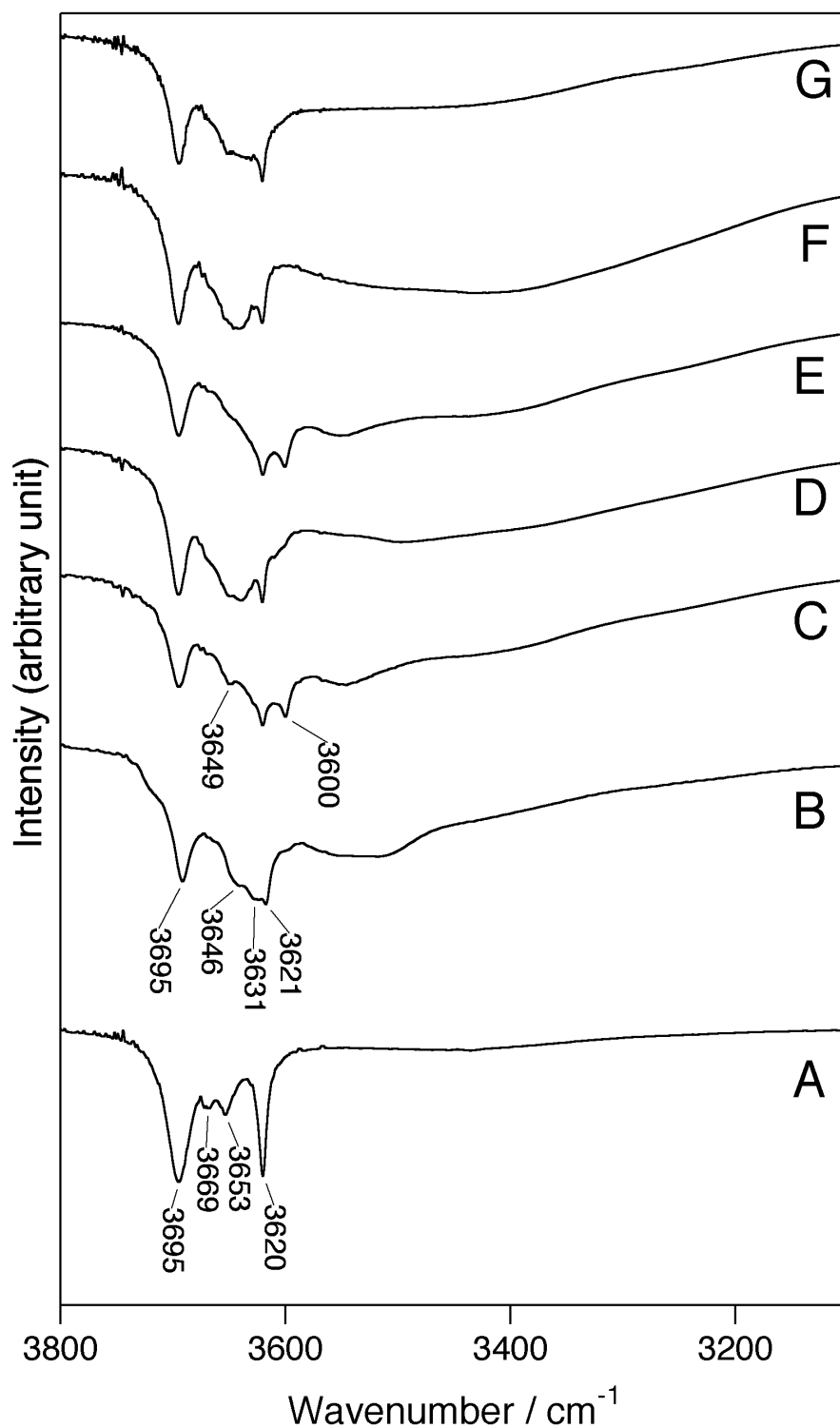
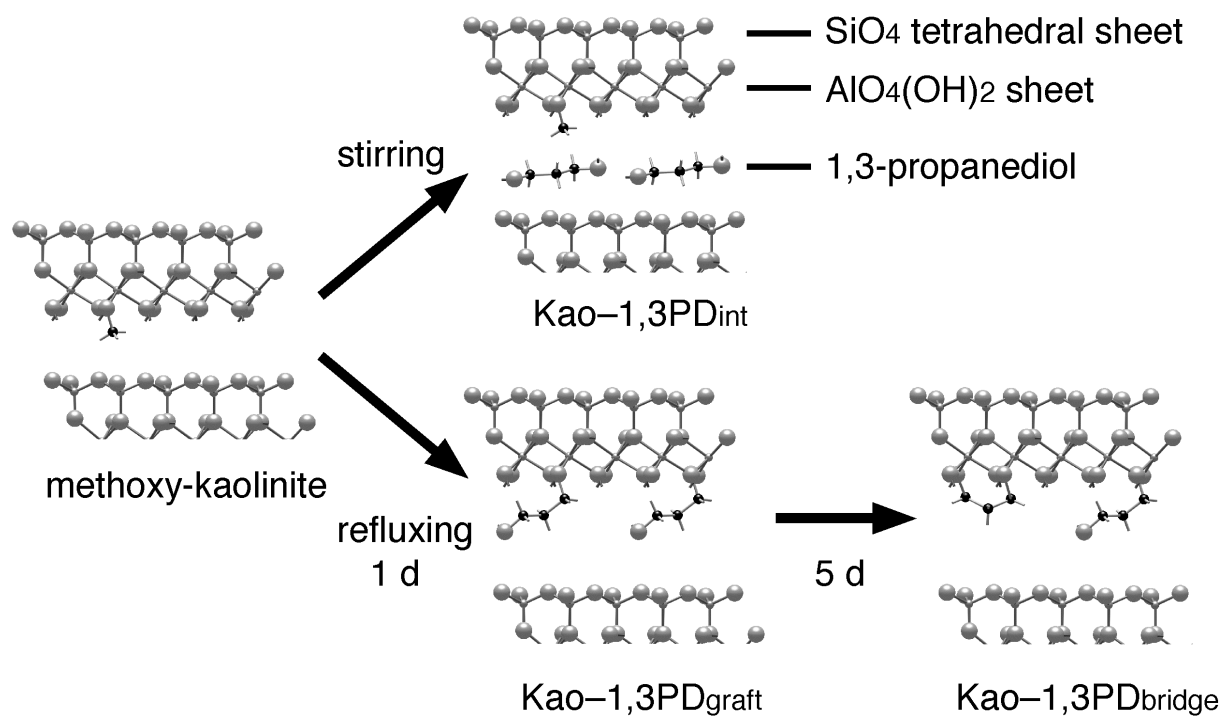


Fig. 2-6 Infrared spectra of (A) kaolinite, (B) methoxy-modified kaolinite, (C) Kao-1,2PD<sub>int</sub>, (D) Kao-1,2PD<sub>graft</sub>, (E) Kao-1,3PD<sub>int</sub>, (F) Kao-1,3PD<sub>graft</sub>, and (G) Kao-1,3PD<sub>bridge</sub>.



Scheme 2-1 Reaction pathways between methoxy-modified kaolinite and 1,3-propanediol.



## CHAPTER 3

Synthesis and Characterization of Organically-Modified kaolin-  
ite with Glycerol



### 3.1 Introduction

Organically modified inorganic layered material was one of the organic-inorganic nanohybrids, and was researched by many authors for the further application of adsorbents, reaction media etc. There are many reports about organically modified layered zirconium phosphates and phosphonates<sup>1-4</sup>.  $\gamma$ -Zirconium phosphate containing polyethyleneoxide pillar has variable size and shape of the cavities between the layers and which could be controlled by chemical means (i.e. pH control)<sup>5</sup>. Selection and/or controlling the amount of organic units made it possible to obtain the organically pillared materials with unique pore size<sup>5,6</sup>. Layered polysilicates such as magadiite and octosilicate were modified with silylating agents<sup>7-9</sup> and alcohols<sup>10</sup>. Magadiite, one of layered polysilicates, modified with organotricholohsiran absorbed alcohols because by the hydrolysis of residual Si-Cl groups new OH groups were introduced nearby interlayer surfaces<sup>8, 11</sup>. Organically modified layered materials such as boehmite (AlOOH)<sup>12-14</sup>, metal hydroxides<sup>15</sup>, layered double hydroxides<sup>16</sup>, FeOCl<sup>17-19</sup>, layered perovskite<sup>20</sup> were also reported. Their structure were composed of two-dimensional inorganic nanosheets covered by organic units and the properties mainly depend on the interactions between inorganic sheet and grafted organic species. Position of reactive groups on the interlayer surface of inorganic layered materials was very important for controlling the bonding manner and ordering of grafted organic species by molecular levels. Organically modification of  $\alpha$ -zirconium phosphate with regular reactive groups produced porous materials with unique pore size by selection of organic species<sup>2,3</sup>. We reported the organic modification of a layered polysilicate octosilicate with unique bonding manner<sup>7</sup>.

Kaolinite, 1:1 type clay mineral, was used in this report as an inorganic layered material for organic modification. Kaolinite has two interlayer surfaces of  $\text{AlO}_4(\text{OH})_2$  octahedral sheet and  $\text{SiO}_4$  tetrahedral sheet, and reactive OH groups were on the interlayer surface of  $\text{AlO}_4(\text{OH})_2$  sheet. Thus, organic modifications of kaolinite were generating the various asymmetric interlayer

## Chapter 3

environments sandwiched by organically modified  $\text{AlO}_4\text{O}_5(\text{OH})_4$  octahedral and  $\text{SiO}_4$  tetrahedral sheets. Some alcohols including methanol<sup>21-23</sup>, ethylene glycol<sup>24, 25</sup>, propanediol<sup>24, 26</sup>, aminoethanol<sup>27</sup>, ethylene glycol monomethyl ether<sup>24</sup>, and diethylene glycol monobutyl ether<sup>24</sup> were reported for organic modification of kaolinite. However, complete organic modification with alcohol did not proceed, and at most, one-third OH groups on the interlayer surface were reacted<sup>21</sup>. Small amount of methoxy groups grafted onto kaolinite improved the reactivity for intercalation, and methoxy-modified kaolinite showed higher reactivity than conventional intermediates for intercalation such as a kaolinite-*N*-methylformamide intercalation compound<sup>28</sup>.<sup>29</sup> Recently we reported the organic modification of kaolinite with propanediols by transesterification of methoxy modified kaolinite, and proposed the model in which one OH group was grafted onto the interlayer surface of kaolinite and residual OH present on the interlayer<sup>26</sup>. Introduced OH group of propanediol must change the interlayer environments different from that of methoxy-modified kaolinite. However amount of alkoxy groups was still low. For controlling the interlayer environment, we believe more functional groups must be introduced.

Here we report the synthesis of kaolinite modified with glycerol. Glycerol was simple triol, and two OH groups were introduced between the layers of kaolinite if one OH group was reacted. Methoxy-modified kaolinite was used for this work as an intermediate, because it has a more reactivity than conventional intermediates.

### 3.2 Experimental

Kaolinite (KGa-1) was obtained from the Source Clay Repository of Clay Minerals Society (U.S.A.) and was used after grinding to pass a 100-mesh sieve. According to a method reported previously<sup>22,23</sup>, wet methoxy-modified kaolinite with the basal spacing of 1.11 nm was obtained by stirring the mixture of methanol and a kaolinite-*N*-methylformamide intercalation compound<sup>30</sup>

at room temperature and was used without any drying process.

Grafting of glycerol proceeded by reaction between wet methoxy-modified kaolinite and glycerol. The mixture was stirred at 140 °C for 1 d. After centrifuging, the sample was washed by acetone several times and was dried *in-vacuo* to obtain glycerol-grafted kaolinite (abbreviated as Kao–Glycerol<sub>graft</sub>). For comparison, a kaolinite–glycerol molecular intercalation compound was prepared by stirring the mixture at room temperature for 1 d and washing by acetone or ethylacetate.

XRD patterns were obtained by Mac Science MXP<sup>3</sup> diffractometer with monochromated Cu Ka radiation. Solid-state <sup>13</sup>C MAS NMR measurements were performed on JEOL JNM-CMX 400 spectrometer with spinning rate of 6 kHz. The chemical shift was referred as external tetramethylsilane (TMS). The Larmor frequency of <sup>13</sup>C was 100.52 Hz. Thermogravimetry-mass spectrometry (TG-MS; Shimadzu TGA-50 thermobalance coupled with a Shimadzu QP1100EX quadrupole mass spectrometer via a stainless capillary column) was performed under a helium flow (40 ml min<sup>-1</sup>) at a heating rate of 10 °C min<sup>-1</sup>. DTA-TG curves were recorded by Mac Science Mac Science TG-DTA 2010S with the heating rate of 10 °C min<sup>-1</sup> under an dry air flow. The organic amount was determined by CHN analyses using a Perkin-Elmer PE-2400II apparatus. Raman spectra were obtained by Perkin-Elmer 2000R spectroscop.

### 3.3 Results and Discussion

Glycerol was intercalated into kaolinite by stirring the suspension of methoxy-modified kaolinite with glycerol at room temperature, which was shown by XRD and <sup>13</sup>C MAS NMR results. The basal spacing of wet sample was slightly expanded from 1.11 nm of wet methoxy-modified kaolinite to 1.16 nm during the reaction (not shown). The product was washed by ethylacetate and was dried *in-vacuo* to obtained Kao-Glycerol<sub>int</sub> (Fig. 3-1B). In the <sup>13</sup>C MAS NMR spectrum of Kao-Glycerol<sub>int</sub>, three signals were observed at 50.8, 63.9, and 72.3 ppm (Fig.

### Chapter 3

3-2B). The signals at 63.9 and 72.3 ppm were assigned to  $-\underline{\text{C}}\text{H}_2\text{OH}$  and  $-\underline{\text{C}}\text{H}(\text{OH})-$  of glycerol, respectively and the signal at 50.8 ppm was due to methoxy group. When a wet kaolinite-glycerol intercalation compound was dispersed into acetone several times and was dried *in vacuo*, the basal spacing of product decreased from 1.16 nm to 0.89 nm (Fig. 3-1C), which was almost same value as that of dry methoxy-modified kaolinite (0.86 nm). This means that most of glycerol between the layers of kaolinite was deintercalated as the case of kaolinite-1,2-(and 1,3-)propanediol intercalation compound<sup>26</sup>. The broadness of the peak and the relative large basal spacing were probably due to residual glycerol between the layers of kaolinite. This is the reason why we concluded that glycerol was molecular intercalated into methoxy-modified kaolinite by stirring at room temperature.

In the mass chromatogram of Kao-Glycerol<sub>int</sub>, the fragments of methanol ( $m/z = 31, 29,$  and 15) were detected at 130 °C with the very small fragments of deintercalated glycerol ( $m/z = 61$  and 43; not shown). At the same temperature, the fragments due to H<sub>2</sub>O ( $m/z = 18$  and 17) were also detected in the mass chromatogram (Fig. 3-3 below). Liquid glycerol was decomposed at 290 °C, and methoxy groups on the interlayer surface of kaolinite was stable until 350 °C<sup>22</sup>. Thus, generation of methanol and H<sub>2</sub>O suggested that glycerol between the layers of kaolinite reacted with methoxy and hydroxy groups on the interlayer surface of methoxy-modified kaolinite at 130 °C. These reactions proceeded by the transesterification and new esterification, and during the reaction H<sub>2</sub>O and methanol were generated, respectively.

Thus, Organic modification of glycerol with kaolinite was attempted by stirring the suspension of methoxy-modified kaolinite with glycerol at 140 °C. After the reaction, the fragments of H<sub>2</sub>O ( $m/z = 18$  and 17) at 130 °C was not observed (Fig. 3-3 above) and organic fragments was not detected until 200 °C.

Glycerol was grafted into the interlayer surface of kaolinite during the reaction at 140 °C, which was shown by XRD and DTA-TG results. After the reaction, the basal spacing was changed from 1.11 nm of wet methoxy-modified kaolinite to 1.09 nm. Different from the case of

a wet kaolinite–glycerol intercalation compound, the basal spacing was not changed after washed by acetone several times (Fig. 3-1D). In the DTA-TG curves of Kao–Glycerol<sub>graft</sub> (Fig. 3-4 solid line), an evident exothermal peak with mass loss were observed at 400 °C. Because organic amounts of methoxy-modified kaolinite were low, the exothermal peak was not observed in the DTA-TG curves of methoxy-modified kaolinite (Table 3-1 and Fig. 3-4 dotted line). These data means that glycerol between the layers of kaolinite was grafted onto aluminosilicate layer.

The reaction pathway was examined by <sup>13</sup>C MAS NMR and CHN data. In the <sup>13</sup>C MAS NMR spectrum of Kao-Glycerol<sub>graft</sub> (Fig. 3-2C), two signals were observed at 72.3 and 65.9 ppm derived from glycerol. The signal assigned to methoxy groups at 50 ppm was still observed, and the relative peak intensity was much lower than that in the <sup>13</sup>C MAS NMR spectrum of Kao-Glycerol<sub>int</sub>. TG-MS data also suggested the elimination of methoxy groups. These data revealed that glycerol was grafted into aluminosilicate layer by the transesterification reaction, as well as the case of organic-modification of kaolinite with 1,2- and 1,3-propanediol<sup>26</sup>. The carbon content of methoxy-modified kaolinite and Kao-Glycerol<sub>graft</sub> were 1.60 and 8.05 mass%, respectively (Table 3-1). If all methoxy groups were reacted with glycerol, the amount of grafted glycerol per Al<sub>2</sub>Si<sub>2</sub>O<sub>5</sub>(OH)<sub>4</sub> was calculated to be 0.73, which was lager than the amount of methoxy groups in methoxy-modified kaolinite (0.37). Transesterification did not affect the amount of alkoxy groups. Mass chromatograph of *m/z*=17, 18 detected the generation of H<sub>2</sub>O during heat treatment of Kao-Glycerol<sub>int</sub>, and the incensement of amount of alkoxy group was also observed in the case of hydroxypropoxy-modified kaolinite (Kao-PD<sub>graft</sub>)<sup>26</sup>. These data showed that glycerol was grafted onto the interlayer surface of kaolinite by two route, i.e., transesterification of methoxy groups and new esterification between AlOH group and glycerol as the case of Kao-PD<sub>graft</sub><sup>26</sup>.

FT-Raman spectra were shown in Figure 5. In Raman spectrum of liquid glycerol (Fig. 3-5D), CH<sub>2</sub> twist, and two C-O stretch vibrations were observed at 1090, 1054 (C1=C3), and 1118 (C=2), respectively<sup>31</sup>. After the molecular intercalation of glycerol, these three bands were observed at 1100, 1055 (C1=C3), and 1115 (sh; C2) cm<sup>-1</sup> (Fig. 3-5B). Grafted glycerol also had

## *Chapter 3*

three bands at 1100, 1028-1063 (C1=C3), and 1119 (sh; C2)  $\text{cm}^{-1}$  (Fig. 3-5C). Comparing the Raman spectra of molecularly intercalated and grafted glycerol, C-O stretching vibration (C1=C3) of grafted glycerol was much broader than that of intercalated glycerol, which suggesting glycerol was grafted into kaolinite with one terminal COH group (C1 or C3).

### **3.4 Conclusion**

Organically modified kaolinite with glycerol and a kaolinite-glycerol intercalation compound were obtained by the reaction between methoxy-modified kaolinite and glycerol at different temperatures. By stirring at 140 °C, organic modification of glycerol proceeded via transesterification of methoxy-modified kaolinite and further esterification. One terminal COH group was probably used for grafting. When the reaction proceeded at RT, glycerol was not grafted and molecularly intercalation into methoxy-modified kaolinite.

### 3.5 References

- 1 G. Alberti, M. Casciola, U. Constantino and R. Vivani, *Adv. Mater.*, 1996, **8**, 291.
- 2 G. Alberti, R. Vivani, F. Marmottini and P. Zappelli, *J. Porous. Mater.*, 1998, **5**, 205.
- 3 A. Clearfield, *Chem. Mater.*, 1998, **10**, 2801.
- 4 A. Clearfield and Z. Wang, *J. Chem.Soc., Dalton Trans.*, 2002, 2937.
- 5 G. Alberti, E. Brunet, C. Dionigi, O. Juanes, M. J. de la Mata, J. C. Rodríguez-Ubis and R. Vivani, *Angew. Chem. Int. Ed. Engl.*, 1999, **38**, 3351.
- 6 G. Alberti, S. Murcia-Mascarós and R. Vivani, *J. Am. Chem. Soc.*, 1998, **120**, 9291.
- 7 D. Mochizuki, A. Shimojima and K. Kuroda, *J. Am. Chem. Soc.*, 2002, **124**, 12082.
- 8 I. Fujita and K. Kuroda, *Chem. Mater.*, in press,
- 9 E. Ruiz-Hitzky and J. M. Rojo, *Nature*, 1980, **287**, 28.
- 10 Y. Mitamura, Y. Komori, S. Hayashi, Y. Sugahara and K. Kuroda, *Chem. Mater.*, 2001, **13**, 3747.
- 11 S. Okutomo, K. Kuroda and M. Ogawa, *Appl. Clay Sci.*, 1999, **15**, 253.
- 12 M. Inoue, M. Kimura and T. Inui, *Chem. Mater.*, 2000, **12**, 55.
- 13 M. Inoue, Y. Kondo and T. Inui, *Chem. Lett.*, 1986, 1421.
- 14 M. Inoue, H. Kominami, Y. Kondo and T. Inui, *Chem. Mater.*, 1997, **9**, 1614.
- 15 S. Ogata, H. Tagaya, M. Karasu and J. Kadokawa, *J. Mater. Chem.*, 2000, **10**, 321.
- 16 V. PrEvot, C. Forano and J. P. Besse, *Appl. Clay Sci.*, 2001, **18**, 3.
- 17 S. Son, S. Kikkawa, F. Kanamaru and M. Koizumi, *Inorg. Chem.*, 1980, **19**, 262.
- 18 S. Kikkawa, F. Kanamaru and M. Koizumi, *Inorg. Chem.*, 1980, **19**, 259.
- 19 S. Kikkawa, F. Kanamaru and M. Koizumi, *Inorg. Chem.*, 1976, **15**, 2195.
- 20 H. Suzuki, K. Notsu, Y. Takeda, W. Sugimoto and Y. Sugahara, *Chem. Mater.*, in press.
- 21 J. J. Tunney and C. Detellier, *J. Mater. Chem.*, 1996, **6**, 1679.

### Chapter 3

- 22 Y. Komori, H. Enoto, R. Takenawa, S. Hayashi, Y. Sugahara and K. Kuroda, *Langmuir*, 2000, **16**, 5506.
- 23 Y. Komori, Y. Sugahara and K. Kuroda, *J. Mater. Res.*, 1998, **13**, 930.
- 24 J. J. Tunney and C. Detellier, *Chem. Mater.*, 1993, **5**, 747.
- 25 J. J. Tunney and C. Detellier, *Clays Clay Miner.*, 1994, **42**, 552.
- 26 T. Itagaki, *J. Mater. Chem.*, in press (See Chapter 2).
- 27 J. J. Tunney and C. Detellier, *Can. J. Chem.*, 1997, **75**, 1766.
- 28 Y. Komori, Y. Sugahara and K. Kuroda, *Chem. Mater.*, 1999, **11**, 3.
- 29 Y. Komori, Y. Sugahara and K. Kuroda, *Appl. Clay Sci.*, 1999, **15**, 241.
- 30 S. Olejnik, A. M. Posner and J. P. Quirk, *Clay Miner.*, 1970, **8**, 421.
- 31 E. Mendelevici, R. L. Frost and T. Kloprogge, *J. Raman Spectrosc.*, 2000, **31**, 1121.

Table 3-1 Organic amounts of alkoxy groups in methoxy-modified kaolinite and organically modified kaolinite with glycerol

	C contents /mass%	alkoxy groups / Al <sub>2</sub> Si <sub>2</sub> O <sub>5</sub> (OH) <sub>4</sub>
Methoxy-modified kaolinite	1.60	0.37
Kao-Glycerol <sub>graft</sub>	8.05	0.73*

\*: Small amount of methoxy groups were detected in <sup>13</sup>C CP/MAS spectrum. Amount of alkoxy groups was calculated when all methoxy groups were reacted with glycerol and methoxy groups did not exist in sample.

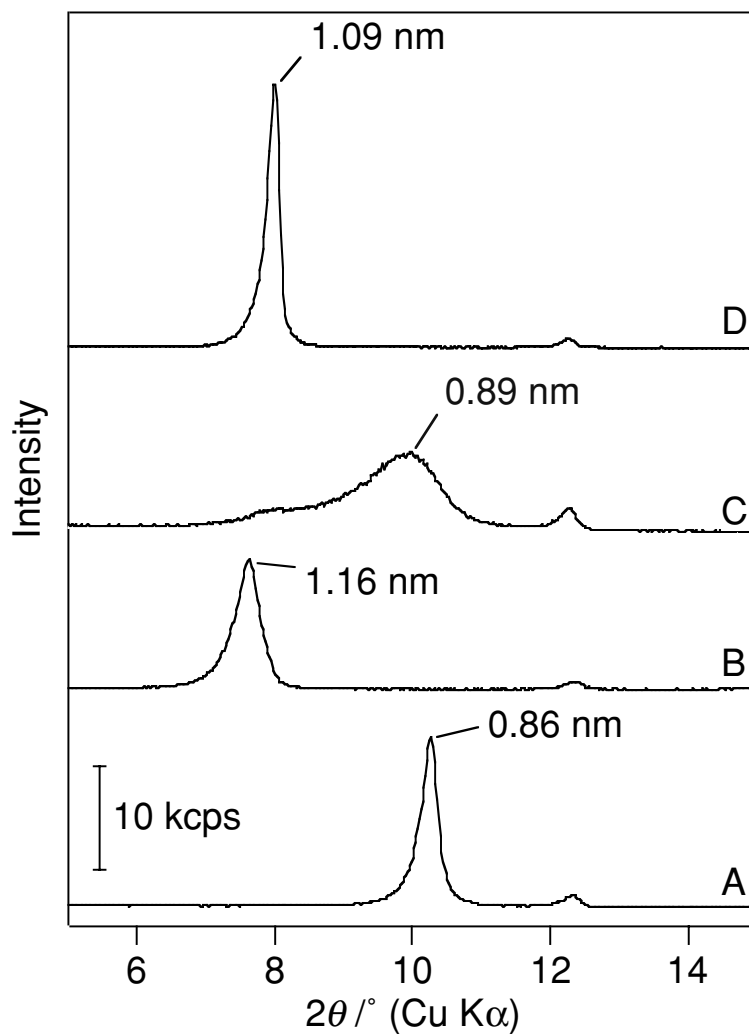


Figure 3-1 XRD patterns of (A) methoxy-modified kaolinite, (B) a kaolinite-glycerol intercalation compound washed by ethylacetate (Kao-Glycerol<sub>int</sub>), (C) a kaolinite-glycerol intercalation compound washed by acetone, and (D) glycerol grafted kaolinite (Kao-Glycerol<sub>graft</sub>)

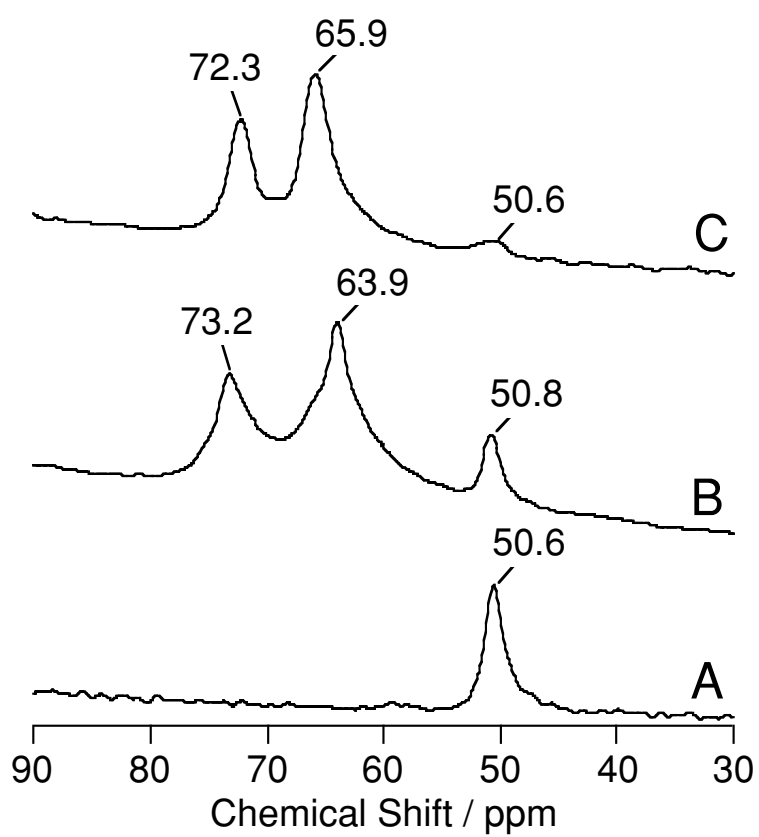


Figure 3-2  $^{13}\text{C}$  MAS NMR spectra without cross polarization of (A) methoxy-modified kaolinite, (B) Kao-Glycerol<sub>int</sub>, and (C) Kao-Glycerol<sub>graft</sub>

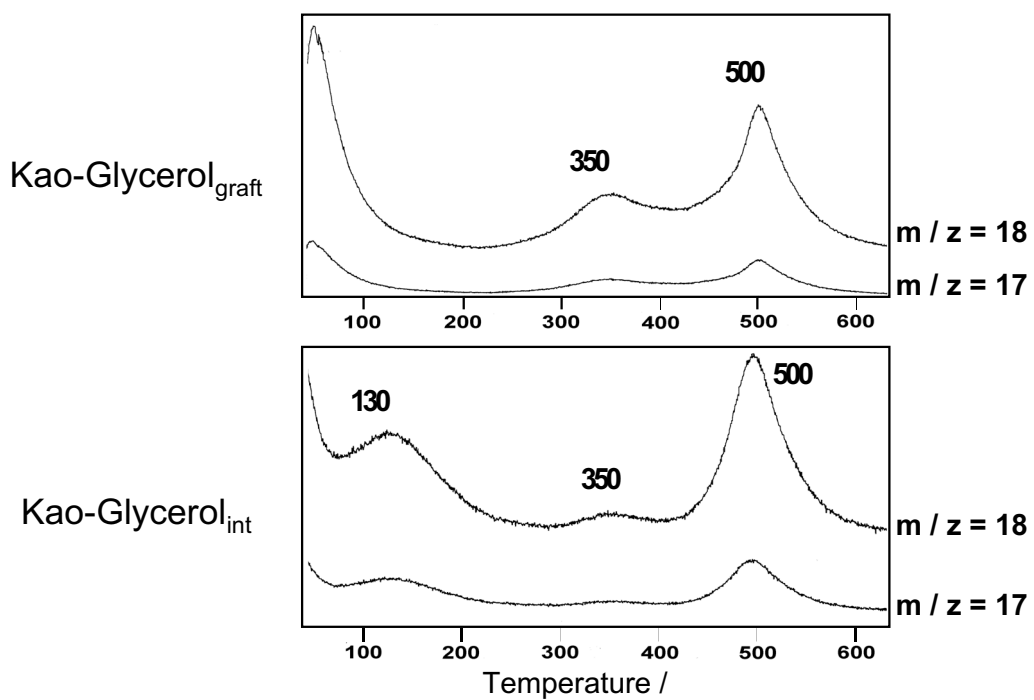


Figure 3-3 Mass chromatograms ( $m/z = 18$  and  $17$ ) of Kao-Glycerol<sub>int</sub> (below) and Kao-Glycerol<sub>graft</sub> (above)

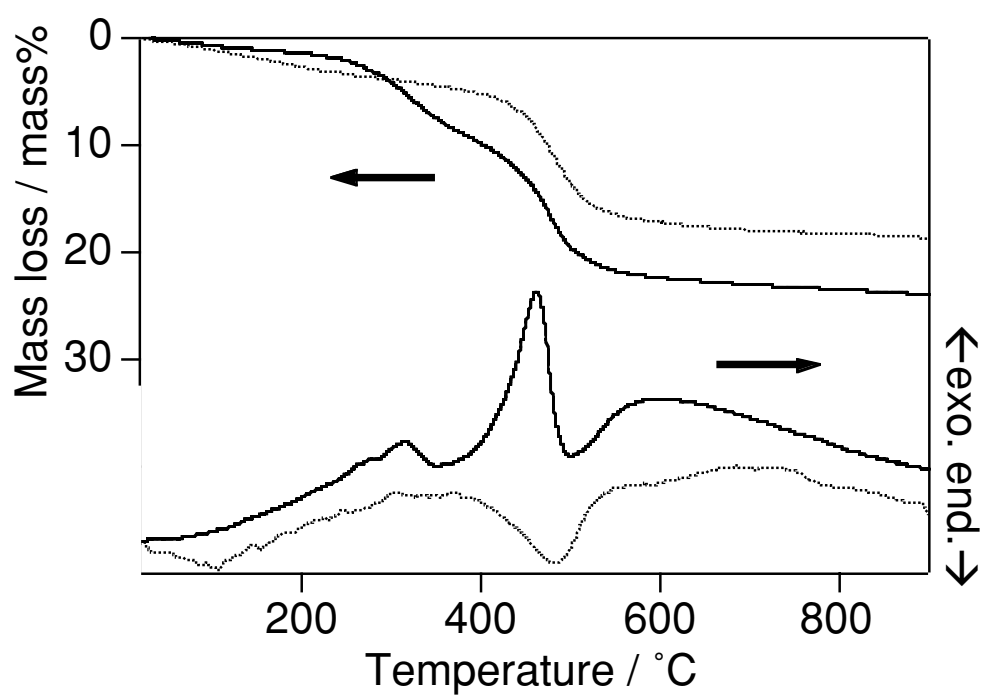


Figure 3-4 DTA-TG curves of methoxy-modified kaolinite (dotted line) and Kao-Glycerol<sub>raft</sub> (solid line).

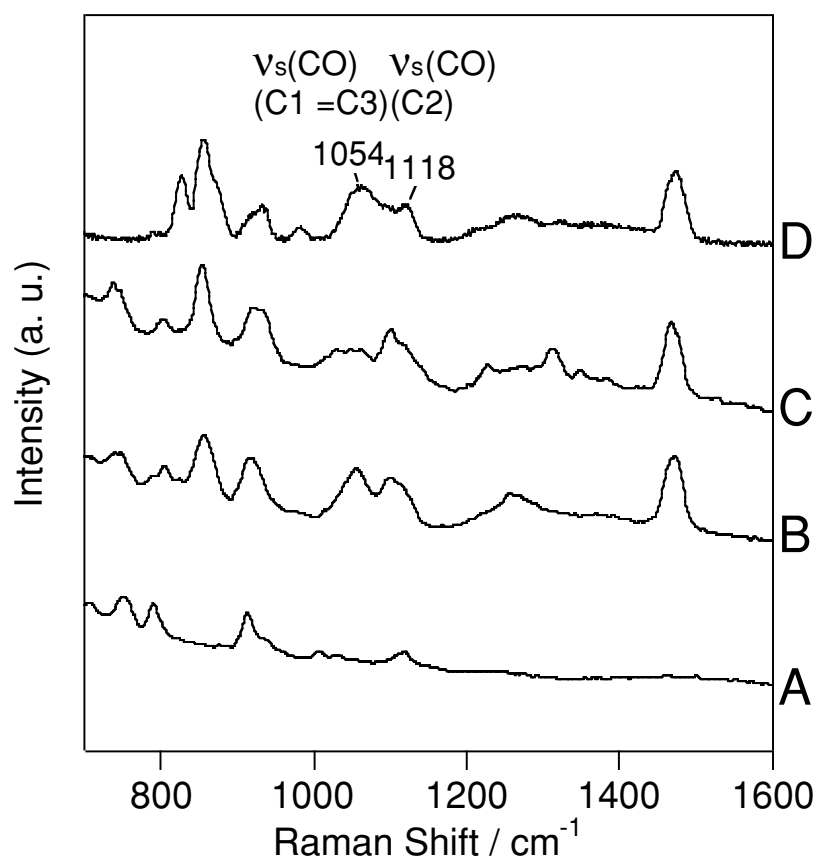


Figure 3-5 Raman spectra of (A) raw kaolinite, (B) Kao-Glycerol<sub>int</sub>, (C) Kao-Glycerol<sub>graft</sub> and (D) liquid glycerol

## CHAPTER 4

### Swelling Behavior of Kaolinite Induced by Organic Modification



## 4.1 Introduction

Organic modification is the route for improving the interlayer environment of inorganic layered materials. For example, zirconium phosphate in which polyethylene oxides chain was bonded to both layers like pillar has variable basal spacing by adsorption / desorption of amine<sup>1</sup>. A layered polysilicate magadiite modified with octyltrichlorosilane has unique interlayer environment, that is, mainly hydrophobic but hydrophilic just only nearby interlayer surface, which enable adsorption of alcohol<sup>2</sup>. Inorganic layered materials which have functional groups on their both interlayer surfaces such as layered zirconium phosphates/phosphonates<sup>3-6</sup>, layered polysilicates, metal dihydroxides<sup>7</sup>, layered double hydroxides<sup>8</sup>, FeOCl<sup>9-12</sup>, and layered perovskites<sup>13</sup> were generally used for organic modification.

Different from these materials, kaolinite ( $\text{Al}_2\text{Si}_2\text{O}_5(\text{OH})_4$ ) is composed of  $\text{Al}_2\text{O}_4(\text{OH})_2$  octahedral and  $\text{SiO}_4$  tetrahedral sheet, and posses OH groups only on  $\text{Al}_2\text{O}_4(\text{OH})_2$  octahedral sheet. Some alcohols<sup>14-21</sup> and phenylphosphonic acid<sup>22</sup> were reported to react with the OH groups on  $\text{Al}_2\text{O}_4(\text{OH})_2$  octahedral sheet. Thus, organically modified kaolinite have two distinctive interlayer surfaces, organic and inorganic interlayer surfaces. Kaolinite is quite unique materials for organic modification on this point. By organic modification new asymmetric interlayer environment is generated and the environment is able to order guest molecules between the layers. After the intercalation of *p*-nitroaniline into methoxy-modified kaolinite, *p*-nitroaniline molecules were ordered in one direction and a kaolinite-*p*-nitroaniline intercalation compound shows SHG property. On the other hand, layer structure of kaolinite was retained by hydrogen bonding between  $\text{Al}_2\text{O}_4(\text{OH})_2$  octahedral and  $\text{SiO}_4$  tetrahedral sheets, which cause kaolinite to be low intercalation properties. Thus, excepting small polar molecules such as *N*-methylformamide and dimethylsulfoxide which were able to be intercalated directly<sup>23</sup>, and guest replacement method was generally needed for the intercalation. Intercalation properties will be improved after organic modification because the number of OH groups decrease and adequate interlayer environment is

## Chapter 4

able to be designed. Our laboratory focused on these characteristics, and prepared some organically modified kaolinite<sup>14-17</sup>. On these processes, I found that kaolinite, typical non-swelling clay mineral, showed the swelling behavior by organic modification of kaolinite. Here I report this phenomenon in this paper.

## 4.2 Experimental

### *Materials*

Well-crystallized kaolinite from Georgia (KGa-1), obtained from the Source Clays Repository of Clay Minerals Society (U.S.A.), was used after grinding for a few minutes to pass a 100-mesh sieve. Ethylene glycol, 1,2-(and 1,3-)propanediol, and aminoethanol (Kanto Chemical Co. Inc.), 1,2-(and 1,3-)butanediol (Tokyo Kasei Kogyo Co., Ltd.), and dehydrated ethylene glycol (Wako Pure Chemical Industries, Ltd.) were used without further purification.

### *Synthetic procedure*

Wet methoxy-modified kaolinite was reacted with several alcohols for the purpose of transesterification and/or adsorption of alcohols. As an example, the reaction between wet methoxy-modified kaolinite was described as follows. At first, methoxy-modified kaolinite was prepared by stirring the suspension of a kaolinite-*N*-methylformamide intercalation compound<sup>23</sup> with methanol several times according the method reported previously<sup>17</sup>. Any drying process was not taken. Next, wet methoxy-modified kaolinite (c.a. 1 g) was dispersed into 100 ml of ethylene glycol and the mixture was refluxed for 1 d under an N<sub>2</sub> flow to obtain kaolinite/ethylene glycol (wet) without any drying process. Kaolinite/ethylene glycol (dry) was obtained after washing kaolinite/ethylene glycol (wet) by acetone several times and drying at 150 °C. Aminoethanol, 1,2-(and 1,3-)propanediol, and 1,2-(and 1,3-)butanediol were also reacted with wet methoxy-modified kaolinite by refluxing for 1 d under an N<sub>2</sub> flow. Detail experimental

conditions were listed in Table 4-1.

To investigate reaction process, the suspension of kaolinite/ethylene glycol (dry) with dehydrated ethylene glycol was refluxed for 1 d. The product was mentioned as kaolinite/alcohols (two times refluxing, wet).

### *Analyses*

Powder XRD patterns were obtained by a Mac Science MXP<sup>3</sup> diffractometer with graphite monochromated CuK $\alpha$  radiation and a Mac Science M03XHF<sup>22</sup> diffractometer with Mn filtered FeK $\alpha$  radiation. The <sup>13</sup>C and <sup>29</sup>Si CP/MAS NMR spectra were recorded at 100.52 MHz and 79.42 MHz with the contact times of 2 and 5 ms using the spinning rates of 10 kHz and 5 kHz, respectively. The <sup>29</sup>Si CP/MAS NMR spectrum of wet sample (kaolinite/ethylene glycol (wet)) was measured by using a sealed tube of polychlorotrifluoroethylene (Kel-F) with the spinning rate of 3 kHz. All the chemical shifts were referred with external tetramethylsilane (TMS). DTA and TG curves were recorded with a MAC Science TG-DTA 2010S instrument under a dry air flow (200 ml min<sup>-1</sup>) with a heating rate of 10 °C min<sup>-1</sup>. SEM images were taken by a Hitachi S2500CX scanning electron microscope.

## **4.3 Results and Discussion**

### *Preparation of kaolinite/ethylene glycol*

After refluxing the suspension of methoxy-modified kaolinite with ethylene glycol, a swelling behavior was observed. In the XRD pattern (Fe) of kaolinite/ethylene glycol (wet) (Fig. 4-1C), four peaks with  $d$  values of 0.72, 0.96, 2.9, 4.9, and 6.4 nm were observed. The peak with the  $d$  value of 0.72 nm was assigned to the basal spacing of residual kaolinite. The  $d$  value of 0.96 is almost equal to that of ethylene glycol-grafted kaolinite<sup>19,20</sup> reported previously (0.95 nm). Though kaolinite (from Georgia, KGa-1) included a small amount of anatase, any

## Chapter 4

other impurities were not observed in the XRD pattern of kaolinite (Fig. 4-1A). The peak intensities of 2.9, 4.9, and 6.4 nm were relatively strong compared with that of 0.96 nm. Thus, the products were derived from not impurities like swelling 2:1 type clay minerals but kaolinite. The reproducibility of the product was very low concerning the basal spacing, and different extraordinary large  $d$  values were observed every time that the sample was prepared. These phases with large  $d$  values were also unstable in air, and the positions and intensities of these peaks were changing with time (Fig. 4-2). After washing kaolinite/ethylene glycol (wet) by acetone and drying at 150 °C, the peaks of 2.9, 4.9, and 6.4 nm disappeared (Fig. 4-1D). From these results, we concluded that these unstable phases with extraordinary  $d$  values were derived from the swelling phase of kaolinite with ethylene glycol.

Ethylene glycol was grafted onto the interlayer of kaolinite during refluxing, which was shown by XRD, <sup>13</sup>C CP/MAS NMR, and DTA-TG results. In XRD pattern of kaolinite/ethylene glycol (dry) (Fig. 4-1D), the peak with the basal spacing of 0.94 nm was observed with the very small peak of residual kaolinite, and the value was almost equal to that of glycol-grafted kaolinite<sup>19, 20</sup> reported previously (0.95 nm). The phases of methoxy-modified kaolinite and swollen kaolinite were not detected. The signal appeared at 64.9 ppm (-CH<sub>2</sub>O-) and the signal intensity at 49.0 due to methoxy group was very weak in the NMR spectrum of kaolinite/ethylene glycol (dry) (Fig. 4-3B). Exothermic peak with evident mass loss was observed at ca. 500 °C in DTA-TG curves of kaolinite/ethylene glycol (wet) (Fig. 4-4). The temperature was higher than the boiling point of liquid ethylene glycol (197.6 °C) and the exothermic peak with mass loss was not observed in DTA-TG curves of methoxy-modified kaolinite (not shown). Thus, this exothermic peak means intercalated ethylene glycol was not desorbed until 400 °C and was decomposed, that is, ethylene glycol was not molecular intercalated but was grafted into aluminosilicate layer. Ethylene glycol was probably reacted with methoxy-modified kaolinite via transesterification same as the cases of propanediols<sup>14</sup> and glycerol<sup>15</sup>.

Solid-state <sup>29</sup>Si CP/MAS NMR spectroscopy was used to examine the <sup>29</sup>Si environments

of kaolinite/ethylene glycol (wet) and (dry). Kaolinite exhibits two  $^{29}\text{Si}$  NMR resonances at  $-90.9$  and  $-91.3$  ppm, which is induced by the interlayer hydrogen bonding between layers or different distances between Si and Al atoms (Fig. 4-5A)<sup>24,25</sup>. By intercalation of organic molecules, this split disappeared and the signals generally shifted to lower frequencies. This shift is caused by the weaker interaction between  $\text{SiO}_4$  tetrahedral sheet and guest molecules than pristine hydrogen bonding between  $\text{SiO}_4$  tetrahedral and  $\text{AlO}_4(\text{OH})_2$  octahedral sheet<sup>26</sup>. In the  $^{29}\text{Si}$  CP/MAS NMR spectra of alcohol-grafted kaolinite, one signal was also observed at lower frequencies<sup>14, 15, 17</sup>. For example, one signal was observed at  $-91.6$  ppm in the  $^{29}\text{Si}$  CP/MAS NMR spectrum of methoxy-modified kaolinite (Fig. 4-5B). In the  $^{29}\text{Si}$  CP/MAS NMR spectra of kaolinite/ethylene glycol (dry) and (wet), the signals were observed at  $-91.9$  and  $-92.1$  ppm with the shoulder to high frequencies, respectively (Fig. 4-5D and C). The  $^{29}\text{Si}$  CP/MAS NMR spectrum of kaolinite/ethylene glycol (wet) was almost same as that of kaolinite/ethylene glycol (dry), which suggesting that the layer of swollen kaolinite was grafted with not methanol but ethylene glycol. The signal at  $-92.1$  ppm in the  $^{29}\text{Si}$  NMR spectrum of kaolinite/ethylene glycol was at highest frequencies of all samples, which may be explained by that in wet condition the interactions between organically modified aluminosilicate (the bonding force of the layers) sheets was weakest because of layer expansion.

Figure 4-6 shows SEM images of kaolinite, methoxy-modified kaolinite and kaolinite/ethylene glycol (dry). The plate-like particles with the particle size from ca. 0.2-1.5  $\mu\text{m}$  were observed in SEM images of kaolinite (Fig. 4-6A) and methoxy-modified kaolinite (Fig. 4-6B). After reaction between methoxy-modified kaolinite and ethylene glycol, significant change concerning particles size and aspect ratio was not observed (Fig. 4-6C).

By the reaction between kaolinite/ethylene glycol (dry) and anhydrous ethylene glycol, the phase due to swollen kaolinite appeared in the XRD pattern of kaolinite/ethylene glycol (two times refluxing) (Fig. 4-1E). This showed that methoxy groups on the interlayer surface of kaolinite and  $\text{H}_2\text{O}$  were not necessary for swollen kaolinite and swelling behavior of kaolinite

## Chapter 4

was probably caused by adsorption of ethylene glycol in ethylene glycol-grafted kaolinite. Proposed reaction scheme between methoxy-modified kaolinite and ethylene glycol was illustrated in Scheme 4-1. At first, transesterification between methoxy-modified and ethylene glycol proceeded. Next, some ethylene glycol-modified kaolinite was swollen into ethylene glycol. Adsorbed ethylene glycol was deintercalated during washing and drying process and ethylene glycol-grafted kaolinite was obtained.

Methoxy-modified kaolinite was reacted with various alcohols (1,2-(and 1,3-)propanediol, 1,2-(and 1,3-)butanediol, and aminoethanol). Fig. 4-7 shows XRD patterns of wet sample and the basal spacings of the products were listed in Table 4-2. In all XRD patterns of wet samples, several basal spacings of c.a. 1 and 3-5 nm were observed in XRD patterns of wet samples (Fig. 4-7C~G). In XRD patterns of dried samples (Table 4-2), the basal spacing of c.a. 1 nm was also observed and the swelling phase disappeared. Organic modification of 1,2-(and 1,3-)propanediol<sup>14, 20</sup> and aminoethanol<sup>18</sup> was reported. These data suggested that these alcohols were adsorbed into alcohol-grafted kaolinite same as the case of ethylene glycol. Diols and aminoethanol with two functional groups probably play the important role in swell of organically modified kaolinite.

### 4.4 Conclusion

Kaolinite partially swelled by the reaction between methoxy-modified kaolinite and ethylene glycol. During the reaction, ethylene glycol was grafted onto the interlayer surface of kaolinite. The swelling behavior was probably caused by intercalation of ethylene glycol to ethylene glycol-grafted kaolinite. Swollen phase was very unstable in air and the basal spacing was changed with time. Several diols and aminoethanol also showed similar swelling behavior. Swelling behavior induced by organic modification will expand a potential of kaolinite as industrial materials and shows a potential for exfoliation of non-swelling clay mineral kaolinite. Next step is to add the properties characteristic to its crystal structure by organic modification.

## 4.5 References

- 1 G. Alberti, E. Brunet, C. Dionigi, O. Juanes, M. J. de la Mata, J. C. Rodríguez-Ubis and R. Vivani, *Angew. Chem. Int. Ed. Engl.*, 1999, **38**, 3351.
- 2 M. Ogawa, S. Okutomo and K. Kuroda, *J. Am. Chem. Soc.*, 1998, **120**, 7361.
- 3 A. Clearfield and Z. Wang, *J. Chem.Soc., Dalton Trans.*, 2002, 2937.
- 4 G. Alberti, M. Casciola, U. Constantino and R. Vivani, *Adv. Mater.*, 1996, **8**, 291.
- 5 G. Alberti, R. Vivani, F. Marmottini and P. Zappelli, *J. Porous. Mater.*, 1998, **5**, 205.
- 6 A. Clearfield, *Chem. Mater.*, 1998, **10**, 2801.
- 7 S. Ogata, H. Tagaya, M. Karasu and J. Kadokawa, *J. Mater. Chem.*, 2000, **10**, 321.
- 8 V. Prévot, C. Forano and J. P. Besse, *Appl. Clay Sci.*, 2001, **18**, 3.
- 9 S. Kikkawa, F. Kanamaru and M. Koizumi, *Inorg. Chem.*, 1980, **19**, 259.
- 10 S. Kikkawa, F. Kanamaru and M. Koizumi, *Inorg. Chem.*, 1976, **15**, 2195.
- 11 S. Son, S. Kikkawa, F. Kanamaru and M. Koizumi, *Inorg. Chem.*, 1980, **19**, 262.
- 12 Z. Takehara, H. Sakaebe and K. Kanamura, *J. Power Sources*, 1993, **43-44**, 627.
- 13 H. Suzuki, K. Notsu, Y. Takeda, W. Sugimoto and Y. Sugahara, *Chem. Mater.*, in press.
- 14 T. Itagaki, *J. Mater. Chem.*, in press (See Chapter 2).
- 15 T. Itagaki, Chapter 3.
- 16 Y. Komori, Y. Sugahara and K. Kuroda, *J. Mater. Res.*, 1998, **13**, 930.
- 17 Y. Komori, H. Enoto, R. Takenawa, S. Hayashi, Y. Sugahara and K. Kuroda, *Langmuir*, 2000, **16**, 5506.
- 18 J. J. Tunney and C. Detellier, *Can. J. Chem.*, 1997, **75**, 1766.
- 19 J. J. Tunney and C. Detellier, *Clays Clay Miner*, 1994, **42**, 552.
- 20 J. J. Tunney and C. Detellier, *Chem. Mater.*, 1993, **5**, 747.
- 21 J. J. Tunney and C. Detellier, *J. Mater. Chem.*, 1996, **6**, 1679.
- 22 J. Guimaraes, P. Peralta-Zamora and F. Wypych, *J. Colloid Interface. Sci.*, 1998, **206**, 281.

## *Chapter 4*

23 S. Olejnik, A. M. Posner and J. P. Quirk, *Clay Miner.*, 1970, **8**, 421.

24 J. G. Thompson, *Clays Clay Miner*, 1984, **32**, 233.

25 P. Barron, R. L. Frost, J. O. Skjemstad and A. J. Koppi, *Nature*, 1983, **302**, 49.

26 J. G. Thompson, *Clays Clay Miner*, 1985, **33**, 173.

Table 4-1 the basal spacings of kaolinite/alcohols (dry)

	the basal spacing / nm	wash	drying
ethylene glycol	6.4, 4.9, 2.9, 0.96	acetone	<i>in vacuo</i>
1,2-propanediol <sup>14</sup>	4.6, 3.8, 1.09	1,4-dioxane	<i>in vacuo</i>
1,3-propanediol <sup>14</sup>	5.8, 4.9, 1.12	1,4-dioxane	<i>in vacuo</i>
1,2-butanediol	4.6, 3.8, 1.09	acetone	<i>in vacuo</i>
1,3-butanediol	4.3, 3.4, 1.16	acetone	<i>in vacuo</i>
aminoethanol	5.0, 4.6, 4.3, 1.08	1,4-dioxane	<i>in vacuo</i>

Table 4-2 the basal spacings of kaolinite/alcohols (dry)

	basal spacing / nm	
	wet	dry
methoxy-modified kaolinite	1.1	0.86
kaolinite/ethylene glycol	6.4, 4.9, 2.9, 0.96	0.94
kaolinite/1,2-propanediol	4.6, 3.8, 1.09	1.08
kaolinite/1,3-propanediol	5.8, 4.9, 1.12	1.11
kaolinite/1,2-butanediol	4.6, 3.8, 1.09	1.18
kaolinite/1,3-butanediol	4.3, 3.4, 1.16	1.16
kaolinite/aminoethanol	5.0, 4.6, 4.3, 1.08	

The basal spacing of wet sample was determined by FeK $\alpha$  radiation, and that of dried sample was by CuK $\alpha$  radiation.

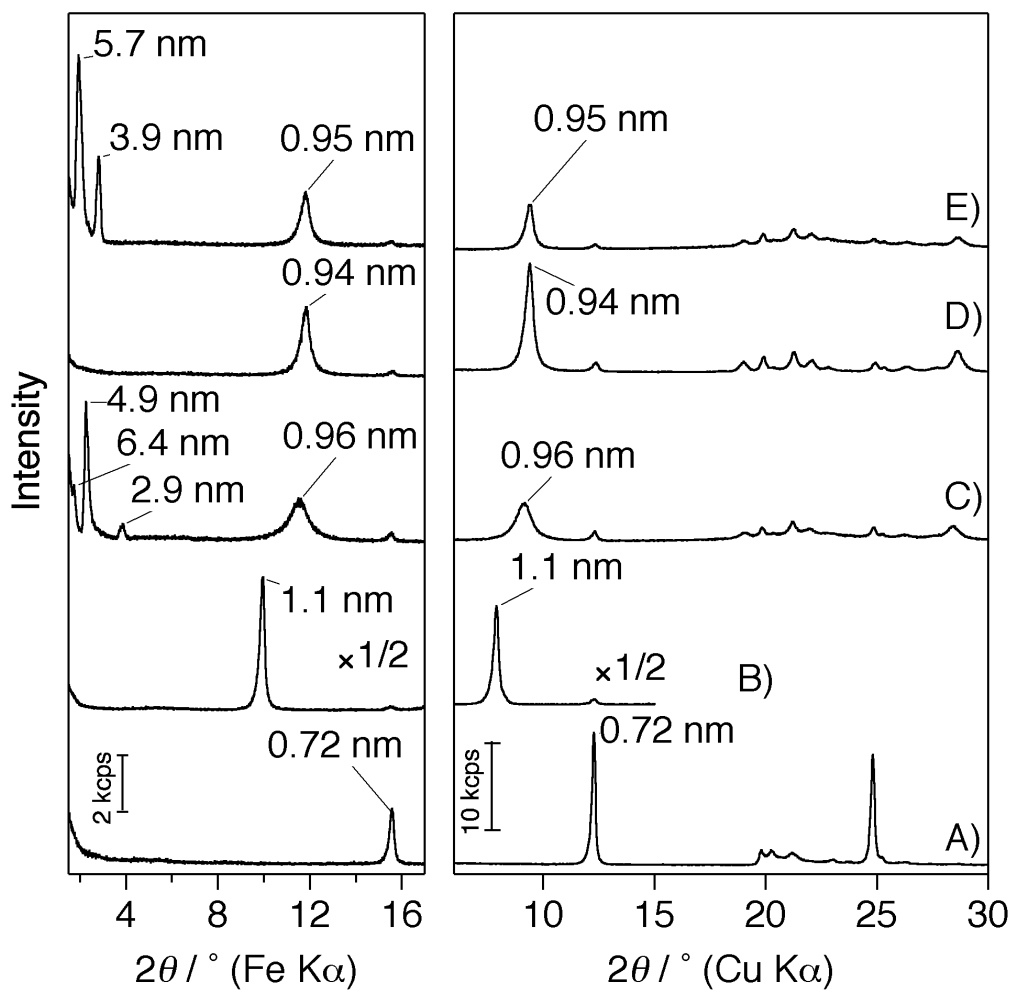


Figure 4-1 XRD patterns of A) kaolinite, B) methoxy-modified kaolinite (wet), C) kaolinite/ethylene glycol (wet), D) kaolinite/ethylene glycol (dry), and E) kaolinite/ethylene glycol (two times refluxing).

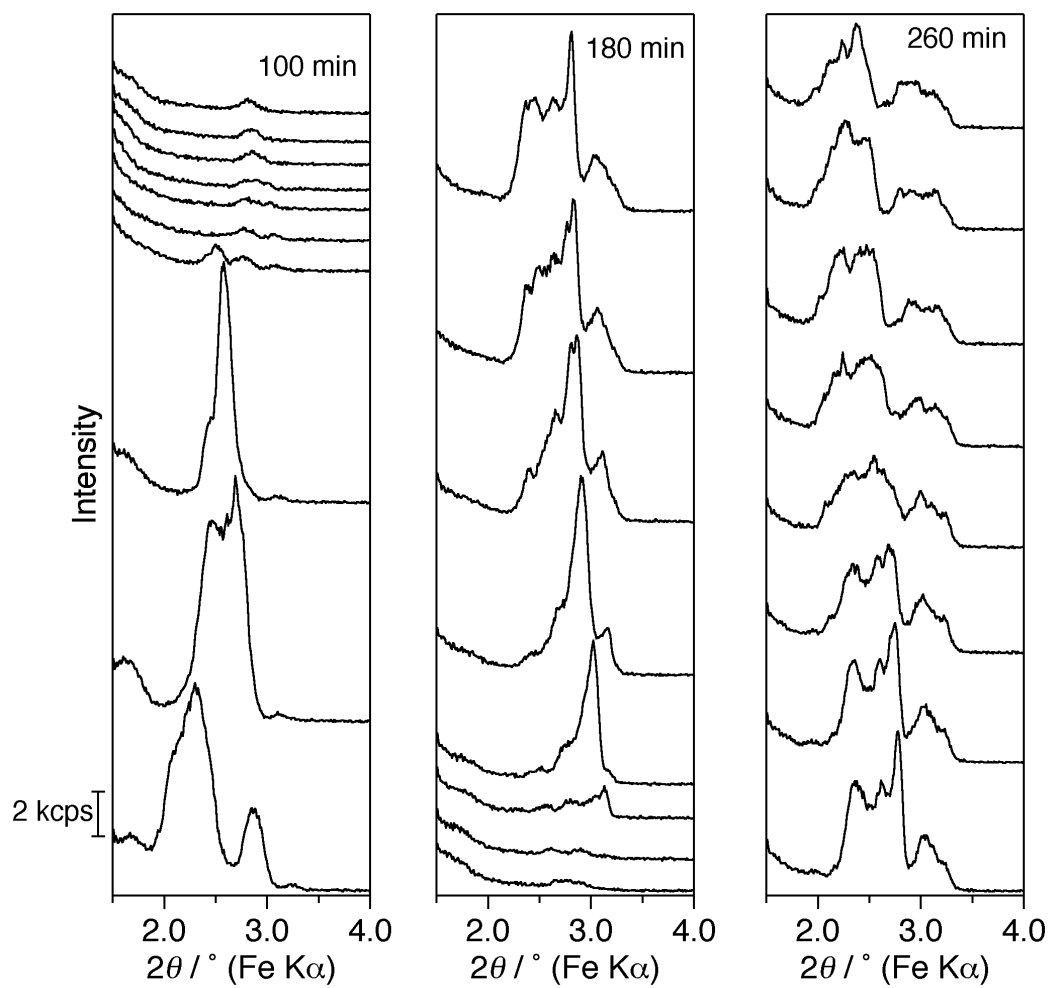


Figure 4-2 XRD pattern of kaolinite/ethylene glycol (wet). Each pattern was recorded every 10 min and sample after 260 min was still wet.

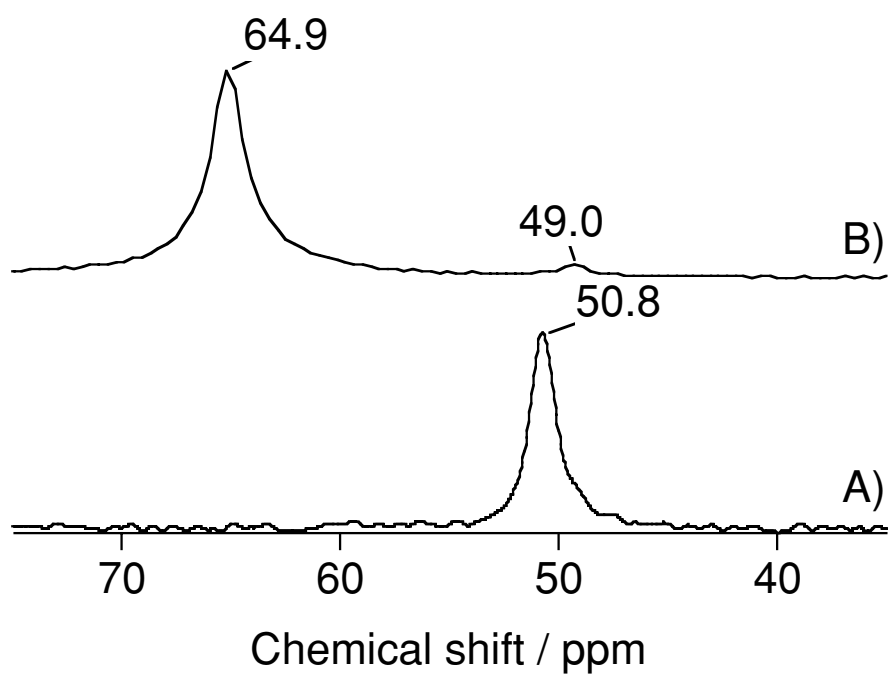


Figure 4-3  $^{13}\text{C}$  CP/MAS NMR spectra of A) methoxy-modified kaolinite (dry) and B) kaolinite/ethylene glycol (dry)

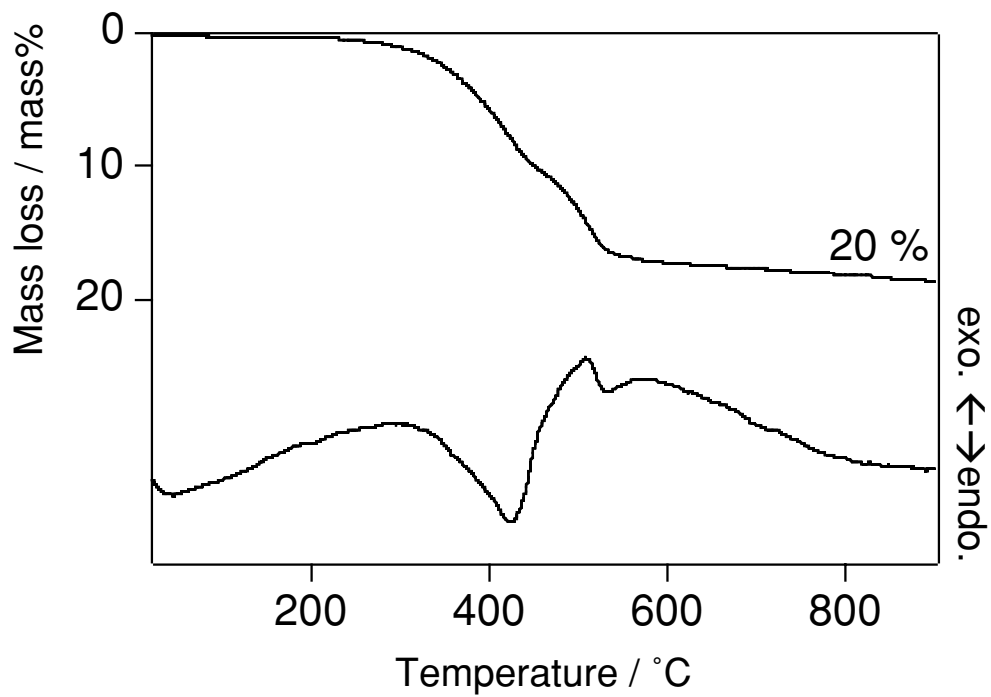


Figure 4-4 DTA-TG curve of kaolinite/ethylene glycol (dry)

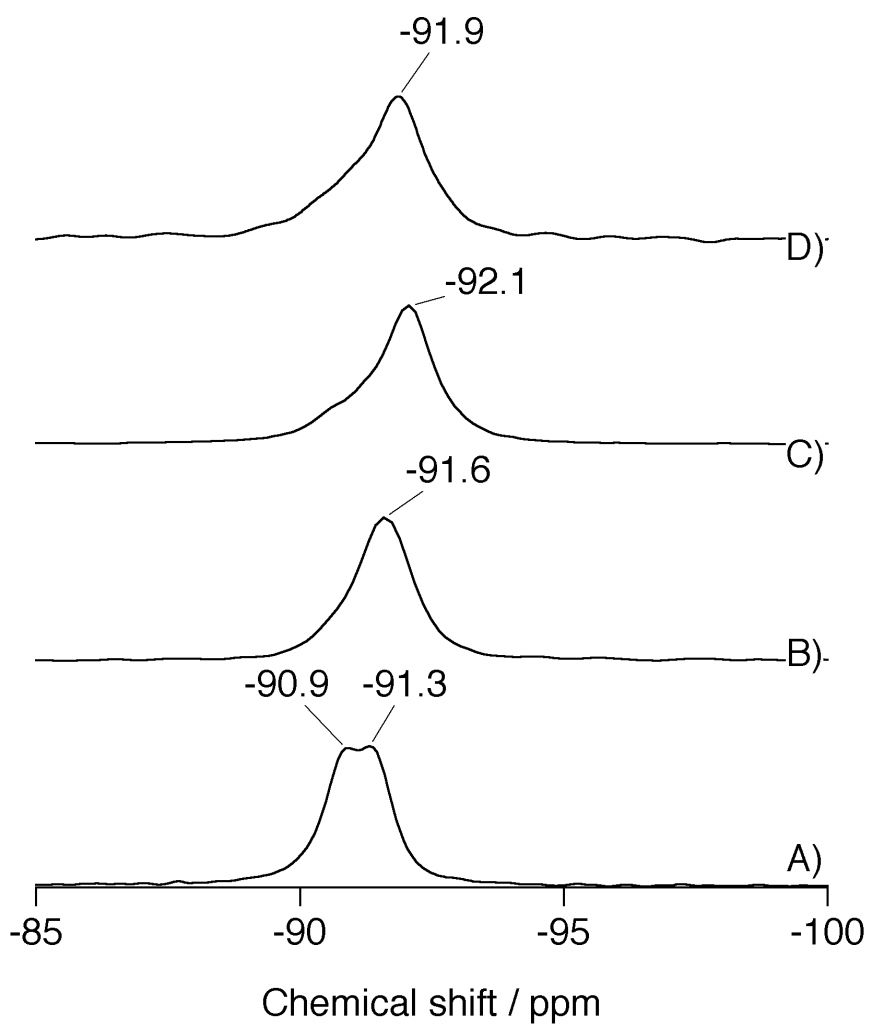
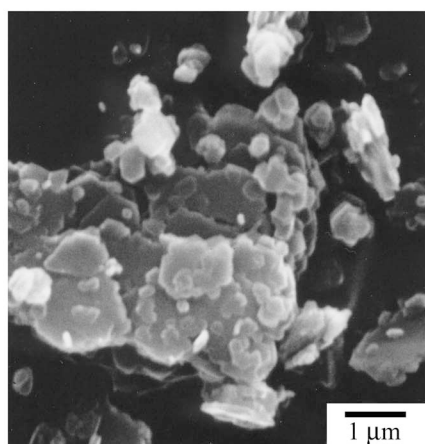
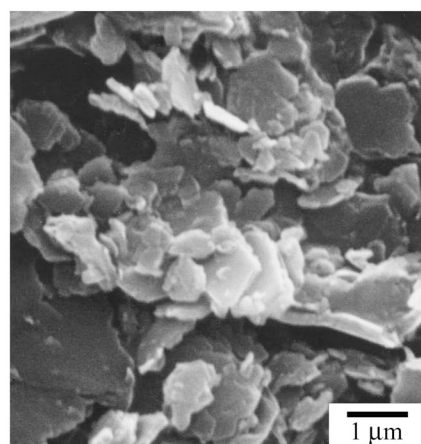


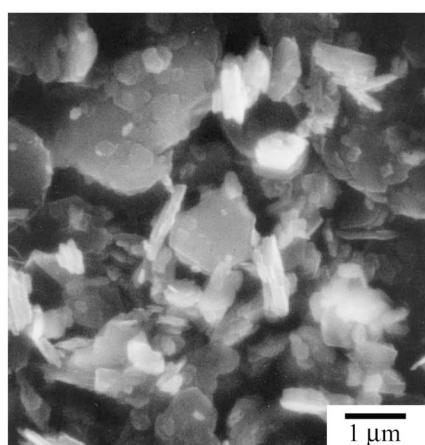
Figure 4-5  $^{29}\text{Si}$  NMR spectra of A) kaolinite, B) methoxy-modified kaolinite, C) kaolinite/ethylene glycol (wet), and kaolinite/ethylene glycol (dry)



**A) kaolinite**



**B) methoxy-modified kaolinite**



**C) Kao-EG<sub>graft</sub>**

Figure 4-6 SEM images of A) kaolinite, B) methoxy-modified kaolinite, and C) kaolinite/ethylene glycol (dry)

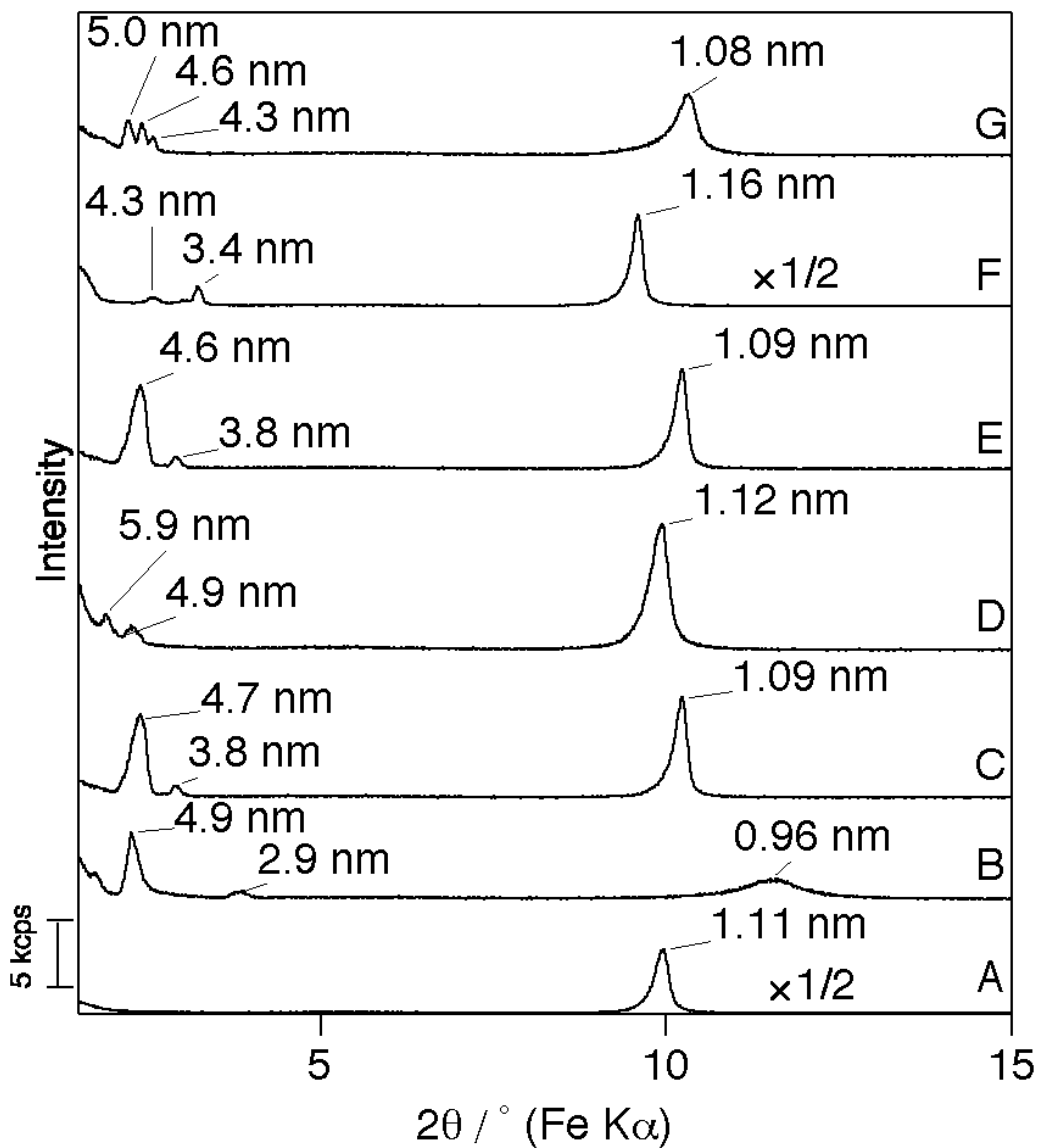
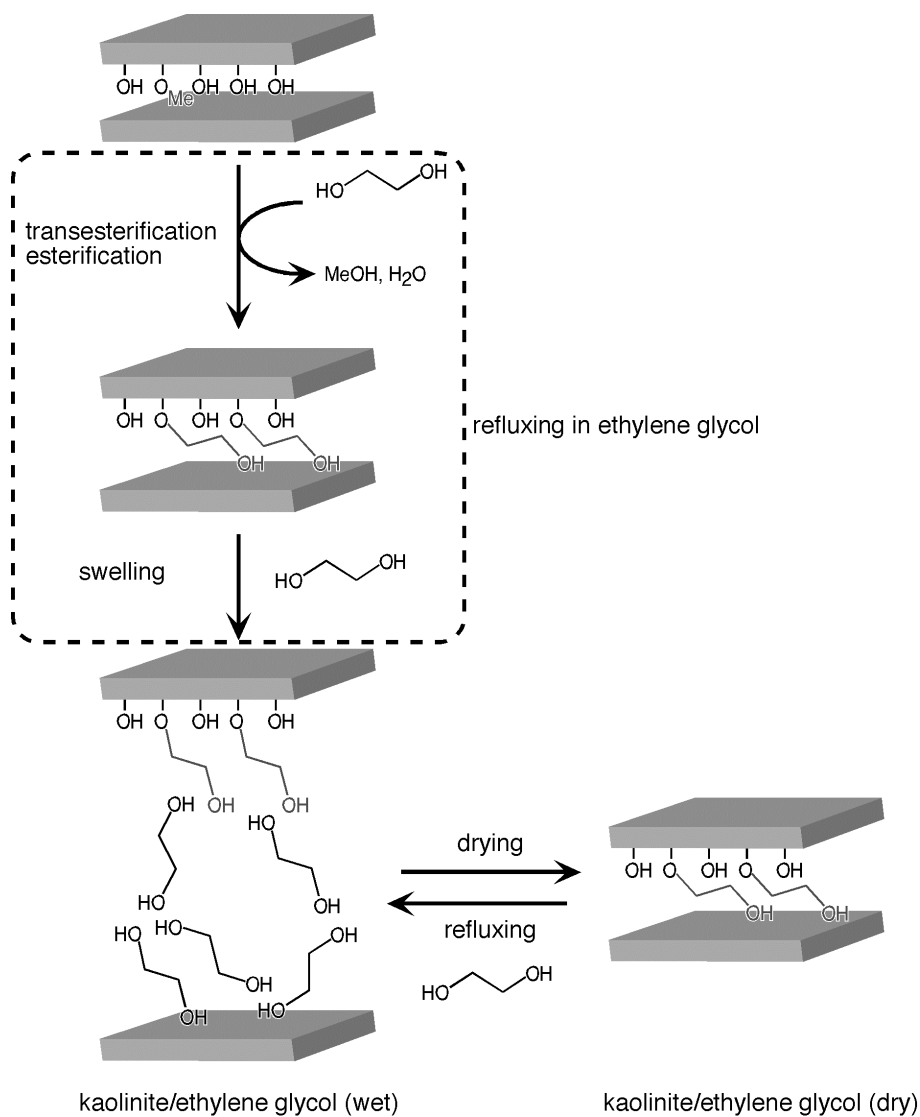


Figure 4-7 XRD patterns of A) methoxy-modified kaolinite (wet), B) kaolinite/ethylene glycol (wet), C) kaolinite/1,2-propanediol (wet), D) kaolinite/1,3-propanediol (wet), E) kaolinite/1,2-butanediol (wet), F) kaolinite/1,3-butanediol (wet), and G) kaolinite/aminoethanol (wet)



Scheme 4-1 Reaction pathway between methoxy modified kaolinite and ethylene glycol



## CHAPTER 5

### Synthesis and Mechanical Properties of Kaolinite/Polymer Nanocomposites



## 5.1 Preparation of a Kaolinite–Nylon 6 Intercalation Compound

### 5.1.1 Introduction

Interactions between inorganic layered materials and organic substances have attracted increasing interest from both scientific and industrial perspectives.<sup>1-4</sup> The intercalation of polymers into inorganic layered materials, such as clay minerals, with a retention of the layered nature is an excellent way to construct novel inorganic-polymer nanoassemblies.<sup>5</sup> A smectite group of clay minerals, such as montmorillonite, has mainly been used because of their excellent intercalation abilities.<sup>6-8</sup> Other types of layered silicates have been used for preparing polymer intercalation compounds to a much lesser degree because of their lower reactivities for the intercalation of polymers. However, an extension of this kind of host material will lead to various layered silicate-based nanocomposites with compositional and structural variations, which can be directed toward new applications.<sup>9</sup>

Kaolinite, a 1:1 type clay mineral, is a unique layered material because the interlayer space is sandwiched by OH groups of octahedral aluminum hydroxide sheets and oxygen atoms of tetrahedral silicate sheets. Because of the inherent hydrogen bonds between the layers, a limited number of small polar guest molecules, such as dimethylsulfoxide (DMSO) and *N*-methylformamide (NMF), are directly intercalated.<sup>10</sup> Guest molecules are intercalated by forming new hydrogen bonds. A guest displacement method has enabled the formation of various kinds of intercalation compounds of kaolinite. So far, intercalation compounds with NMF,<sup>10</sup> ammonium acetate<sup>11</sup>, and methanol<sup>12</sup> have mainly been used as intermediates for guest displacement reactions. In particular, a kaolinite–methanol intercalation compound has been found to be an excellent intermediate that can be used for the intercalation of relatively large molecules, such as alkylamines,<sup>13</sup> *p*-nitroaniline,<sup>14</sup>  $\epsilon$ -caprolactam<sup>15</sup>, and poly(vinylpyrrolidone).<sup>16</sup>

Kaolinite–polymer intercalation compounds have been prepared by two methods. Some

## Chapter 5

polymers are directly intercalated,<sup>16-18</sup> and the others are intercalated by the *in situ* polymerization of preintercalated monomers between the layers of kaolinite.<sup>11, 19-21</sup> The number of polymers, which are intercalated directly, is so limited that the route utilizing preintercalated monomers is important. In addition to vinyl polymerization,<sup>11, 19, 20</sup> I have reported a polycondensation reaction of  $\beta$ -alanine [ $\text{H}_2\text{N}-(\text{CH}_2)_2-\text{COOH}$ ].<sup>21</sup> Therefore, the formation of a kaolinite–nylon 6 intercalation compound is expected by an *in situ* polymerization reaction of 6-aminohexanoic acid (AHA) [ $\text{H}_2\text{N}-(\text{CH}_2)_5-\text{COOH}$ ]. The nanocomposites of nylon 6 with kaolinite may possess better properties over nylon-smectite hybrids<sup>22-24</sup> because of the high crystallinity, high aspect ratio, and confined interlayer environment of kaolinite.

In this study, as a first step toward nylon-kaolinite hybrids, the intercalation of AHA and its polymerization reaction were investigated. The intercalation of several kinds of  $\omega$ -amino acid with shorter carbon chains has been reported.<sup>21, 25</sup> However, the formation of a kaolinite–AHA intercalation compound has not been successful because of its large size and low ability to form an intercalation compound with kaolinite, though AHA molecules are intercalated into vermiculite and montmorillonite.<sup>26, 27</sup> To overcome this difficulty, I employed a guest displacement reaction using a kaolinite–methanol intercalation compound as an intermediate. Furthermore, I carried out an *in situ* polymerization reaction by a heat treatment under a nitrogen flow. By comparing with a kaolinite– $\beta$ -alanine intercalation compound,<sup>21</sup> the interactions between kaolinite and AHA and its polymerization behavior are discussed.

### 5.1.2 Experimental

#### *Materials*

Kaolinite used in the present study was KGa-1, well-crystallized Georgia kaolinite obtained from the Source Clays Repository of Clay Minerals Society (U.S.A.).<sup>28</sup> The sample was used

after grinding to pass a 100-mesh sieve. AHA was obtained from Junsei Chemical Co., Ltd.

### ***Preparation of a Kaolinite–AHA Intercalation Compound and in situ Polymerization***

The intercalation of AHA was performed by a fine guest displacement method using a kaolinite–methanol intercalation compound as the intermediate, because no intercalation reactions of AHA took place by utilizing kaolinite, a kaolinite–NMF intercalation compound, or a kaolinite–ammonium acetate intercalation compound. Because the basal spacing of a dried kaolinite–methanol intercalation compound decreased to 0.86 nm, a wet kaolinite–methanol intercalation compound with a larger spacing (1.11 nm, Fig. 5-1b) was prepared according to a method reported previously.<sup>12, 29</sup> At first, a kaolinite–NMF intercalation compound (basal spacing, 1.08 nm) was prepared, and then a guest displacement reaction between NMF and methanol was conducted. The wet kaolinite–methanol intercalation compound was added into a saturated AHA solution (solvent (methanol : water = 1 : 3), AHA (740 g/l)) and the mixture was stirred at 30 °C for 3 h. A slight excess of AHA was found in the medium. The product was centrifuged and dried in a desiccator. *In situ* polymerization of the kaolinite–AHA intercalation compound was performed by a heat treatment in a tube furnace at 250 °C for 1 h under a nitrogen flow. For a comparison, bulk AHA without kaolinite was also heated under the same conditions.

### **5.1.2 Characterization**

XRD patterns were obtained by using a Mac Science MXP<sup>3</sup> diffractometer with monochromated CuK $\alpha$  radiation. Solid-state <sup>13</sup>C and <sup>29</sup>Si CP/MAS NMR measurements were performed on a JEOL GSX-400 spectrometer with a spinning rate of 5 kHz. The Larmor frequencies of <sup>13</sup>C and <sup>29</sup>Si were 100.40 MHz and 79.30 MHz, respectively. The chemical shifts were expressed with respect to tetramethylsilane. Infrared spectra (IR) were recorded on a Perkin-Elmer Spectrum ONE FTIR spectrometer using the KBr-disk technique. The amounts

of organic fractions were determined by a CHN analysis using a Perkin-Elmer PE-2400II apparatus. TG and DTA curves were obtained on a Mac Science 2000S instrument. The heating rate was 10 °C min<sup>-1</sup> under a nitrogen flow. A TG-MS analysis was performed on a combined Shimadzu TGA-50 and GCMS-QP1100EX under a He atmosphere at a heating rate of 10 °C min<sup>-1</sup>.

### 5.1.3 Results and Discussion

#### *Preparation of a Kaolinite-AHA Intercalation Compound*

Figure 5-1c shows the XRD pattern of the product. The basal spacing of the product is 1.23 nm, which is larger than those of kaolinite (0.72 nm; Fig. 5-1a) and the kaolinite–methanol intercalation compound (1.11 nm; Fig. 5-1b), indicating the intercalation of AHA into kaolinite. Higher order diffraction peaks (002, 003, and 004) are also observed (not shown). The intensities of the peak at 10.6 ° (0.84 nm) due to crystalline AHA adsorbed on the surface and the broad peak at around 10 ° (~0.86 nm) due to an unreacted phase (dried kaolinite–methanol intercalation compound)<sup>29</sup> are very weak. On the basis of both the interlayer distance of the product (0.51 nm) and the molecular size of AHA (ca. 0.42 × 0.51 × 1.00 nm), it is very likely that AHA molecules take a monolayer arrangement between the layers of kaolinite. The value of the basal spacing (1.23 nm) is larger than those of the kaolinite intercalation compounds with ω-amino acids containing shorter carbon chains (β-alanine, 1.17 nm; γ-aminobutyric acid, 1.20 nm; δ-aminovaleric acid, 1.21 nm).<sup>21, 26</sup> However, the slight degree of the increment with the chain length indicates that the direction of the carbon chains of ω-amino acids is basically parallel to the plane of the layers.

Figure 5-2b shows the <sup>13</sup>C CP/MAS NMR spectrum of the kaolinite–AHA intercalation compound. The signals due to CH<sub>2</sub> groups of AHA appear at ca. 27 ~ 30 and 40.1 ppm. They are

broader than those of bulk AHA (Fig. 5-2a), suggesting that the methylene chains are distorted by a restriction in the interlayer space of kaolinite. The signal at 50 ppm is due to the methoxy groups bound to hydroxy groups of kaolinite.<sup>29</sup> On the other hand, two signals due to C=O groups at 182.3 and 185.0 ppm are detected. The chemical shift of the first signal at 182.3 ppm is very similar to that in the spectrum of AHA (Fig. 5-2a; 182.4 ppm). The second signal is a peculiar one for an intercalation compound, which may be related to the AHA molecules, distorted by the restriction. The presence of two kinds of carbonyl groups has also been reported for a kaolinite–poly(vinylpyrrolidone) (PVP) intercalation compound,<sup>16</sup> in which signals at 176.2 and 182.9 ppm were observed (175.3 ppm for bulk PVP).

Figure 5-3 shows the IR spectra in the range between 1200 and 1800  $\text{cm}^{-1}$ . In the spectrum of the kaolinite–AHA intercalation compound, the bands due to  $\delta_{\text{as}}(\text{NH}_3^+)$  (1623 and 1652  $\text{cm}^{-1}$ ),  $\delta_{\text{s}}(\text{NH}_3^+)$  (1539  $\text{cm}^{-1}$ ) and  $\nu(\text{COO}^-)$  (1390 and 1561  $\text{cm}^{-1}$ ) are observed.<sup>30</sup> Because the intensity of the bands due to  $\nu(\text{NH}_2)$  (3279 and 3433  $\text{cm}^{-1}$ ; not shown) and  $\nu(\text{COOH})$  (1681  $\text{cm}^{-1}$ ) are very small, most of AHA molecules are present as zwitterions. The positions of these bands are very similar to those of the crystalline state, indicating that the hydrogen bondings of these functional groups are similar to those in the crystalline state. Interactions among the AHA molecules are possibly strong, even in the intercalation compound.

Figure 5-4 shows the IR spectra in the OH stretching region. In the spectrum of kaolinite, four bands at 3620, 3651, 3669, and 3693  $\text{cm}^{-1}$  appear (Fig. 5-4a). The band at 3620  $\text{cm}^{-1}$  is assigned to an internal OH group, and the others to outer surface OH groups. By intercalation reactions, the outer OH groups may be perturbed and the OH groups hydrogen-bonded with guest species show new bands at lower wavenumbers, whereas the internal OH group is not influenced.<sup>10</sup> Thus, taking the band at 3620  $\text{cm}^{-1}$  as a reference, interactions between OH groups and guest species can be observed. By the intercalation of AHA, the intensity of the band at 3693  $\text{cm}^{-1}$  decreases and a broad band at around 3640  $\text{cm}^{-1}$  appears (Fig. 5-4b), indicating the formation of new hydrogen bonds between the OH groups and the AHA molecules. Compared

## Chapter 5

with a kaolinite- $\beta$ -alanine intercalation compound,<sup>21</sup> a relatively large band at around  $3640\text{ cm}^{-1}$  appears, whereas the band at  $3603\text{ cm}^{-1}$  is not detected. Therefore, the hydrogen bonds of the OH groups with AHA molecules may be weaker than that with  $\beta$ -alanine.

The Si environments of kaolinite are influenced by the intercalation of guest species. In the  $^{29}\text{Si}$  NMR spectrum of the kaolinite-AHA intercalation, the signal at  $-91.4\text{ ppm}$  is observed (Fig. 5-5b), whereas kaolinite shows a doublet at  $-90.7$  and  $-91.3\text{ ppm}$  (Fig. 5-5a). As for a kaolinite- $\beta$ -alanine intercalation compound, the signal at  $-90.4\text{ ppm}$  has been reported.<sup>21</sup> Therefore, the signal at  $-91.4\text{ ppm}$  for the kaolinite-AHA intercalation compound denotes that the interactions between the silicate sheets and AHA molecules are different from those in the case of  $\beta$ -alanine.

The amount of AHA was estimated by a CHN analysis (Table 5-1). The contents of the carbon and nitrogen are 20.8 and 3.8 mass%, respectively, and the molar ratio of C/N is found to be 6.3. The slight deviation from 6.0 for the chemical composition of AHA is explained by the presence of methoxy groups bound to kaolinite.<sup>29</sup> On the basis of the nitrogen content, 1.2 molecules of AHA per a kaolinite unit of  $\text{Al}_2\text{Si}_2\text{O}_5(\text{OH})_4$  are present. On the other hand, the amount of AHA on the surface of kaolinite is estimated to be 0.3 molecules per the unit, which was deduced from a sample prepared by mixing kaolinite with AHA dissolved in the solvent. Consequently, the amount of AHA in the interlayer space of kaolinite is 0.9 molecules per  $\text{Al}_2\text{Si}_2\text{O}_5(\text{OH})_4$ . When DMSO, a much smaller molecule, is intercalated into kaolinite, the amount of DMSO is 1 molecule per the unit.<sup>31</sup> The basal spacing of a kaolinite-DMSO intercalation compound is 1.12 nm, which is not so larger than that of a kaolinite-AHA intercalation compound (1.23 nm). On the other hand, an intercalation compound of kaolinite with  $\epsilon$ -caprolactam (basal spacing 1.31 nm) has 0.7 molecules per the unit. Consequently, it is suggested that the AHA molecules are closely packed in the interlayer space.

The intercalation of AHA into kaolinite is more difficult than those of  $\omega$ -amino acids with shorter carbon chains, such as  $\beta$ -alanine.<sup>21, 26</sup> Thus, a guest displacement reaction using the

kaolinite–methanol intercalation compound as an intermediate was required. When the intermediate was stirred in a saturated solution of AHA in methanol, no reaction took place because of low solubility of AHA in methanol (8 g/l). Although the use of an aqueous solution of AHA was advantageous for increasing the concentration of AHA, water molecules were selectively intercalated. Therefore, AHA dissolved in the mixed solvent of methanol and water (1:3) was utilized. The long carbon chain of AHA molecules, whose direction is almost parallel to the layer, may be disadvantageous for forming an intercalation compound.

### ***In situ Polymerization of the Kaolinite–AHA Intercalation Compound***

The thermal behavior of the kaolinite–AHA intercalation compound under a nitrogen flow was investigated by TG-DTA (Fig. 5-6). An endothermic reaction with mass loss starts at 190 °C. Because the start of melting and polymerization of bulk AHA is about 210 °C, the endothermic peaks are assigned to the melting and polymerization of AHA. The lower endothermic temperature than that of bulk AHA indicates the peculiar environment of AHA molecules between the layers of kaolinite. The experimental mass loss between 190 and 330 °C (24 mass%) is much larger than that calculated by simple polycondensation of AHA (5 mass%). Additionally, the mass chromatograph between 180 and 260 °C by TG-MS analysis shows the signals of the parent ion of AHA and its fragments (e.g.  $m/e = 55, 85$  and  $113$ ). These results indicate that partial volatilization of AHA took place with almost simultaneous melting and a polycondensation reaction. Above 370 °C, the endothermic peaks with mass loss due to the decomposition of organic substances and the dehydroxylation of kaolinite are observed. Based on the thermal behavior, I carried out the polymerization of AHA by a thermal treatment at 250 °C for 1 h.

The polymerization of AHA was confirmed by an IR analysis. In the spectrum of the product after a heat treatment (Fig. 5-3c), the bands due to  $\delta_{as}(\text{NH}_3^+)$ ,  $\delta_s(\text{NH}_3^+)$ , and  $\nu(\text{COO}^-)$  disappear and amide I ( $1637 \text{ cm}^{-1}$ ) and amide II ( $1550 \text{ cm}^{-1}$ ) are observed, indicating the formation of nylon 6 by the amide bond ( $-\text{CONH}-$ ).<sup>32</sup> Compared with those of bulk nylon 6, which is

## Chapter 5

prepared by heating AHA molecules under the same conditions (Fig. 5-3d), the bandwidths due to the amide I and II are obviously narrow. Therefore, the interactions among the guest molecules in the confined region are limited, compared with those in the bulk state, where three dimensional interactions are present.

Figure 5-4c shows the OH stretching bands of the heated product. In the spectrum, the characteristic band at  $3644\text{ cm}^{-1}$  is observed and its width is narrower than that of the product before the heat treatment, indicating that characteristic hydrogen bonds between OH groups and the guest species is present. Because the band at  $3645\text{ cm}^{-1}$  is observed in the spectra of kaolinite–2-pyrrolidone<sup>20</sup> and  $\epsilon$ -caprolactam intercalation compound,<sup>15</sup> the band may be assigned to the hydrogen bonds between the OH groups and the amide groups.

The basal spacing of the thermally treated product was 1.16 nm (Fig. 5-1d). Judging from the interlayer distance of 0.44 nm, nylon 6 takes a monolayer arrangement between the layers. The value of the basal spacing is smaller than that before the heat treatment (1.23 nm), and the decrease by 0.07 nm is comparable to that in the case for  $\beta$ -alanine (0.06 nm).<sup>21</sup> Therefore, the decrease in the basal spacing is caused by a polycondensation reaction and a simultaneous rearrangement of the hydrogen bondings between the OH groups and the guest species.

In the  $^{13}\text{C}$  CP/MAS NMR spectrum of the heated product (Fig. 5-2c), the signals due to  $\text{CH}_2$  groups at 37.3, 40.0 and around 30 ppm and  $\text{C}=\text{O}$  groups at 173.8 and 177.1 ppm are observed. All of the signals are due to nylon 6.<sup>33</sup> No signals, except for those related to the nylon 6 and methoxy groups (50 ppm), are observed, indicating no side reactions by the heat treatment. The deviation in the chemical shift from the bulk nylon 6 (Fig. 2d) may be due to interactions between kaolinite and nylon 6. Especially, the signal at 177.1 ppm is a peculiar one for an intercalation compound, indicating unique interactions between the OH groups of kaolinite and the  $\text{C}=\text{O}$  groups of nylon 6, as well as the kaolinite–AHA intercalation compound.

The  $^{29}\text{Si}$  CP/MAS NMR spectrum of the heated product shows a change in the interaction between the silicate sheets and the guest molecules (Fig. 5-5c). By a heat treatment, the signal

at  $-91.4$  ppm with a full width at half maximum (FWHM) of  $1.74$  ppm changed to a signal at  $-91.7$  ppm with a FWHM of  $1.70$  ppm. The change in the chemical shift by the polymerization reaction denotes a new interaction between the silicate sheets and nylon 6. On the other hand, the FWHM of the signal was very similar to that before the heat treatment, indicating well-ordered interactions between the silicate sheets and nylon 6 as the kaolinite-AHA intercalation compound.

The amount of organics was estimated. The contents of carbon and nitrogen atoms were  $12.3$  and  $2.3$  mass%, respectively (Table 5-1). On the basis of the nitrogen content,  $0.5$  unit of nylon 6  $[-\text{CONH}(\text{CH}_2)_5-]$  per a kaolinite unit  $[\text{Al}_2\text{Si}_2\text{O}_5(\text{OH})_4]$  was present. The molar ratio of C/N was  $6.2$ , which is very similar to as that of the intercalation compound before the heat treatment. These results indicate that no decomposition reactions occurred, although some amounts of organic materials were reduced by volatilization.

The reaction of kaolinite with AHA is comparable to those of the smectite group, such as montmorillonite (mont).<sup>27</sup> The basal spacings of the mont-AHA intercalation compounds are  $0.41 \sim 0.82$  nm depending on the kind of the interlayer cations. When they were heated at  $240 \sim 250$  °C, AHA molecules in the interlayer space were polymerized to form nylon 6. Although the interlayer distance of  $0.46 \sim 1.32$  nm of the mont-nylon 6 intercalation compounds are larger than that of the kaolinite-nylon 6 intercalation compound, the layers of mont are not exfoliated.<sup>35</sup> On the other hand, when montmorillonite modified with large organic cations, such as alkylammonium cations or  $\omega$ -amino acid, with long chains were used, the formation of nylon-mont hybrids with exfoliation of the layers has been reported.<sup>7, 8, 23</sup> As for kaolinite, the layers are neutral and immobilizing organic cations in the interlayer space by charge balance is impossible. However, a modification of hydroxy groups with methanol has been reported recently.<sup>29, 34</sup> In the future, if the kaolinite modified with large organic species is available, the formation of polymer-kaolinite hybrids may be produced.

### 5.1.4 Conclusions

A kaolinite–nylon 6 intercalation compound was prepared by an *in situ* polymerization of AHA. The intercalation of AHA was achieved by using both a kaolinite–methanol intercalation compound and AHA dissolved in a mixed solvent of methanol and water (1:3). AHA molecules were present in a zwitterion form and took a monolayer arrangement between the layers of kaolinite. By a heat treatment at 250 °C under a nitrogen flow, AHA molecules were polymerized to form a kaolinite–nylon 6 intercalation compound. The preparation of kaolinite intercalation compounds with  $\omega$ -amino acid with longer carbon chains and their polymerization reactions is feasible under improved experimental conditions. Future applications of these organically modified kaolinites for polymer–clay nanocomposites are expected.

### 5.1.5 References

- 1 D. W. Bruce and D. O'Hare, *"Inorganic Materials," 2nd Ed*, John Wiley & Sons (1996).
- 2 M. Ogawa and K. Kuroda, *Chem. Rev.*, **95**, 399 (1995).
- 3 M. Ogawa and K. Kuroda, *Bull. Chem. Soc. Jpn.*, **70**, 2593 (1997).
- 4 E. Ruiz-Hitzky and P. Aranda, *An. Quim., Int. Ed.*, **93**, 197 (1997).
- 5 B. K. G. Theng, *"Formation and Properties of Clay-Polymer Complexes,"* Elsevier, New York, (1979).
- 6 E. P. Giannelis, *Adv. Mater.*, **8**, 29 (1996).
- 7 G. Lagaly, *Appl. Clay Sci.*, **15**, 1 (1999).
- 8 P. C. LeBaron, Z. Wang, and T. J. Pinnavaia, *Appl. Clay Sci.*, **15**, 11 (1999).
- 9 Y. Komori and K. Kuroda *In "Polymer-Clay Nanocomposites,"* ed. by T. J. Pinnavaia and G. Beall, John Wiley & Sons (2000).
- 10 B. K. G. Theng, *"The Chemistry of Clay-Organic Reactions,"* Adam Hilger, London (1974).
- 11 Y. Sugahara, S. Satokawa, K. Kuroda, and C. Kato, *Clays Clay Miner.*, **36**, 343 (1988).
- 12 Y. Komori, Y. Sugahara, and K. Kuroda, *J. Mater. Res.*, **13**, 930 (1998).
- 13 Y. Komori, Y. Sugahara, and K. Kuroda, *Appl. Clay Sci.*, **15**, 241 (1999).
- 14 K. Kuroda, K. Hiraguri, Y. Komori, Y. Sugahara, H. Mouri, and Y. Uesu, *Chem. Commun.*, **22**, 2253 (1999).
- 15 Y. Komori, A. Matsumura, T. Itagaki, Y. Sugahara, and K. Kuroda, *Clay Sci.*, **11**, 47 (1999).
- 16 Y. Komori, Y. Sugahara, and K. Kuroda, *Chem. Mater.*, **11**, 3 (1999).
- 17 J. J. Tunney and C. Detellier, *Chem. Mater.*, **8**, 927 (1996).
- 18 J. E. Gardolinski and L. C. M. Carrera, *J. Mater. Sci.*, **35**, 3113 (2000).
- 19 Y. Sugahara, S. Satokawa, K. Kuroda, and C. Kato, *Clays Clay Miner.*, **28**, 137 (1990).
- 20 Y. Sugahara, T. Sugiyama, T. Nagayama, K. Kuroda, and C. Kato, *J. Ceram. Soc. Jpn.*, **100**, 413 (1992).

## Chapter 5

- 21 T. Itagaki, Y. Komori, Y. Sugahara, and K. Kuroda, *Book of Abstracts, 42<sup>nd</sup> Annual Meeting of the Clay Science Society of Japan*, p.74, (1998).
- 22 Y. Kojima, A. Usuki, M. Kawasumi, A. Okada, T. Kurauchi, and O. Kamigaito, *J. Polym. Sci. Part A: Polym. Chem.*, **31**, 983 (1993).
- 23 A. Usuki, Y. Kojima, M. Kawasumi, A. Okada, Y. Fukushima, T. Kurauchi, and O. Kamigaito, *J. Mater. Res.*, **8**, 1179 (1993).
- 24 T. Watari, T. Yamane, S. Moriyama, T. Torikai, Y. Imaoka, K. Suehiro, and H. Tateyama, *Mater. Res. Bull.*, **32**, 719 (1997).
- 25 M. Sato, *Clays Clay Miner.*, **47**, 793 (1999).
- 26 F. Kanamaru and V. Vand, *Am. Mineral.*, **55**, 1550 (1970).
- 27 C. Kato, K. Kuroda, and M. Misawa, *Clays Clay Miner.*, **27**, 129 (1979).
- 28 H. V. Olphen and J. J. Fripiat, *"Data Handbook for Clay Materials and Other Non-metallic Minerals,"* Pergamon (1979).
- 29 Y. Komori, H. Enoto, R. Takenawa, S. Hayashi, Y. Sugahara, and K. Kuroda, *Langmuir*, **16**, 5506 (2000).
- 30 C. G. Lagrange, *Can. J. Chem.*, **56**, 663 (1978).
- 31 S. Hayashi, *J. Phys. Chem.*, **99**, 7120 (1995).
- 32 H. Arimoto, *J. Polym. Sci. A*, **2**, 2283 (1964).
- 33 A. Okada, M. Kawasumi, I. Tajima, T. Kurauchi, and O. Kamigaito, *J. Appl. Polym. Sci.*, **37**, 1363 (1989).
- 34 J. J. Tunney and C. Detellier, *J. Mater. Chem.*, **6**, 1679 (1996).

Table 5-1 CHN data of the kaolinite-AHA intercalation compounds before and after the heat treatment at 250 °C.

	Content / mass% C/N		(molar ratio)
	C	N	
Kaolinite-AHA	20.8	3.8	6.3
heat treated product	12.3	2.3	6.2

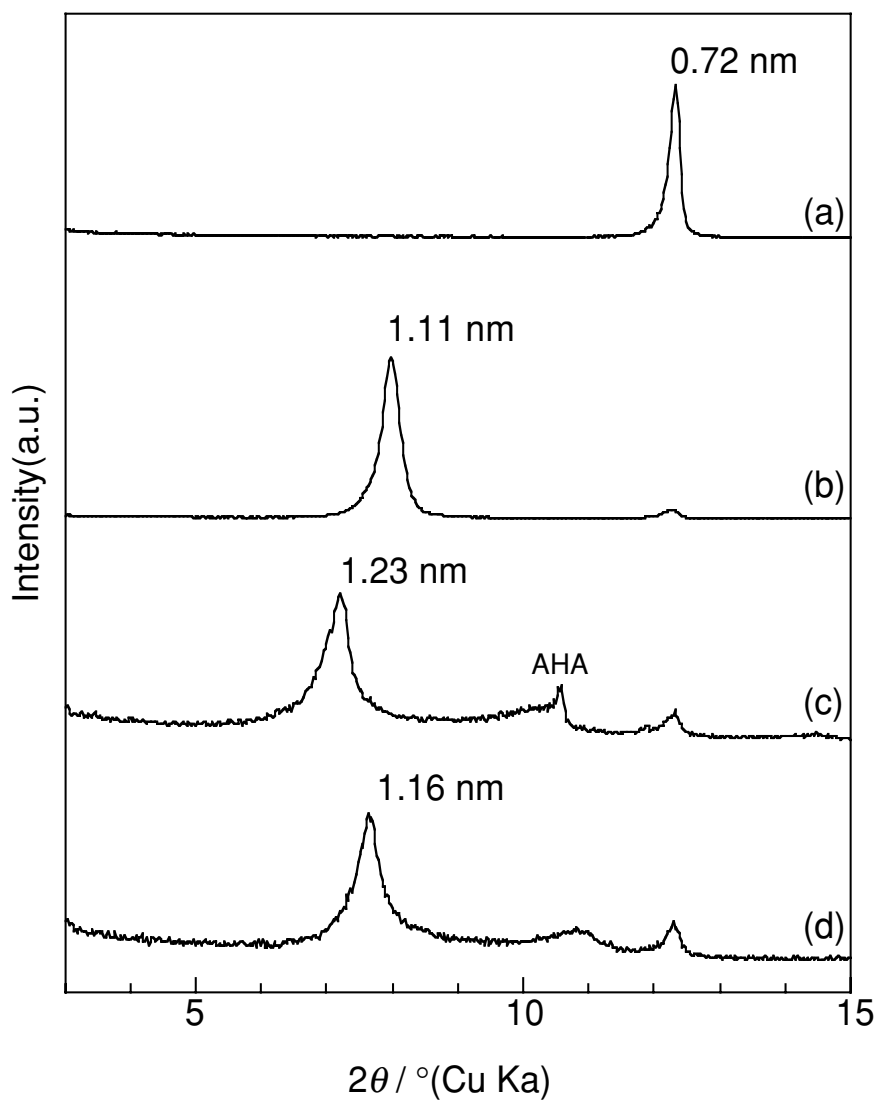


Figure 5-1 XRD patterns of (a) kaolinite, (b) kaolinite–methanol intercalation compound under wet conditions, (c) kaolinite–AHA intercalation compound, and (d) kaolinite–AHA intercalation compound heated at  $250^\circ\text{C}$ .

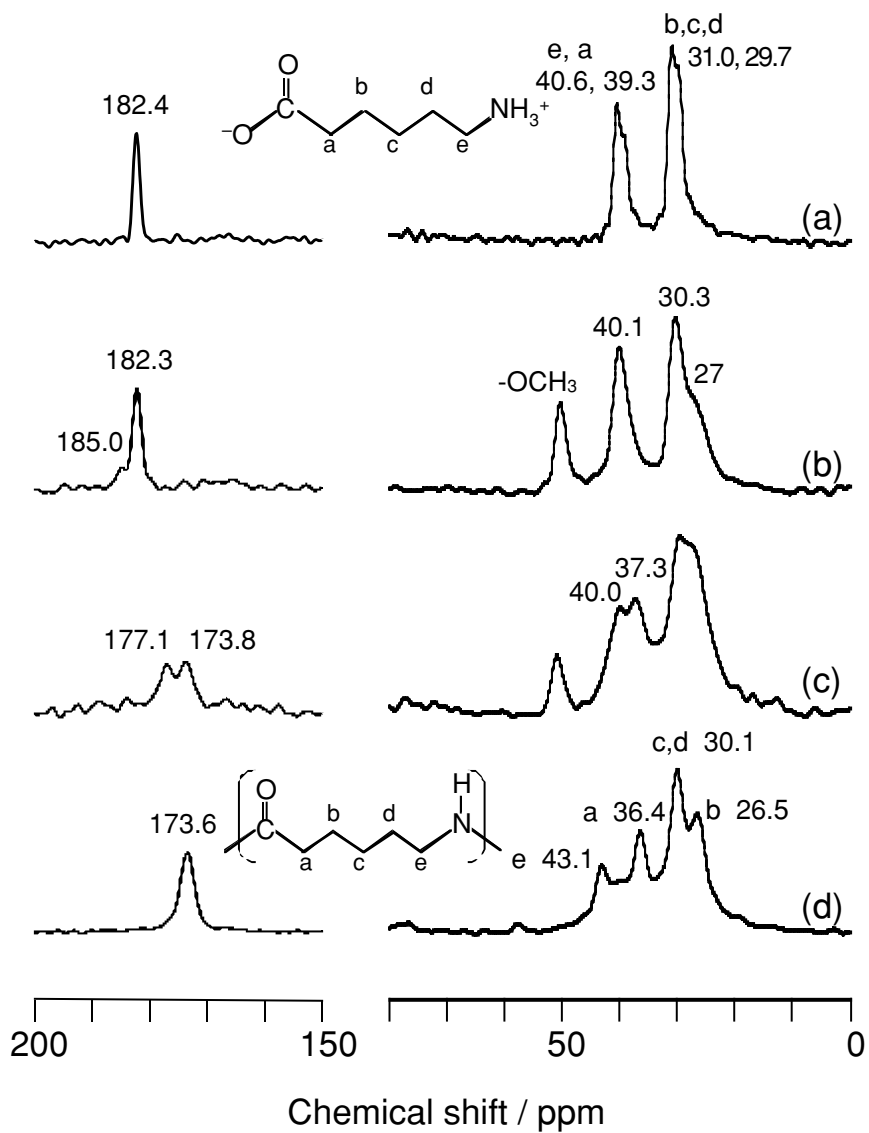


Figure 5-2  $^{13}\text{C}$  CP/MAS NMR spectra of (a) AHA, (b) kaolinite-AHA intercalation compound, (c) kaolinite-AHA intercalation compound heated at 250 °C, and (d) AHA heated at 250 °C (nylon 6).

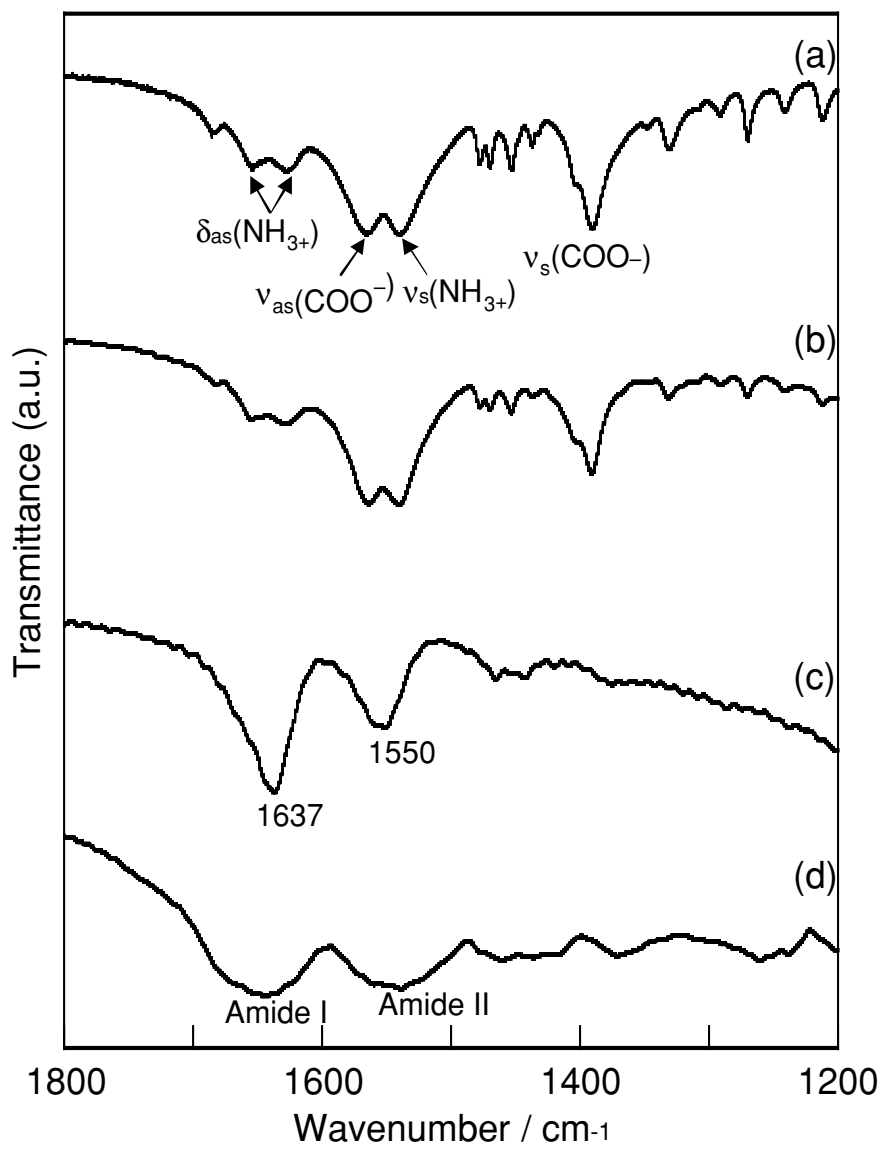


Figure 5-3 IR spectra of (a) AHA, (b) kaolinite–AHA intercalation compound, (c) kaolinite–AHA intercalation compound heated at 250 °C, and (d) AHA heated at 250 °C (nylon 6).

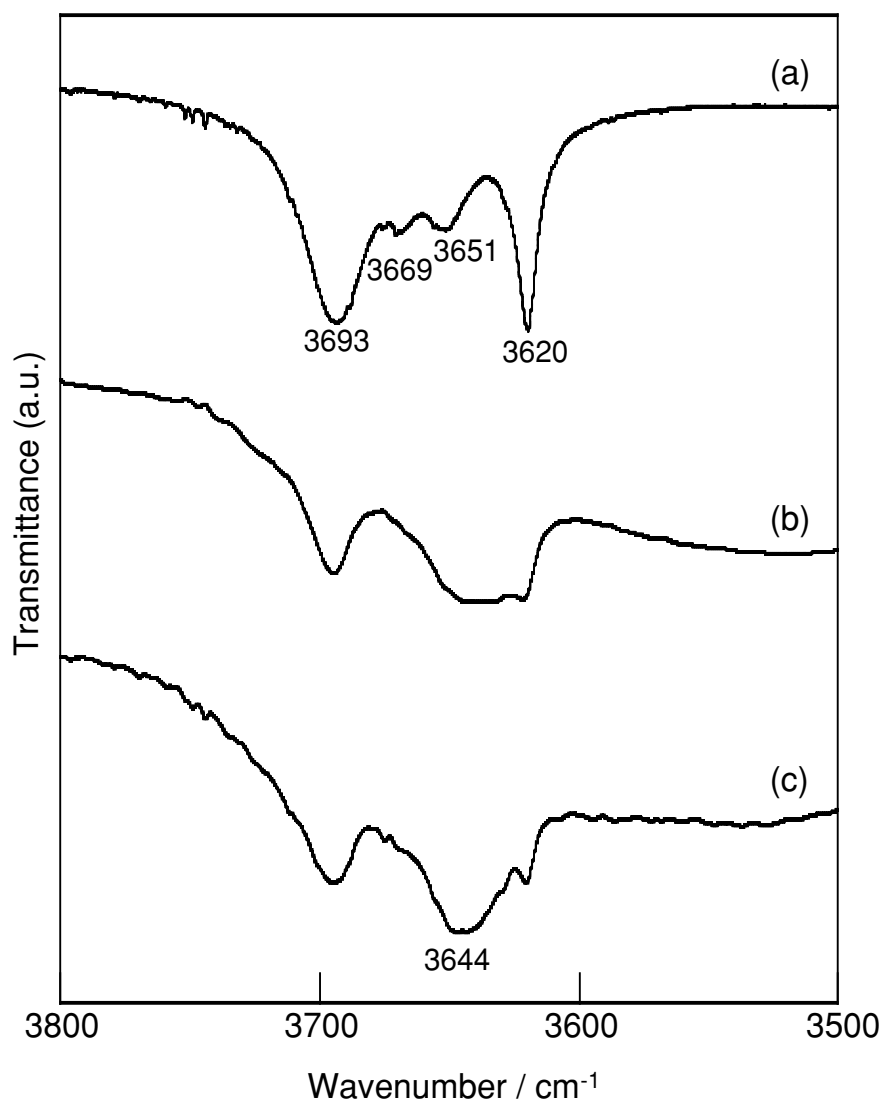


Figure 5-4 IR spectra of (a) kaolinite, (b) kaolinite–AHA intercalation compound, and (c) kaolinite–AHA intercalation compound heated at 250 °C.

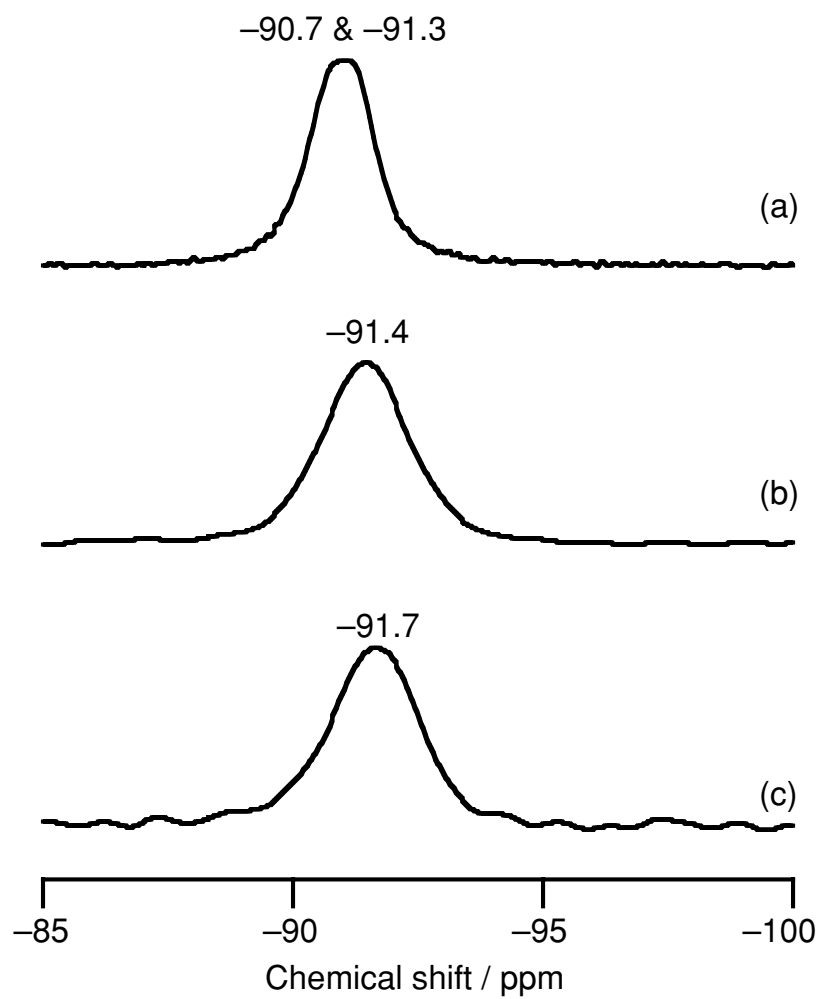


Figure 5-5  $^{29}\text{Si}$  CP/MAS spectra of (a) kaolinite, (b) kaolinite-AHA intercalation compound, and (c) kaolinite-AHA intercalation compound heated at 250 °C.

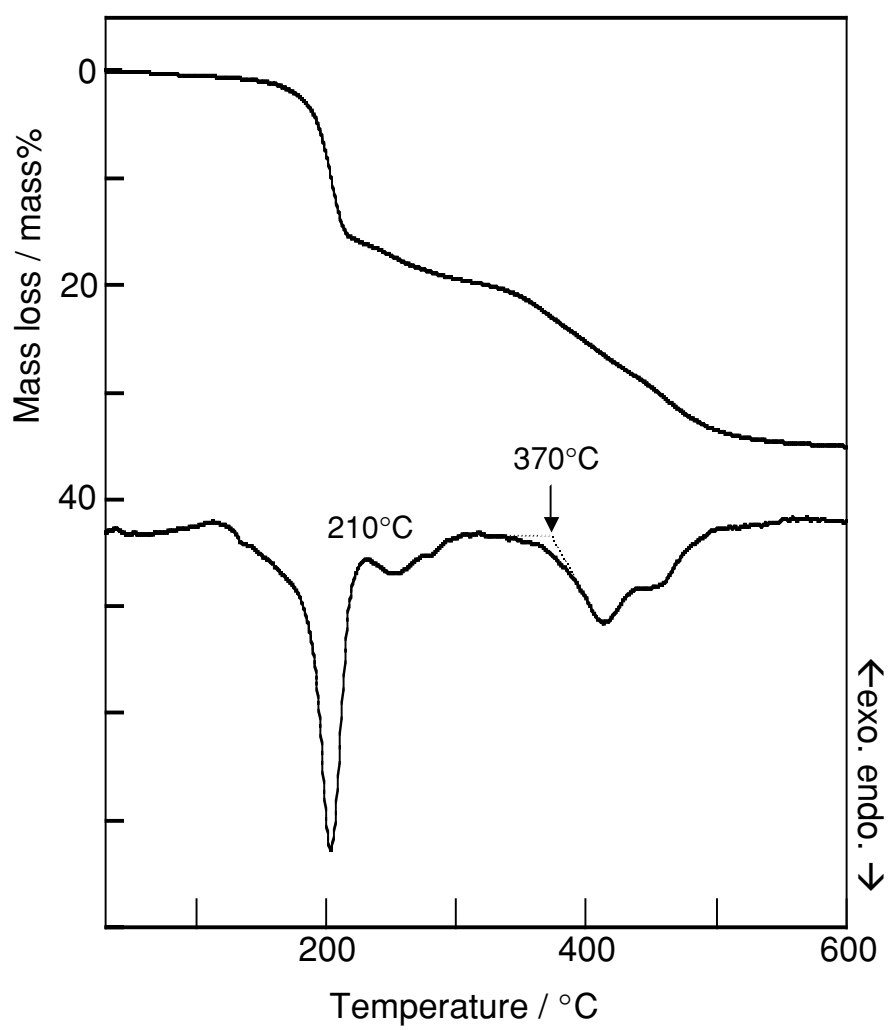


Figure 5-6 TG-DTA curves of the kaolinite-AHA intercalation compound.

## 5.2 Preparation of Kaolinite–Nylon6 Composites by Blending

### Nylon6 and a Kaolinite–Nylon6 Intercalation Compound

#### 5.2.1 Introduction

Polymer/clay nanocomposites, in which exfoliated smectite clay nanosheets are highly dispersed in polymer matrices, exhibit excellent tensile property, gas-barrier property, thermostability, flame retardance, etc.<sup>1-3</sup> Polymers utilized for this purpose are various, including nylon,<sup>4, 5</sup> epoxy resin,<sup>6, 7</sup> polyurethanes,<sup>8</sup> polyimides,<sup>9</sup> nitrile rubber,<sup>10</sup> polyesters,<sup>11</sup> poly(propylene),<sup>12, 13</sup> poly(styrene),<sup>14, 15</sup> and polysiloxanes.<sup>16</sup> However, the kind of clays used for the formation of this type of nanocomposites is limited to swelling smectite clays, such as montmorillonite. It has been pointed out that the property of polymer/clay nanocomposites also depends on the kind of smectite clays.<sup>5</sup> This prompted me to survey the possibility of the formation of this type of nanocomposites by the use of different kinds of clays.

Kaolinite, a 1:1 type clay mineral, is different from 2:1 type smectite clay minerals and has a larger aspect ratio. The surface of the aluminosilicate is composed of SiO<sub>4</sub> tetrahedral sheets and AlO<sub>2</sub>(OH)<sub>4</sub> octahedral sheets which can be utilized for the formation of hydrogen bondings with some polymers. Due to its unique structural feature, polymer/kaolinite nanocomposites would exhibit different behaviors from those of polymer/smectite nanocomposites. However, the intercalation capability of kaolinite for polymers is very low and only several intercalation compounds with limited polymers have been reported.<sup>17-22</sup> Komori *et al.* have recently clarified that methoxy-modified kaolinite<sup>23</sup> is an excellent intermediate for intercalating various organic species<sup>24</sup> and we reported the formation of a kaolinite–nylon6 intercalation compound<sup>25</sup>. In the present study, blended composites were prepared by employing nylon6 as a polymer matrix and a kaolinite–nylon6 intercalation compound or kaolinite as an inorganic filler, and their mechanical properties were measured. Because there are no reports on

the mechanical properties of kaolinite–organic intercalation compounds blended with polymers, the present results contribute to the prediction of the properties of polymer/kaolinite nanocomposites to be developed in future where the nanosheets of kaolinite would be well dispersed in polymer matrices.

### **5.2.2 Experimental**

A kaolinite–nylon6 intercalation compound (abbreviated as kaolinite–nylon6) was prepared according to a method reported previously by using a kaolinite–6-aminohexanoic acid (AHA) intercalation compound as a precursor.<sup>25</sup> Nylon6/kaolinite–nylon6 was obtained by melt mixing between nylon6 (commercial grade, 1015B, Ube Industries Co.) and kaolinite–nylon6 by a twin-screw extruder (S-1KRC, Kurimoto Ltd.). The temperature of nylon6 was 240 °C and a rotational speed was 300 rpm with the amount of feed by 1300 g h<sup>-1</sup>. Nylon6 blended without clay (nylon6 (blended)) and with unmodified kaolinite (nylon6/kaolinite) were prepared for comparison. Nylon6 Clay Hybrid (NCH,<sup>4, 5</sup> commercial grade, 1015C2, Ube Industries Co.), composed of organically modified smectite and nylon6, was used as a reference. Tensile and Izod impact tests were carried out according to the methods of ASTM D-638 and ASTM-D256, respectively.

### **5.2.3 Results and Discussion**

After the blending for the formation of nylon6/kaolinite–nylon6, the basal spacing of kaolinite–nylon6 was slightly reduced to 1.15 nm from that of original kaolinite-nylon6 (not shown). This result indicates that the layered structure of kaolinite was not exfoliated but retained. The mechanical properties of the samples are listed in Table 5-2. Tensile strength and tensile modulus of nylon6 were improved after blending with kaolinite or kaolinite–nylon6. The reinforced effect of nylon6 with kaolinite–nylon6 in tensile modulus is slightly larger than that

## *Chapter 5*

with kaolinite. The slight increase of nylon6/kaolinite–nylon6 is probably due to the newly generated interactions between the polymer matrix and intercalated nylon6. Some of the guest polymers should reside outer surfaces and/or near the edge of the clay platelets. The values of the Izod impact strength of nylon6/kaolinite and nylon6/kaolinite–nylon6 were equivalent to that of nylon6, though they were lower than that of nylon6 (blended).

When a kaolinite–AHA intercalation compound (kaolinite-AHA) was used for blending instead of kaolinite–nylon6, all the mechanical properties were lowered. We reported that half AHA molecules between the layers are polymerized and the others are deintercalated at 250 °C under an N<sub>2</sub> atmosphere.<sup>25</sup> The condition of the heat treatment was similar to that of the blending. Consequently, the decrease in the mechanical properties may be attributed to the deterioration of the nylon6 matrix by deintercalated AHA molecules.

The tensile moduli of the samples were slightly lower than that of NCH. The values of the tensile strength were much lower than that of NCH. However, the kaolinite-based composites and NCH exhibited almost similar impact strength. The effect of kaolinite should arise from the surface of each particle because the mineral was not exfoliated. The surface of kaolinite particles, as described above, is covered by abundant OH groups which can be interacted with nylon6 matrices. The particle size of kaolinite is larger than that of montmorillonite, which might also be attributed to the effect. Kaolinite–nylon6 has an additional effect for the increase in the interactions with the polymer matrix because the surface and the edge of kaolinite are covered by sorbed nylon6 at least partly.

### **5.2.4 Conclusions**

The increase in tensile moduli of the composites derived from nylon6 blended with kaolinite or a kaolinite–nylon6 intercalation compound was confirmed whereas the layered structure was retained. The change in the properties is most likely due to the surface structure and the crystallite

size of kaolinite. Although polymer/kaolinite nanocomposites, in which exfoliated kaolinite nanosheets are dispersed in polymer matrices, are not known at present, the study here strongly suggests that higher dispersion of kaolinite crystallites in polymers should have larger interfaces between the kaolinite surface and polymers, which would result in further increase in the properties of these polymer clay systems. The next step is a search for highly versatile intermediates derived from kaolinite, utilized for intercalation of polymers and the following exfoliation.

### 5.2.5 References

- 1 *Appl. Clay Sci.* **15** (1999) Special issue on clay mineral-polymer nanocomposites.
- 2 “*Polymer-Clay Nanocomposites*,” ed. by T. J. Pinnavaia and G. Beall, John Wiley & Sons (2000).
- 3 E. P. Giannelis, *Adv. Mater.* **8** (1996) 29.
- 4 A. Usuki, Y. Kojima, M. Kawasumi, A. Okada, Y. Fukushima, T. Kurauchi and O. Kamigaito, *J. Mater. Res.* **8** (1993) 1179.
- 5 Y. Kojima, A. Usuki, M. Kawasumi, A. Okada, Y. Fukushima, T. Kurauchi and O. Kamigaito, *J. Mater. Res.* **8** (1993) 1185.
- 6 P. B. Messersmith and E. P. Giannelis, *Chem. Mater.* **6** (1994) 1719.
- 7 T. Lan and T. J. Pinnavaia, *Chem. Mater.* **6** (1994) 2216.
- 8 Z. Wang and T. J. Pinnavaia, *Chem. Mater.* **10** (1998) 3769.
- 9 K. Yano, A. Usuki, A. Okada, T. Kurauchi and O. Kamigaito, *J. Polym. Sci., Part. A: Polym. Chem.* **31** (1993) 2493.
- 10 Y. Kojima, K. Fukumori, A. Usuki, A. Okada and T. Kurauchi, *J. Mater. Sci. Lett.* **12** (1993) 889.
- 11 P. B. Messersmith and E. P. Giannelis, *J. Polym. Sci., Part. A: Polym. Chem.* **33** (1995) 1047.

## Chapter 5

- 12 Y. Kurokawa, H. Yasuda and A. Oya, *J. Mater. Sci. Lett.* **15** (1996) 1481.
- 13 A. Usuki, M. Kato, A. Okada and T. Kurauchi, *J. Appl. Polym. Sci.* **63** (1997) 137.
- 14 T. L. Porter, M. E. Hagerman, B. P. Reynolds, M. P. Eastman and R. A. Parnell, *J. Polym. Sci., Part. B: Polym. Phys.* **36** (1998) 673.
- 15 A. Akelah and A. Moet, *J. Mater. Sci.* **31** (1996) 3589.
- 16 S. D. Burnside and E. P. Giannelis, *Chem. Mater.* **7** (1995) 1597.
- 17 Y. Sugahara, S. Satokawa, K. Kuroda and C. Kato, *Clays Clay Miner.* **36** (1988) 343.
- 18 Y. Sugahara, S. Satokawa, K. Kuroda and C. Kato, *Clays Clay Miner.* **38** (1990) 137.
- 19 Y. Sugahara, T. Sugiyama, T. Nagayama, K. Kuroda and C. Kato, *J. Ceram. Soc. Jpn.* **100** (1992) 413.
- 20 Y. Komori, Y. Sugahara and K. Kuroda, *Chem. Mater.* **11** (1999) 3.
- 21 J. J. Tunney and C. Detellier, *Chem. Mater.* **8** (1996) 927.
- 22 J. E. Gardlinski, L. C. M. Carrera, M. P. Cantao and F. Wypych, *J. Mater. Sci.* **35** (2000) 3113.
- 23 Y. Komori, H. Enoto, R. Takenawa, S. Hayashi and K. Kuroda, *Langmuir*, **16** (2000) 5506.
- 24 Y. Komori, Y. Sugahara and K. Kuroda *J. Mater. Res.* **13** (1998) 930.
- 25 A. Matsumura, Y. Komori, T. Itagaki, Y. Sugahara and K. Kuroda, *Bull. Chem. Soc. Jpn.* **74** (2001) 1153.

Table 5-2 Mechanical properties of blended composites

	Clay content /wt%	tensile strength / MPa	tensile modulus / GPa	Izod impact strength (with notch) /J m <sup>-1</sup>
nylon6	0	74.0	1.13	27.8
nylon6 (blended)	0	72.7	1.16	34.5
nylon6/kaolinite	1.42	79.2	1.29	27.7
nylon6/kaolinite-AHA	1.48	77.0	1.25	21.6
nylon6/kaolinite-nylon6	1.38	80.4	1.33	27.7
NCH	1.80	89.1	1.36	25.4



# CHAPTER 6

## CONCLUSION



Various kinds of kaolinite–organic intercalation compounds were prepared by appropriate methods, i.e. transesterification and *in-situ* polymerization methods, and their structures and properties were investigated.

Propanediols (1,2- and 1,3-propanediols) were grafted on to the interlayer surface of kaolinite via transesterification of methoxy-modified kaolinite. This is the first report to prepare organically modified kaolinite by transesterification. Grafting occurred on the AlOH groups of the interlayer surface, which provided unique interlayer environments surrounded by both hydroxy groups of diols and silicate layers. Residual OH group of propanediol has a potential for further modification. When the reaction time was increased, 1,3-propanediol partially forms a bridge type grafting where both OH groups were bonded. Amounts of alkoxy groups per  $\text{Al}_2\text{Si}_2\text{O}_4(\text{OH})_5$  were increased during the reaction, which showed not only transesterification but also further esterification also proceeded. On milder conditions, 1,2- and 1,3-propanediols were not grafted onto the interlayer surface but molecularly intercalated. The difference between propanediol-grafted kaolinites and kaolinite-propanediol intercalation compounds were discussed by using spectroscopic data. This method is suit for other large alcohols because methoxy-modified kaolinite is a versatile intermediate.

By utilizing this method, glycerol-modified kaolinite was prepared. After the reaction, the basal spacing of product was expanded to 1.09 nm. The covalent bonding between kaolinite and glycerol was shown by DTA-TG data. Raman spectroscopy suggested that one terminal OH group of glycerol was used for bonding.

Swelling behavior of organically modified kaolinite was investigated. By refluxing the mixture of ethylene glycol and methoxy-modified kaolinite, some organically modified kaolinite was swollen into ethylene glycol. The reaction pathway is proposed as follows. At first, transesterification between methoxy-modified kaolinite and ethylene glycol proceeded. Then, ethylene glycol-grafted kaolinite was swollen into ethylene glycol. Same behavior was also observed in the case of refluxing the mixture of methoxy-modified kaolinite and other alcohols

## Chapter 6

such as propanediols, butandriols, and aminoethanol. These data showed that organic modification improved the properties of kaolinite, and swelling behavior of kaolinite, known as non-swelling clay mineral, is firstly reported.

On the other hand, a kaolinite–nylon6 intercalation compound was prepared by *in-situ* polymerization of 6-aminohexanoic acid. Between the layers of kaolinite, 6-aminohexanoic acid were present in a zwitterion form with a monolayer arrangement. By heating the kaolinite–6-aminohexanoic acid at 250 °C, intercalated 6-aminohexanoic acid was polymerized and a kaolinite–nylon 6 intercalation compound was obtained.

As an application of kaolinite–polymer intercalation compounds, blended composites (Nylon 6/Kaolinite-Nylon 6) were prepared by employing nylon6 as a polymer matrix and a kaolinite–nylon 6 intercalation compound as a filler and the mechanical properties were measured. The reinforced effect of a kaolinite–nylon 6 intercalation compound was slightly higher than that of kaolinite. Though the layer structure of kaolinite was retained, Nylon 6/Kaolinite-nylon 6 showed almost similar impact strength to nylon 6-clay hybrid in which nanosheet derived from smectite were dispersed into nylon 6 matrix. These data showed that kaolinite–polymer intercalation compounds and kaolinite-polymer hybrids have a potential for an inorganic filler.

A 1:1 type clay mineral kaolinite is a unique material with two different interlayer surfaces,  $\text{SiO}_4$  tetrahedral and  $\text{AlO}_4(\text{OH})_2$  octahedral sheet, and has high crystallinity and high aspect ratio. Several kaolinite–organic intercalation compounds utilizing these features were prepared.

Kaolinite reacted with various alcohols on the interlayer surface of  $\text{AlO}_5(\text{OH})_2$  to form two-dimensional inorganic-organic nanohybrids with interlayer regions sandwiched by organic and inorganic sheets. Organic modification of kaolinite affected the interlayer environments and alcohols were absorbed into the new interlayer space of organically modified kaolinite. The additional properties induced by organic modification such as swelling behavior should wide the various use of kaolinite

The reinforce effects of a kaolinite-nylon 6 intercalation compound, prepared by *in-situ* polymerization of 6-aminohexanoic acid, to nylon 6 matrix is quite high, which was demonstrated in chapter 5. This showed the efficiency of kaolinite–polymer intercalation compound as an inorganic filler, and also imply that of exfoliated nanosheet derived form kaolinite.



## List of Publications

- 1) Preparation of a kaolinite- $\epsilon$ -caprolactam intercalation compound  
*Clay Sci.*, **11**, 47 (1999).
- 2) Preparation of a kaolinite-nylon6 intercalation compound  
*Bull. Chem. Soc. Jpn.*, **74**, 1153 (2001).
- 3) Preparation of Kaolinite-Nylon6 Composites by Blending Nylon6 and a Kaolinite-Nylon6 Intercalation Compound  
*J. Mater. Sci. Lett.*, **20**, 1483 (2001).
- 4) Synthesis of a kaolinite-poly( $\beta$ -alanine) intercalation compound  
*J. Mater. Chem.*, **11**, 3291 (2001).
- 5) Organic modification of the interlayer surface of kaolinite with propanediol by transesterification  
*J. Mater. Chem.* in press.



## *Acknowledgement*

I would like to express my grateful acknowledgement to Professor Kazuyuki Kuroda in Waseda University for valuable advice, helpful discussion, careful reviewing of the manuscript, and continuous encouragement. I wish to thank to Professor Tetsuya Osaka in Waseda University for his support and encouragement. I deeply appreciate to Professor Yoshiyuki Sugahara in Waseda University for valuable advice and discussion.

A special debt of gratitude goes to Dr. Shigeo Satokawa in Tokyo Gas Co., Ltd. and Dr. Yoshihiko Komori in National Institute of Advanced Industrial Science and Technology (AIST) for valuable suggestions. I acknowledge Dr. Makoto Kato and Dr. Arimitsu Usuki in Toyota central Research & Development Labs. Inc. for measurements of mechanical properties. Special thanks are also due to Dr. Hiroyasu Furukawa in National Institute of Advanced Industrial Science and Technology (AIST), Dr. Atsushi Shimojima, and Mr. Tetsuro Shigeno in Waseda University for their earnest discussion and encouragement. I am deeply indebted to Professor Dermot O'Hare and Dr. Alex Norquist in Oxford University for their helpful discussion.

I would like to express my acknowledgement to Miss Asako Matsumura, Mr. Hiroyuki Kurachi, Miss Miho Nakagawa, and Mr. Junnosuke Murakami for experimental supports. Thanks to their supports, I have accomplished my thesis.

Finally I thanks to my parents for financial supports and continuous encouragement.

